# Improving the technical properties of recycled aggregates for road construction

Solomon Adomako

UiA University of Agder

Doctoral Dissertations at the University of Agder 428

Solomon Adomako

# Improving the technical properties of recycled aggregates for road construction

Doctoral Dissertation for the Degree *Philosophiae Doctor (PhD)* at the Faculty of Engineering and Science, Specialization in Civil Engineering

University of Agder
Faculty of Engineering and Science
2023

Doctoral dissertations at the University of Agder 428
ISSN: 1504-9272
ISBN: 978-82-8427-145-3

© Solomon Adomako, 2023

Print: Make! Graphics
Kristiansand

# Preface

This doctoral thesis is submitted in partial fulfillment of the requirements for the degree of Philosophiae Doctor at the University of Agder (UiA). The research was carried out at the Department of Engineering and Science of UiA in Grimstad, Norway, under the supervision of Christian John Engelsen (Chief Scientist at SINTEF and Professor at UiA) and Rein Terje Thorstensen (Professor at UiA).

Solomon Adomako

Grimstad, Norway

May 2023

*“We have to put an end to those bad long-standing habits of squandering natural resources. Sustainable building materials or green building materials can be the solution.”*

*Sustainability for All.*

# Acknowledgments

This PhD study was conducted at the Department of Engineering and Science of the University of Agder. The study contributed to Work Package Two (WP2) of the project titled "More Efficient and Environmentally Friendly Road Construction (MEERC)," funded by the Research Council of Norway.

First, I would like to thank my distinguished supervisors, Christian John Engelsen (Chief Scientist at SINTEF and Professor at UiA) and Rein Terje Thorstensen (Professor at UiA), for their invaluable guidance throughout my PhD. You took me through this exciting and research-based experiential journey and sharpened my understanding at every step. I would like to emphasize that your constructive and stimulating comments, discussions, and advice, as well as the help you provided in writing my scientific papers, are deeply appreciated.

My sincere gratitude goes to Associate Professor Diego Maria Barbieri of the Norwegian University of Science and Technology (NTNU) for his support during the repeated load triaxial test campaign at NTNU campus in Trondheim.

I would like to thank Velde Miljø in Sandnes for the maximum collaboration and opportunity to visit the recycling facility during my PhD.

I am extremely grateful to Anette Heimdal and Rita Sølvi Ditlefsen for their support and encouragement. I enjoyed the BYGGLAB work environment. Both your presence and the waffle-making experience were fantasies, and I appreciate the time we spent together.

Special thanks go to Emma Elisabeth Horneman of the Faculty of Engineering and Science for your maximum collaboration and care throughout my stay. I also would like to express my gratitude to Professor Ephrem Taddesse for being a significant anchor in which you always asked about my progress.

The MEERC team (Mehrdad, Ingrid, Una, Otto, and Mequanent) deserves excellent gratitude. We built a beautiful scientific community in our office. The inspiring discussions on the scope of MEERC and research updates were a remarkable experience. Our self-acclaimed motto that our office is the best in the entire department motivated me to always be with you.

I would like to express my heartfelt gratitude to my dear mother and late father for believing in me and investing in my education. Your unwavering love and support have had a profound impact on both my personal and academic life and have helped shape me into the person I am today. I would also like to thank

my beloved wife and son, Yvonne, and Ezekiel, for their unyielding support and belief in me.

Lastly, I would like to express my profound appreciation for the support and encouragement offered by Winston, my siblings and all my friends -Oscar, Immanuel, and Antoine, who supported me in various ways.

# Abstract

Sustainable construction, operation and maintenance of road infrastructure are currently of high priority in Norway. The development of the highway standards and specifications (e.g., N200) plays an important role, so that optimized use of recycled excavation materials and crushed concrete is achieved in the sub-base and base layers.

Generally, factors that hinder the use of EM include geological complexity (i.e., composition of mechanically weak rocks), the absence of declaration policies, and a standard framework to characterize the testing frequency of general properties. Considering their application in permitted quantities in the base layer, it is expected that compliance with the mechanical performance, that is, Los Angeles (LA) and micro-Deval (MD) and other geometric properties designed for conventional materials will be met. In addition, given the related geological complexity, it is essential to identify the effects of chemical and mineralogical features, as this may enhance the opportunity to classify geological variations and optimize the performance by mixing the masses with other materials.

In this study, the first approach involved the identification of knowledge gaps pertaining to the relationship between the local geology and the mechanical performance (LA and MD) of the aggregates. Considering this, state of the art studies on the geological influences on the properties of rock aggregates were performed. It was demonstrated that the global synergy of the influence of weathering on geological parameters (mineralogy, grain size and crystal size, grain shape, and porosity) and the extent to which they affect the overall performance remain important criteria in material selection. This pertains to excavation materials given the large geological make-up and may help end-users to understand the different roles played by mineralogy and other textural properties.

Second, this study presents a documented baseline for the mechanical stability of excavation materials and assesses their mineralogical and chemical influences. The approach consisted of mixing protocols, such as intermixing with other materials as a mechanical stabilizing technique. The experimental protocol involved LA and MD tests and repeated load triaxial tests (RLTT). Generally, in the cases of LA and MD, the local excavation materials met the current technical criteria for the base layer. However, if weak rocks, such as phyllite, make up the composition, a limited target of ≤ 40% would be tolerable. The findings on the

mineralogical influence demonstrated that phyllosilicates (mica and chlorite) predominantly contributed to the low mechanical performances. In addition, it was demonstrated that if excavation materials are potentially composed of soluble materials such as masonry rubble, careful consideration should be given to the mixing level.

Regarding the stiffness and deformation properties, as analyzed by Hicks and Monismith's model and Uzan's model, respectively, it was shown that as the bulk stress increased excavation materials produced higher stiffness response than phyllites. At the intermix level, the stiffness was higher at 25% substitution by phyllites compared to 50%. Hence, the performance was sensitive to the increased phyllite content. On the other hand, the permanent deformation behavior did not show significant variations despite the reported values of the degree of mobilized friction angle ρ(°), and incremental friction angle φ(°) which describe mobilized and maximum shear strength, respectively. These findings provide valuable input to future guidelines in predicting the bearing capacities for roads constructed with recycled materials.

Finally, this study demonstrated the extended performance of recycled aggregates derived from concrete sludge by the Re-Con Zero dry washing technology (RCZ) applied as feedstock in wet recycling of excavation materials to increase material circularity. The results showed a general trend of increased LA and MD with increased feeding of RCZ. The acid solubility results indicated that cement paste remained on the particles after the wet recycling process and parts of the cement paste was size reduced (< 1.6 mm) in the LA-testing process.

The content of chemical species of potential concern was generally low and complied with Norwegian waste regulations. In addition, the low Cr(VI) content indicates low leaching of Cr upon carbonation and a decrease in pH when used under real conditions.

These findings contribute to maximizing sustainable use of resources in Norway and may help end -users with increased understanding of handling techniques and the use of recycled aggregates from excavation masses.

# Sammendrag

Bærekraftig utbygging, samt drift og vedlikehold av veganlegg, er høyt prioritert i Norge. I dette arbeidet er også utviklingen av vegnormalene (f.eks. N200) viktig, slik at bruken av resirkulerte gravemasser (engelsk: Recycled Excavation Materials, REM) og knust betong i bære- og forsterkningslag kan optimaliseres.

Generelt sett inkluderer faktorer som hindrer bruken av REM geologisk kompleksitet (dvs. sammensetning av mekanisk svake bergarter), tydeligere prosedyrer og regler på hvilke egenskaper som bør deklareres og hvor hyppig dette skal utføres. Visse krav til mekaniske egenskaper må oppfylles for at masser skal tilates brukt i veikroppen, herunder Los Angeles- (LA) og micro-Deval (MD)-verdier. På grunn av den geologiske kompleksiteten er det også viktig å identifisere kjemiske og mineralogiske egenskaper. Dette kan forbedre mulighetene til å blande materialer med ulike egenskaper, og derved øke utnyttelsen av masser som i utgangspunktet ikke tilfredsstiller kvalitetskravene.

Den første tilnærmelsen i denne studien var å identifisere av kunnskapshull angående forholdet mellom lokal geologi og mekanisk ytelse (LA og MD) av tilslag. Med tanke på dette ble det utført state-of-the-art studier om geologisk påvirkning på egenskapene til tilslag. Det ble demonstrert at synergien av påvirkninger av forvitring på geologiske parametere (mineralogi, kornstørrelse og krystallstørrelse, kornform og porøsitet) og i hvilken grad de påvirker den generelle ytelsen, forblir viktige kriterier i materialvalg. Dette er relevant for gravemasser med varierende geologisk sammensetning hvor funnene i studien kan bidra til økt innsikt i hvordan mineralogien og teksturen påvirker egenskapene. Neste skritt I studien var å dokumentere den mekaniske stabiliteten til de resirkulerte gravemassene og vurdere mineralogiske og kjemiske påvirkninger. Tilnærmingen besto av blandingsteknikker, for eksempel blanding med andre materialer som en mekanisk stabiliseringsteknikk. De eksperimentelle metodene var LA og MD-tester og treaksialtester (RLTT). I hovedsak tilfredsstilte de resirkulerte gravemassene gjeldende krav for bære- og forsterkningslag, målt ved LA- og MD-verdier. Når sammensetningen inneholdt betydelige andeler av svake bergarter som fylitt, ville en maksimal innblandingsmengde på ≤ 40 % være akseptabelt. Funnene om den mineralogiske påvirkningen viste at fyllosilikater (mika og kloritt) hovedsakelig bidro til den lave

mekaniske ytelsen. I tillegg ble det vist at hvis gravemasser består av porøse materialer som mursteinrester, bør det gjøres en vurdering av innblandingsnivået.

Når det gjelder stivhets og deformasjonsegenskaper analysert i henhold til Hicks og Monismith's modell og Uzan's modell, ble det vist at resirkulerte gravemasser påvirket stivhetsutviklingen positivt sammenlignet med fyllittmaterialene. Det ble påvist høyere stivhetsrespons ved 25% substitusjon av resirkulerte gravemasser med fyllitt enn ved 50 % substitusjon. Derfor var ytelsen følsom overfor økt innhold av fyllitt. På den annen side så viste permanent deformasjonsadferd ingen betydelige variasjoner til tross for rapporterte verdier av graden av mobilisert friksjonsvinkel ρ(°) og inkrementell friksjonsvinkel φ(°), som beskriver henholdsvis mobilisert og maksimal skjærstyrke. Disse funnene gir verdifull informasjon til retningslinjer for å evaluere bæreevnen til vei bygget med resirkulerte materialer.

Site steg i denne studien var å evaluere ytelsen til resirkulerte tilslag fra betongslam ved bruk av Re-Con Zero tørrvasketeknologi (RCZ). RCZ tilslag ble blandet med gravemasser og resirkulert i våtprosess for å øke materialenes sirkularitet. Resultatene viste en generell trend med økt LA og MD-ytelse med økende RCZ innblanding. Resultatene fra syreløselig andel, viste at det resirkulerte tilslaget inneholdt sementpasta og at en andel av sementpastaen ble nedknust (< 1.6 mm) i LA testen. Dette antyder tilstedeværelsen av en godt herdet pasta. Innholdet av farlige stoffer, var generelt lavt og i samsvar med norske avfallsregler. I tillegg indikerer det lave Cr(VI) innholdet at det kan forventes lav utlekking av Cr ved karbonatisering og en reduksjon i pH under reell bruk av tilslaget.

Disse funnene bidrar til å maksimere bærekraftig bruk av gravemasser i Norge og kan hjelpe sluttbrukere med økt forståelse av håndteringsmetoder og bruk av resirkulert tilslag fra gravemasser.

# Publications

This thesis is based on papers published or submitted for publication in peer-reviewed journals.

**PAPER A**

**S. Adomako**, C. J. Engelsen, R. T. Thorstensen, and D. M. Barbieri, "Review of the Relationship between Aggregates Geology and Los Angeles and Micro-Deval Tests," *Bulletin of Engineering Geology and the Environment*, vol. (80), pp. 1963-1980, 2021. doi:10.1007/s10064-020-02097-y

**PAPER B**

**S. Adomako**, C. J. Engelsen, T. Danner, R. T. Thorstensen, and D. M. Barbieri, "Recycled aggregates derived from excavation materials-Mechanical performance and identification of weak minerals,"*Bulletin of Engineering Geology and the Environment*, vol. (81), no. 8, pp. 1-12, 2022. doi:10.1007/s10064-022-02817-6

**PAPER C**

**S. Adomako**, C. J. Engelsen, R. T. Thorstensen, and D. M. Barbieri, "Repeated Load Triaxial Testing of Recycled Excavation Materials Blended with Recycled Phyllite Materials," *Materials*, vol. (15), no. 2, pp. 621, 2022. doi: 10.3390/ma15020621

**PAPER D**

**S. Adomako**, C. J. Engelsen, L.T. Døssland, T. Danner, and R. T. Thorstensen "Technical and environmental properties of recycled aggregates produced from concrete sludge and excavation materials," *Case Studies in Construction Materials*, vol. (19), 2023. doi:10.1016/j.cscm.2023.e02498

The following papers were published during the PhD studies but were not included in this thesis.

**PAPER E**

**S. Adomako**, R. T. Thorstensen, N. Akhtar, M, Norby, C.J. Engelsen, T. Danner, and D.M. Barbieri, "Evaluating the Effect of Mineralogy and Mechanical Stability of Recycled Excavation Materials by Los Angeles and Micro-Deval Test, "*Eleventh International Conference on the Bearing Capacity of Roads, Railways and Airfields,* vol. (1), pp. 131-138, 2021. doi: 10.1201/9781003222880-13

**PAPER F**

**S. Adomako,** A. Heimdal, and R. T. Thorstensen, "From Waste to Resource– Utilising Residue from Ready-Made Concrete as New Aggregate, "*Nordic Concrete Research*, vol. (64), pp. 1- 10, 2021. doi:10.2478/ncr-2021-0010

# Contents

Preface ..... vi
Acknowledgments ..... viii
Abstract ..... x
Sammendrag ..... xii
Publications ..... xiv
Abbreviations ..... xvii
1. Introduction ..... 1
   1.1 Excavation materials-Overview ..... 1
   1.2 Factors affecting recycling of excavation materials ..... 2
   1.3 Selected approach for mechanical characterization ..... 3
   1.4 Research objective ..... 8
2. Geological influences on the performance of mixed recycled aggregates ..... 9
   2.1 Performance related to mineralogy ..... 9
   2.2 Performance related to textural composition ..... 11
3. Fragmentation and wear resistance of recycled mixed materials ..... 13
   3.1 Performance related to changes in the source ..... 13
   3.2 Mixing of materials ..... 13
   3.3 Hard and weak mineral constituents in mixed fractions ..... 16
4. Mechanical properties of recycled mixed materials ..... 19
   4.1 Resilient modulus ..... 19
   4.2 Permanent deformation ..... 22
   4.3 Discussion ..... 24
5. Developing recycled aggregates with Re-Con Zero Technology ..... 26
   5.1 Dry washing with two-component admixture ..... 26
   5.2 Physical and geometric properties ..... 27
   5.3 Mechanical characterization by Los Angeles and micro-Deval test ..... 28
   5.4 Solubility related to paste content in recycled aggregates ..... 29
   5.5 Environmental properties of recycled aggregates from concrete waste . 30
6. Conclusions and future work ..... 32
   6.1 Main conclusions ..... 32
   6.2 Limitations and future work ..... 34
Bibliography ..... 35
Appended papers ..... 48

# Abbreviations

| | |
|---|---|
| COPC | Chemical Species of Potential Concern |
| ELGIP | European Large Geotechnical Institute Platform |
| EM | Excavation material |
| FI | Flakiness Index |
| LA | Los Angeles |
| Lim | Limestone |
| MD | Micro-Deval |
| NPRA | Norwegian Public Roads Administration |
| PD | Permanent Deformation |
| PGr | Porphyritic Granite |
| PSD | Particle-Size Distribution |
| RCA | Recycled Concrete Aggregate |
| RCZ | Recycled Aggregate from Concrete Sludge by Re-Con Zero Technology |
| RCZ-F | Feedstock sampled at Velde |
| RCZ-$F_0$ | Feedstock sampled at Ølen Betong |
| REM | Recycled Excavation Material |
| RESGRAM | Recycled Aggregates from Excavation Masses |
| RLTT | Repeated Load Triaxial Test |
| RPM | Recycled Phyllite Material |
| UGM | Unbound Granular Material |
| XRD | X-Ray Diffraction |

# 1. Introduction

## 1.1 Excavation materials-Overview

Surface and underground construction activities lead to significant removal of earth materials and are key drivers of environmental pollution [1-4]. The primary components of these masses include virgin soil and rocks; however, other wastes, such as asphalt, wood, volatile solids, and concrete rubble, may also be present [3]. In Europe, excavation materials are regarded as one of the largest sources of waste (by volume) and are reported to be five times the amount of household waste [5].

For example, considering only excavated soil, data from the European Large Geotechnical Institute Platform (ELGIP) suggest that France is one of the largest producers with an annual production of approximately 7-10 million tons [6]. Generally, the disparity in the amount of excavation materials generated from one country to another reflects the action plan-(s) adopted to manage them. Therefore, it is worth noting that while some countries have implemented specific legislative guidelines to encourage recycling practices and the use of high-quality excavation materials [7], others have not fully embraced the potential sustainability benefits and instead primarily utilize these materials as coverings. It is important to consider that this may be influenced by economic structures and differing sustainability policies.

The newly launched strategy for a sustainable built environment in the European Union encompasses the fundamental objective to promoting safe, sustainable, and circular use of excavation masses [8]. This development may help member states formulate a solid framework to ensure harmony in the tracing, recycling, and utilization of surplus excavation masses within the circular economy.

In Norway, the national narrative on becoming environmentally friendly includes the increased promotion of the use surplus materials from excavation operations based on quality and technical performance [6]. Considering this, national projects, such as *Kortreist stein* (short-traveled aggregates) and *RESGRAM* (recycled aggregates from excavation masses), were designed to develop technological processing solutions for the sustainable use of high-quality excavation and tunnel

materials and increase competitiveness among local contractors and practitioners. This increased the understanding of handling techniques, practices, and the use of these materials in concrete and road pavement and served as a demonstration of the commitment to leverage key resources in the country. Conceptually, these developments will contribute to achieving the 2030 targets set by the United Nations Sustainable Development Goals. Goal number 11.6 under sustainable cities and communities is targeted toward the reduction of the adverse per capita environmental impact of cities, including paying special attention to air quality, and municipal and other waste management. In addition, goal number 12.2 under the caption of natural resources seeks to achieve sustainable management and efficient use of natural resources [9].

## 1.2 Factors affecting recycling of excavation materials

While the management of excavation materials varies among construction activities, several factors such as, geology [4, 10, 11], legislative and regulatory policies [6, 12], and management (organizational and logistics) [6] impede the use of these materials. Geological complexity is of particular interest because it influences (1) the performance of recycled materials, (2) decisions regarding the need to formulate standard frameworks to convert and use these materials for construction, and (3) the economic and environmental implications if the materials are landfilled because of low-quality performance. Therefore, advances toward their use in construction have been slow in various parts of the world.

The lack of mandatory regulations and supervision regarding legislative policies is a significant issue, as many countries have not yet implemented them. As a result, the responsibility of determining the fate of these materials is left solely in the hands of developers and contractors. For example, in New York City, an estimated annual cost of 60 million USD is incurred because of non-existent policies for complete retention and on-site use [13]. In addition, other scenarios that require permit applications to perform risk assessments do not have a harmonized application procedure [6].

Some studies used material flow analysis to design the life cycle chain of materials, including recycling and disposal [14, 15]. A specific focus on the flow

of input and output is regarded as an essential management design, given its consistency with the mass balance concept [16]. To manage construction waste, some researchers have used this model to project increased generation in the future [17-21]. This means that the descriptive flow of excavation materials from construction operations necessitates the expansion of waste management or treatment capacities and increases the utilization options if properties and suitability for infrastructure are established.

This study focuses on this concept by evaluating the technical performance of recycled aggregates derived from excavation materials and other sources. In addition, this study investigated the chemical and mineralogical influences based on local geology and their effect on performance. Using this approach, this study lays the foundation for describing the influential parameters and how materials may be mixed to establish stabilized results from which end -users may refer during the selection process. This approach leads to a more sustainable use of resources because a large volume of excavation materials may be used.

## 1.3 Selected approach for mechanical characterization

The selection and application of materials in unbound construction primarily depend on their mechanical and geometric properties. Unbound granular materials (UGMs) provide a sufficient structural response to traffic loads in flexible pavements. The feasible application of excavation materials for unbound construction requires that these materials pass criteria assessments and withstand common problems associated with unbound construction such as, frost-heave damage, fatigue cracking, rutting, and depressions [22, 23].

In Norway, the road construction guide describes the Los Angeles test (LA), micro-Deval test (MD), and other geometric properties, including flakiness index (FI) and particle-size distribution (PSD), which constitute the criteria for the performance assessment of UGM. **Table 1** lists the quality requirements for base layer materials where the mechanical strength is characterized by the assessment of fragmentation and wear resistance. Furthermore, function-based repeated load triaxial tests (RLTTs) are beneficial for investigating the deformation (stiffness and permanent strain) properties of unbound aggregates under rapid repeated loading [24-

36]. Considering this, the general focus on characterizing the strength of the UGM may be linked to its impact on seasonal climatic conditions (moisture, frost, and temperature) and stress distribution [37], which can only be achieved in real full -scale applications.

One important observation is that while the Norwegian road criteria recommend the application of recycled aggregates, the use of excavation materials (recycled) is only allowed in the subbase, compared to recycled crushed concrete, which also constitutes the description of materials and is applicable in both the base and subbase layers. Furthermore, the traffic groups in the regulation are categorized from low to heavy traffic, following the orders A, B, C, D, E, and F (see **Table 2** for details). Traffic group A was designated as low -traffic roads, sidewalks, bicycle lanes, and parking lots. Traffic groups E and F were designated as highways. The LA and MD criteria for recycled materials applied in traffic group A are $\leq 40$ and $\leq 25$, respectively. In traffic groups B to F, the specified criteria for LA and MD for recycled materials are $\leq 35$ and $\leq 20$. Recycled aggregates from excavation materials and other construction work (denoted as Bm in the regulations) are recommended in traffic groups A to D as recycled crushed concrete (Gjb), as shown in **Table 2**. Crushed rock was the only material allowed in traffic groups A to F.

**Table 1** Material properties and quality requirements for (Gk) crushed gravel, (Fk) crushed rock, and (Gjb) crushed concrete in N200 (2022 edition) [38].

| **Base layer requirement** | |
|---|---|
| **Material properties** | **Quality requirement** |
| **Mechanical strength** | |
| Los Angeles value | ≤ 35 |
| Micro-Deval value | ≤ 15 |
| **Humus content** | |
| Humus content for crushed gravel | < 1% |
| **Geometrical properties** | |
| Flakiness index | ≤ 25 |
| **Grain grading** | |
| Maximum fines content (< 63 μm) | |
| 0/22 (Gk &Fk)<br>0/32 (Gk, Fk & Gjb) | ≤ 7% |
| 0/45 (Gk, Fk & Gjb) | ≤ 5% |
| 0/63 (Fk & Gjb) | ≤ 3% |

**Table 2** Traffic groups for base and subbase layers in relation to the number of equivalent 10 tons axles.

| **Traffic groups** | **Equivalent of 10 tonnes axles (N)** | **Traffic group base layer** | | | **Traffic group subbase** | |
|---|---|---|---|---|---|---|
| | | **Type of material** | **Upper support base layer** | **Lower support base layer** | **Type of material** | **Subbase** |
| A | < 500 000 | Fk | A | A-C | G | A |
| B | 500 000 – 1 000 000 | Ag | A-F | A-F | Gk | A-C |
| C | 1 000 000 – 2 000 000 | Ap | A-C | A-F | Fk | A-F |
| D | 2 000 000 – 3 500 000 | Gja | A-C | A-D | Gjb | A-D |
| E | 3 500 000 – 10 000 000 | Ak | A-B | A-D | Bm | A-D |
| F | > 10 000 000 | | | | | |

Ag represents asphalt gravel

Ap and Gja represent asphalt crushed stone and recycled crushed asphalt, respectively
Ak represents crushed asphalt
G represents gravel, and Gjb and Bm are crushed concrete and excavation material
N and traffic groups were determined based on the average number of heavy vehicles (ÅDTT).

In view of quality improvement, a new study proposing composition criteria and requirements for recycled aggregates applied in road construction in Norway is presented in **Table 3.** This study highlights four classifications based on differences in the source material. These included crushed concrete (Gjb I), excavation materials (Gjn I), mixed proportions of crushed concrete and excavation materials (Gjbn I), and a concrete and brick mixture (Gjb II). Gjb I and Gjn I are characterized by high MD coefficients ≤ 15%, which indicate potential applications in roads with high mean traffic roads, and currently the Norwegian Roads Public Administration has allowed Gjb I and Gjn I (i.e., Bm) in traffic group D.

**Table 3** Proposed classes for N200 in composition and requirements for recycled materials [39]

| **Material and test classification** | **Material composition** | | | |
|---|---|---|---|---|
| | **Gjb I**<br>$Rc_{90}$, $Rb_{10}$-, $Ra_{5}$-, $Rg_{2}$-, $X_{1}$-, $FL_{5}$- | **Gjn I**<br>$Ru_{90}$, $Rc_{5}$-, $Rb_{5}$-, $Ra_{5}$-, $Rg_{2}$-, $X_{1}$-, $FL_{5}$- | **Gjbn I**<br>$Ru_{50}$, $Rc_{50}$-, $Rb_{10}$-, $Ra_{5}$-, $Rg_{2}$-, $X_{1}$-, $FL_{5}$- | **Gjb II**<br>$Rcub_{90}$, $Rb_{40}$-, $Ra_{5}$-, $Rg_{2}$-, $X_{2}$-, $FL_{5}$- |
| Rc | ≥ 90 % | < 10 % | < 50 % | - |
| Ru | - | ≥ 90 % | ≥ 50 % | - |
| Rb | ≤ 10 % | < 5 % | < 10 % | ≤ 40 % |
| Rc + Ru + Rb | - | - | - | ≥ 90 % |
| Ra | ≤ 5 % | ≤ 5 % | ≤ 5 % | ≤ 5 % |
| Rg | ≤ 2 % | ≤ 2 % | ≤ 2 % | ≤ 2 % |
| X | ≤ 1 % | ≤ 1 % | ≤ 1 % | ≤ 2 % |
| FL | ≤ 5 $cm^3/kg$ | ≤ 5 $cm^3/kg$ | ≤ 5 $cm^3/kg$ | ≤ 5 $cm^3/kg$ |
| Oven-dried density | ≥ 2000 $cm^3/kg$ | ≥ 2100 $cm^3/kg$ | ≥ 1800 $cm^3/kg$ | ≥ 1500 $cm^3/kg$ |
| Saturated and surface-dried density | ≥ 2100 $cm^3/kg$ | ≥ 2200 $cm^3/kg$ | ≥ 2000 $cm^3/kg$ | ≥ 1800 $cm^3/kg$ |
| Water Absorption | < 10 % | < 5 % | < 10 % | < 20 % |
| LA | ≤ 35 % | ≤ 35 % | ≤ 35 % | ≤ 40 % |
| MD | ≤ 15 % | ≤ 15 % | ≤ 20 % | ≤ 25 % |

Rc, concrete, concrete products, mortar, and concrete masonry units

Ru, unbound aggregate, natural stone, hydraulically bound aggregate
Rb, clay masonry units (i.e. bricks and tiles), calcium silicate masonry units, aerated non -floating concrete
Ra, bituminous materials
Rg, glass
X, cohesive (i.e. clay and soil) miscellaneous: metals (ferrous and non-ferrous), non -floating wood, plastic and rubber, and gypsum plaster
FL, floating material in volume

The LA test is one of the fundamental tests used to investigate aggregate resistance to fragmentation or crushing impact. Developed in the 1920s by the Municipal Laboratory of Los Angeles [40], this test has gained wide acceptance and is well established in several standards worldwide. The test is performed on specific aggregate gradations based on the application purpose (e.g., road or railway ballast) and in a dry state. In the 1950s, the Norwegian Public Roads Administration (NPRA) first used the test to investigate ballast materials [41]. EN-1097-2 is the European standard, and AASHTO T-96 (American Association of State Highway and Transportation Officials) and ASTM-C131 (American Society for Testing and Materials) are the North American test procedure standards. An example of the maximum LA values reported for different road design codes for various applications are presented in **Paper A.**

The MD test was developed in the 1960s in France and was used to investigate the wear resistance of rock aggregates [42]. Some similarities exist between MD and LA, such as the size range of the test sample. MD is performed under moisturized conditions. Changes in the form, texture, and angularity commonly occur because of the wear of mineral components in traffic; hence, the MD test best describes the wear resistance of aggregates under these conditions [43]. Some authors have mentioned that compared to LA, the MD test correlates with the conditions that occur in the field [44-46]. Applicable standards, denoted as ASTM-D6928, AASHTO T327, and EN-1097-1, specify the MD test procedures in North America and Europe, and an example of the maximum MD values for different applications is presented in **Paper A**.

## 1.4 Research objective

The main research objective of this thesis is to demonstrate how final recycled aggregates from excavation masses and other sources can be intermixed and used in unbound applications, and in quantities higher than current production levels. A comprehensive multidisciplinary approach is used to characterise the properties from a physical, mechanical, and geochemical perspective. The main objective was further divided into specific objectives which have been addressed in the four journal papers included in the thesis:

- The influence of geology on the mechanical performance of rock aggregates **(Paper A**). This essentially compensates for the global synthesis of geological influences, which may be suitable for end -users during material selection and mechanical characterization.
- The mechanical performance of excavation materials mixed with other rock materials and the effects of intrinsic geological properties (mineralogy and chemical composition) **(Paper B and Paper C)**. This involved investigating how changes in the source affect the overall performance by establishing the technical performance of mixed materials and illustrating the tolerable amount of foreign rock materials that may be substituted.
- The performance of final recycled aggregates from concrete sludge using the Re -Con Zero dry washing technology and applied as feedstock in wet recycling excavation materials **(Paper D)**. The goal was to investigate the technical performance of recycled aggregates from these sources in separate and mixed conditions and identify the environmental properties with respect to chemical constituents by comparing them with Norwegian waste regulations. This approach can contribute to the sustainable use of recycled materials.

# 2. Geological influences on the performance of mixed recycled aggregates

To select high -quality rock materials, it is desirable to have some knowledge of local geological conditions which entails the degree of alteration in mineral features and textural characteristics by weathering and hydrothermal action. Such a preliminary assessment could lead to general knowledge for improving the properties, if required [47]. The influence of geology on rock performance has been extensively studied by various researchers. Some studies date back to the 1970s and the 1980s [48, 49]. Given that the scope of geological factors is wide and related investigations of their influences differ, it is essential to create a global synthesis of influential factors, recognizing that rocks of the same group could have different mineralogical and textural properties [47, 50]. In the illustration of the use of recycled materials from different sources for the same purpose as conventional rocks, this is particularly important given the scope of the local geology. Considering this, **Paper A** presents a state-of-the-art review of the influence of geological properties, (i.e., mineralogy, grain and crystal size, grain shape, and porosity), on the LA and MD performances of rock aggregates.

## 2.1 Performance related to mineralogy

In the case of mineralogy, the distinct roles of primary and secondary minerals were discussed. In short, primary minerals are formed during the solidification of magma; hence, they are the main minerals that geologists use to determine the rock type. Secondary minerals are formed by the alteration of primary minerals through weathering or hydrothermal actions [51]. The inherent characteristics of any mineral in the aforementioned groups provide information on its performance behavior. The findings of this study show that the fundamental roles of primary minerals, such as quartz, feldspar, and mica are intrinsically linked to LA and MD performances. Regarding, the degree of influence, emphasis has been placed on the dominance of quartz and the proportionality of quartz and feldspar [52-55]. These two minerals had hardness values of 7 and 6, respectively, based on the

scratching resistance on the Mohs mineral hardness scale. Nonetheless, one observation was that the role of quartz or both minerals in determining the strength performance did not always follow a consistent pattern [56]. Other studies that employed different test methods have also reported similar narratives, although these were less common. A study that explored the influence of quartz or the quartz-feldspar ratio on the compressive strength of granite rocks concluded that there is a tendency for strength to decrease as the amount of quartz decreases [57]. Another study that investigated the influence of mineralogy found that compared to quartz, K-feldspar had no relationship with compressive strength [58]. It has been mentioned regarding both minerals that the absence of a cleavage structure in quartz contributes to increased strength, and in feldspar, the development of micro -fissures and cleavage patterns generally decreases the compressive strength [59]. Similarly, negative correlations between quartz and K-feldspar and the performance of igneous rocks have been reported [60]. In the same study, strong correlations were observed between plagioclase and igneous rocks. For sedimentary rocks, an initial increase in strength was observed, which later decreased as the content of plagioclase increased. Further reduction in strength with increasing quartz content and little correlation with the content of K-feldspar were also reported [60]. These findings have resulted in attempts to distinguish between the different roles of quartz and feldspar minerals in assessing mechanical performance. One study reported different encounters in relation to the failure mechanism of rocks and concluded that K-feldspar influences the tensile strength, whereas quartz has a profound effect on the compressive strength [61]. This justifies the importance of studying other textural characteristics to gain a broad understanding of the behavior and influence of local geology.

This study also discusses the issue of disposition or mineral alignment classified by crystal size and features, as essential components in mineralogy. For example, rocks characterized by a degree of foliation develop cleavage patterns that promote breaks along weak parts. These developments occur during the alteration process, including changes into primary minerals due to chemical weathering or hydrothermal action. Other specifically altered geological characteristics resulted in the development of secondary minerals.

Further discussions on the effects of secondary and accessory minerals also showed that it is only appropriate to reach conclusions based on quantity. This adds to the reported findings that $\leq 20\%$ of mica does not significantly affect the strength

performance, and Figure 3 in **Paper A** shows a specific pattern of reported LA performance of rocks composed of less amount of mica related minerals (i.e., biotite and muscovite). Similar developments are observed in **Paper B**. In this case, minerals constituted by a low amount of secondary but high primary content may be described by the ratio of secondary to primary minerals [50]. Although the influence of mica is generally known, it has been claimed that the mineral has no direct effect on strength properties particularly LA. However, when the mineral forms a plane foliation, it creates mechanically weak discontinuities and leads to fracture propagation along the path of orientation [62]. This may explain why one study referred to the distribution and structural formation of grain boundaries as factors in decisions regarding its effect [63].

Other findings reported in this study include the impact of the test methods (i.e., LA and MD), on the degree of crushing and wear of the mineral components. This is particularly essential, given that minerals behave differently in different test methods, as previously mentioned. Simple correlation coefficients have mainly been used to describe the relationships among different rock types [50, 64-66].

## 2.2 Performance related to textural composition

Compositional textures in grains and crystal sizes with varying dispositions and layer arrangements contribute to resistance to crushing and wear impact. Generally, the micro -crack development that appears in the intragranular region of the texture can further propagate into major cracks and lead to disintegration. Thus, typical grain sizes forming fine -to -medium grained textural feature were $< 1$ mm, whereas rocks composed of multiple textural features were characterized by weak boundary interlocks, which was also reflected in the performance. In a model-based investigation, mineral grains were found to significantly affect crack propagation paths [67]. This description shows the orientation of the matrix and fits the description of the dynamics of the transformation that may have occurred during development. Compared to mineralogy, where rocks (granite into granite gneiss) can have similar mineralogical components after transformation, the structure of the textural orientation (i.e., planer matrix) undergo significant changes.

Although good estimates are derived in terms of describing the grain and crystal sizes, quantitative analysis of the dispersion effect of these parameters may be challenging. In this context, the texture coefficient principle fit to describe the relationship between textural characteristics and the mechanical performance [68, 69]. Nevertheless, the texture coefficient equation does not account for other important parameters, such as weathering, and altered minerals, matrix type, and mineralogical composition [69].

At the macro -structural scale, the morphological shape descriptor (i.e., grain shape) was found to be the most important parameter. The shape descriptor was classified by three main features (form, surface texture, and angularity), showing the independent effects to these parameters on the behavior under crushing or wear impact. In this case, it is essential to emphasize that both LA and MD play critical roles, given the relationship between changes into particle morphology and test duration. One conclusion is that the apex region of rocks defined by angular features is more likely to experience rapid degradation than those defined by the form and surface texture. Similarly, in a recent study that explored the characteristics of grains between fresh and used railway ballast, the authors demonstrated that particles of a more angular shape have asperities (roughness) that are more prone to damage than particles characterized by a less angular shape [70]. These findings may be related to the effect of elongated and flaky particles, which confirms the reasons for considering rocks with a low flakiness index for roads, and concrete applications [71-73]. Another noteworthy observation is that after 90 minutes of the MD test, the grain breakages did not appear to significantly change to the grain size distribution [70]. Such a response shows the wear resistance behavior of the rocks. Generally, unlike the direct crushing impact of LA, which leads to particle fragments, the wear impact of MD leaves distinct visible features on any of the scale dependencies (i.e., form, angularity, or surface texture). Both methods contribute to mass loss and affect the LA and MD strengths.

This study created a synthesis of the most essential geological features and their impact on the mechanical performance, highlighting the importance of understanding these characteristics in detail particularly for excavation materials which is diverse in composition and performance. In addition, the study highlighted that the assessment of the impact of local geology should be based on the global nature of geological features and not just a few identified textural parameters.

# 3. Fragmentation and wear resistance of recycled mixed materials

## 3.1 Performance related to changes in the source

As previously mentioned, different sources of materials in recycled excavation materials account for variations in the strength performance [34, 74]. This limits extended use of the final product. Specific demonstrations of mixing materials with varying performance in quantities suitable for achieving higher strength are optimal, given that most of these mixtures are well suited for road and concrete applications [28, 32, 34, 75, 76]. This approach contributes to the development of a control framework and tolerance values crucial for selection.

In this study, a demonstration of mixed criteria of recycled excavation material (REM) with recycled phyllite material (RPM) and other materials in varying quantities were demonstrated. The mechanical performance of the mixtures was investigated using the LA and MD tests. These tests constitute the standard procedure for investigating the materials used in road construction and concrete production. The LA test assesses the degree of resistance to fragmentation or crushing, whereas the MD test assesses the degree of resistance to wear. Detailed test methods are described in both **Papers A** and **B**, together with diagrams illustrating the test set -up.

## 3.2 Mixing of materials

The mixing part consisted of selected materials, such as RPM, porphyritic granite (PGr), limestone (Lim) and REM. Therefore, RPM was mixed with REM and PGr, as shown in **Table 4**. Considering that REM may be used in unbound applications, limiting the RPM is essential. Hence, in this context, mixing RPM, which is characterized by phyllosilicates (mica and chlorite) with REM or other materials helped establish a mix ratio suitable for satisfactory performance.

The fractions indicated by < 1.6 mm and > 1.6 mm were collected for analysis of mineralogy. The minerals found in the pulverized part provided good information on the behavior of the mineral features in relation to the impact of the test method and how this influenced the global performance of the mixtures. Similarly, limestone (Lim) was mixed with REM to investigate the effect of calcium carbonate minerals (CaCO3).

**Table 4** Mixing level of RPM and PGr in REM and fractions for X-ray diffraction (XRD) analysis

| Sample name | Mix proportion RPM (%) | The fraction used for XRD |
|---|---|---|
| RPM(4/16) | 100 | 4/16 mm |
| RPM100 | 100 | <1.6 mm after LA |
| RPM100(>1.6) | 100 | >1.6 mm after LA |
| RPM100 MD | 100 | <1.6 mm after MD |
| PGr100 | 100 | <1.6 mm after LA |
| RPM80-REM20 | 80 | <1.6 mm after LA |
| RPM60-REM40 | 60 | <1.6 mm after LA |
| RPM40-REM60 | 40 | <1.6 mm after LA |
| RPM20-REM80 | 20 | <1.6 mm after LA |
| RPM80-PGr20 | 80 | <1.6 mm after LA |
| RPM60-PGr40 | 60 | <1.6 mm after LA |
| RPM40-PGr60 | 40 | <1.6 mm after LA |
| RPM20-PGr80 | 20 | <1.6 mm after LA |
| REM(4/16) | 0 | 4/16 mm |
| REM100 | 0 | <1.6 mm after LA |
| REM100(>1.6) | 0 | >1.6 mm after LA |
| REM100 MD | 0 | <1.6 mm after MD |

The LA and MD performances of the mixtures in **Table 4** are shown in **Figure 1**.These values were compared with the criteria for the base and subbase layers in Norway. The LA values for REM, RPM and Lim in the pure state were 28%, 26%, and 33%, respectively, whereas the MD values were 6%, 26% and 29%, respectively. In addition, the LA and MD of PGr have been reported to be 18% and 9%, respectively. From this standpoint, both RPM and REM showed similar LA performances; however, the MD varied considerably. The MDs of both RPM and Lim were the critical parameters since the values did not meet the $\leq$ 15-20% limit value established in the Norwegian Road Construction Guidelines [38].

A previous study reported a similar LA value of 25% for quartz phyllite obtained from tunnel excavation [77].

In another study, the LA of phyllite was 17%, indicating a good resistance to fragmentation, and compliance with most LA requirements for aggregates [78]. Generally, the performance of phyllites varies from low to moderate depending on the development of schistosity [79].

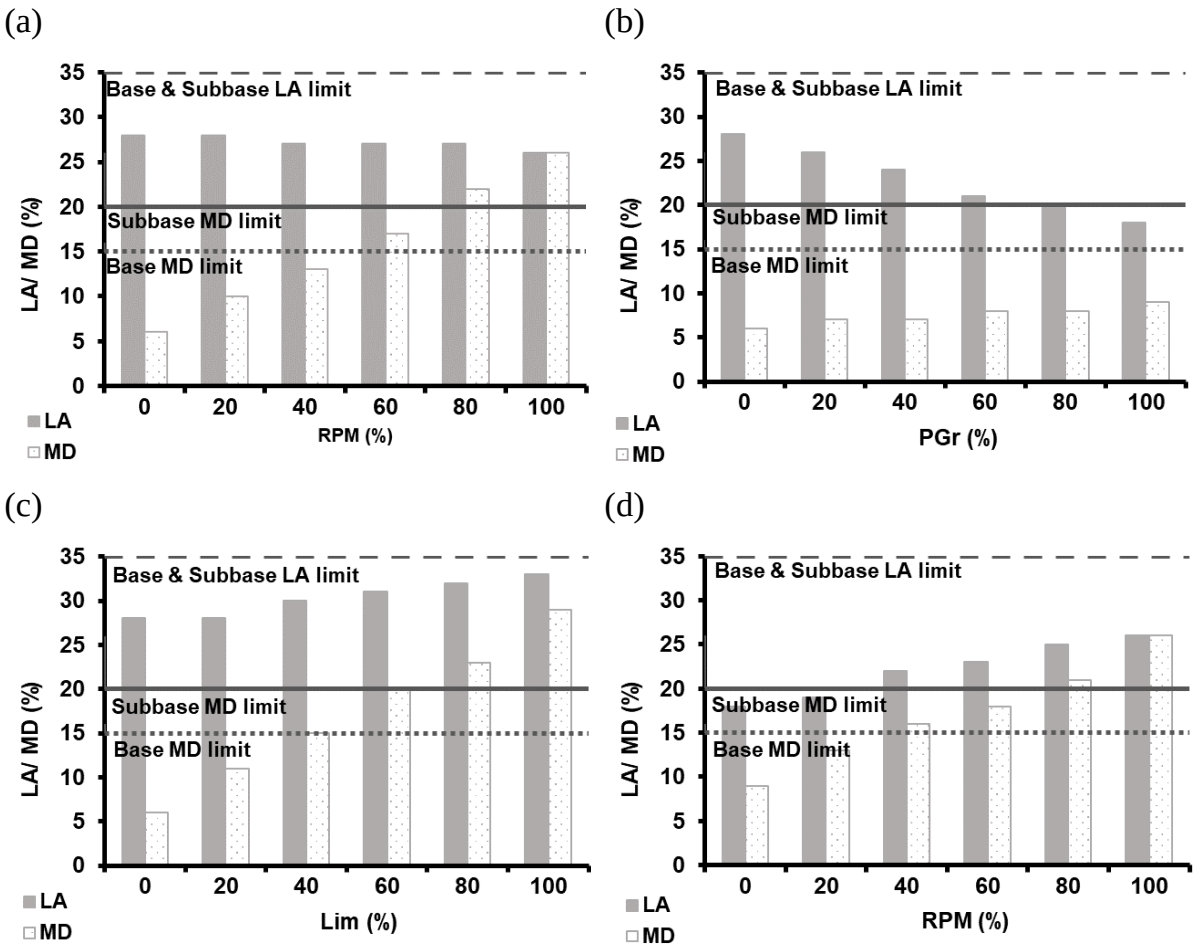


**Figure 1** LA and MD performance of a) RPM premixed with REM, b) PGr premixed with REM, c) Lim premixed with REM, and d) RPM premixed with PGr.

At the mixing level of RPM with REM, a 40% mix ratio of RPM could be tolerated in REM to achieve satisfactory MD performance (**Figure 1a**). Thus, the mixing approach was effective in maximizing the use of the weakest material, -RPM. Studies that have reported the performance of materials obtained from excavation activities in most cases have shown considerable differences in LA and

MD [34, 56, 80]. In one specific case, linear trend distributions were established to describe the relationship between hard and weak excavated rocks, which had been mixed in different quantities [34]. The resulting distribution highlighted low performances with an increased content of weak rocks. In **Figure 1b**, PGr was mixed with REM and the performance showed the competitiveness of REM against a hard rock material such as PGr, since no significant variation in the MD results was shown, compared with the LA. A previous study reported the LA performance of five PGr rocks with different textural characteristics within the range of 25-28% [54], which is similar to the LA of REM obtained in this study. At this point, REM has a competitive edge given its sustainability (i.e., economic, and environmental benefits).

The other mixture produced in this study comprised of limestone and REM ( **Figure 1c**). It was convenient to introduce Lim in the mix given that excavation materials collected from the field may be composed of carbonated concrete products. Lim contains a significant amount of calcium carbonate ($CaCO_3$), and in this context, the effect of $CaCO_3$ on performance was assessed. Based on the results shown in **Figure 1c**, the MD value is significantly high, indicating a lower resistance to wear by Lim compared to REM. Considering this, maximum premixed level of the two materials indicated that as high as $\leq 40\%$ of limestone was appropriate to comply with MD limit value. This indicates that the crushed concrete materials intermixed in REM comply with the MD limits because carbonated crushed concrete does not contain high $CaCO_3$ equivalent in a 40% mixture with limestone. **Figure 1d** shows the LA and MD performances of RPM and PGr. The results showed that MD is a critical parameter in RPM, and the maximum RPM content must be limited to approximately 20-30%.

## 3.3 Hard and weak mineral constituents in mixed fractions

The diffractograms from the X-ray diffraction (XRD) analysis on fine fractions < 1.6 mm and > 1.6 mm after LA and MD following the outline in **Table 4** are shown in **Figure 2**. The diffractograms for the RPM showed biotite, muscovite, microcline/orthoclase, anorthite, and chlorite as the main minerals. The intense peaks of mica and chlorite observed in RPM were expected owing to the geological

nature of the material. In contrast, REM showed quartz, clinochlore, microcline/orthoclase, and plagioclase as dominant minerals and a lower quantity of mica and chlorite. The diffractograms of the PGr samples were similar to those of the REM, except that a distinct mica peak was observed.

For the RPM-REM mixtures, the increased peaks of mica and chlorite matched the increased amounts of RPM. Regarding mechanical strength, both minerals clearly showed less resistance to LA crushing. Similarly, the RPM-PGr mixtures showed weak mineral accumulation in the pulverized fraction. The general influence of weak minerals, such as mica and chlorite, on LA and MD performance of rocks was extensively demonstrated in **Paper A**. Conclusions reached in this context state that the extent of effect by phyllosilicates depended on the amount present (e.g., $\leq 20\%$), structural formation, and distribution of the grain boundaries [47, 80].

This study further highlighted the relationship between the test methods and minerals in the REM and RPM, as shown in Figure 10 of **Paper B**. Compared with LA, increased peaks associated with the wear of mica and chlorite in the MD test were observed. A probable explanation is that (a) the wear nature of the test method and (b) the moisturized condition of the test enhanced the wear effect. Accordingly, the degree of wear in MD tests depends on the mineral contents [81]. It is important to emphasize that the conclusions reached in this case has been found by some authors regarding the relationship between MD and minerals found in other rock sources [66, 74, 80].

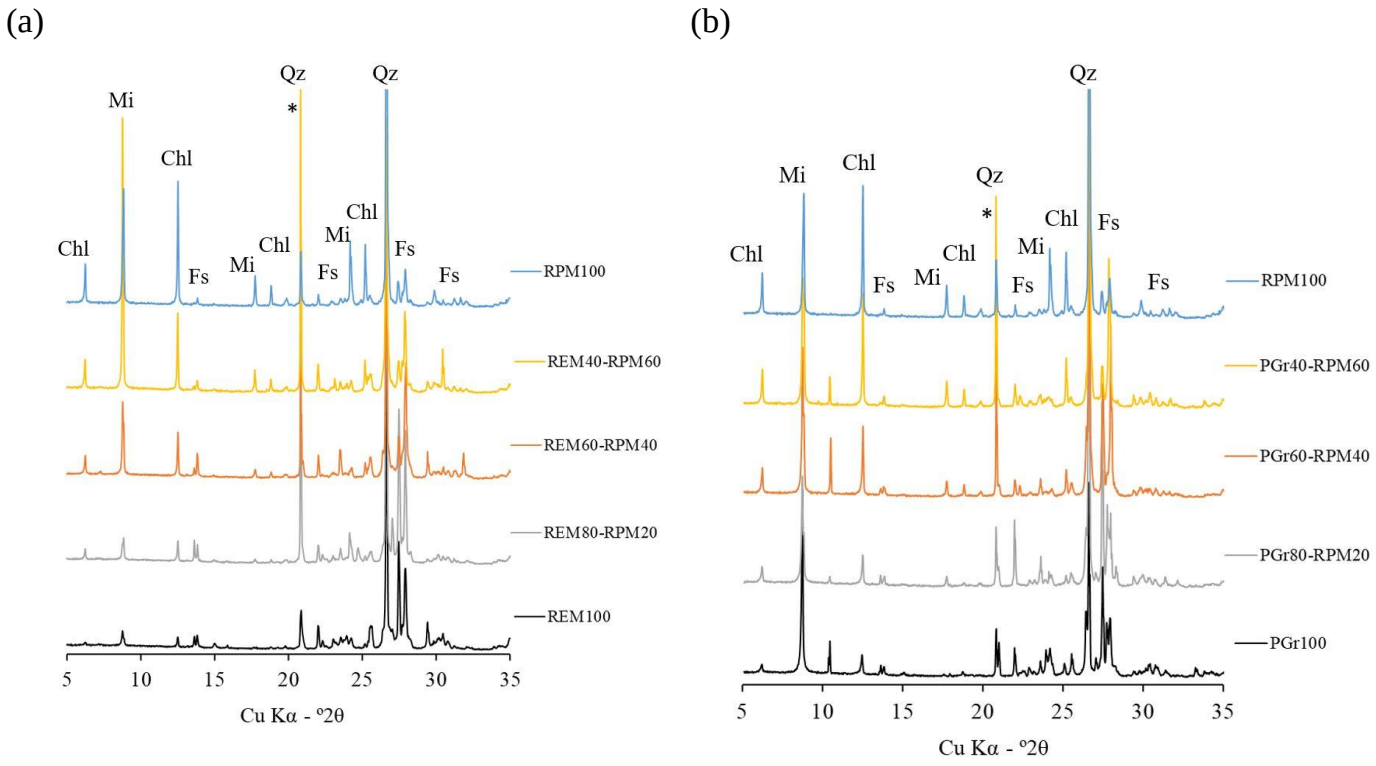


**Figure 2** X-ray diffraction results showing mineral accumulation and changes in the fine fraction (<1.6 mm) after the LA test of (a) RPM-REM and (b) RPM-PGr blends, marked with the prominent peaks of the main mineral phases (Chl = chlorite, Mi = mica, Fs = feldspar, and Qz = quartz).* indicates an artefact (“ spottiness”) caused by abnormal high intensity of a large grain in diffraction position (here quartz). Peaks around 11º 2θ observed in some diffractograms might be associated with cyclosilicate minerals (e.g., cordierite/indialite).

# 4. Mechanical properties of recycled mixed materials

## 4.1 Resilient modulus

The resilient modulus $M_R$ parameter provides information on the material stiffness at different load levels. The $M_R$ is expressed as:

$$M_R = \frac{\sigma_d}{\varepsilon_r}, \quad \text{(Eq. 1)}$$

where $\sigma_d$ is the applied deviatoric stress given as the difference between the repeated axial stress $\sigma_1$and confining pressure $\sigma_3$, and $\varepsilon_r$ is the resilient axial strain [36, 82]. The stress state, including the confining pressure acting in all the directions, is as shown in **Figure 3**. The application of the deviatoric stress followed a sinusoidal pattern, which increased stepwise at each stress state exerted by the confining pressure.

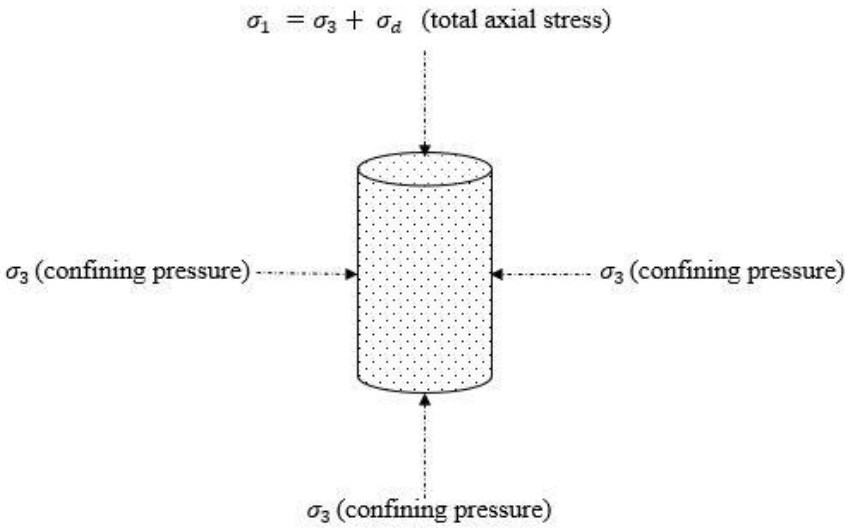


**Figure 3** Principal stresses in resilient modulus.

In principle, both the resilient and permanent strain response under a moving wheel load are described as the (a) recovery to the original position after the

load is removed and (b) gradual accumulation to deformation, respectively. In an attempt to establish a performance-based response for the behavior of REM and RPM blends, RLTT was performed in **Paper C**. The objective is to determine the effect of the RPM on the deformation behavior of the blends.

The k-θ model by Hicks and Monismith describes the relationship between $M_R$ and θ and is assessed by numerical regression. In this case, θ represent the sum of the principal stresses [83], and the model is described in (Eq. 2).

$$M_R = k_1 \sigma_a \left(\frac{\theta}{\sigma_a}\right)^{k_2}, \quad \text{(Eq. 2)}$$

where $\sigma_a$ is the reference pressure set as 100 kPa, the bulk stress θ is the sum of the principal stresses, and $k_1$ and $k_2$ are regression parameters. In the present study, RPM was substituted with REM at 0%, 25%, 50%, and 100%, and the stiffness behaviour was assessed by Hicks and Monismith's models as shown in **Figure 4** .

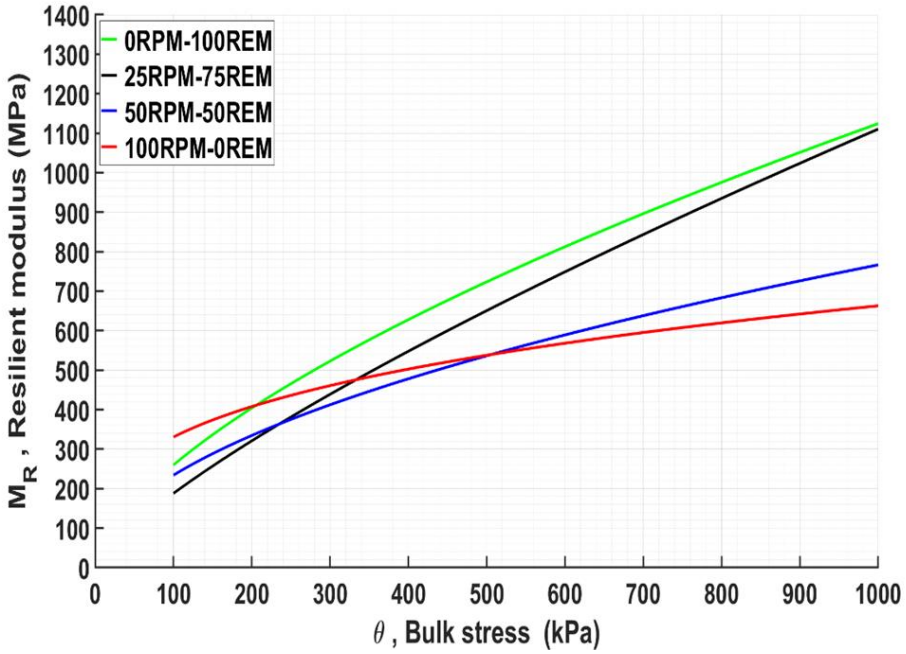


**Figure 4** Resilient modulus of REM and RPM in blended and unblended condition based on Hicks and Monismith's model.

The stiffness responses of the pure and blended materials significantly varied. Based on the performance trend, REM100 is stiffer than RPM100. This obser-

vation demonstrates the potential of resisting traffic impacts under unbound conditions. Here, particles became well compounded to effectively receive and transfer loads through a particle-to-particle contact medium. This is related to the stress-hardening effect in granular materials, given the high $M_R$ values at a high axial stress and constant confining pressure [84].

An interesting observation was the stiffness behavior of the materials at θ of 100 kPa. Within this range, the RPM stiffness was slightly higher. This behavior may be due to the steady packing density and re-orientation at the early stages of compaction because the RPM with a high flakiness index (FI) was characterized by a large surface area. Hence, compared with the REM with an FI of 12%, the FI of RPM was found to be 31%. **Paper B** reported other physical and mechanical properties of both materials. The stiffness behavior of the materials indicated that the inherent material properties had a significant impact on performance.

Regarding the blended mixtures, it was expected that the performance of the REM75 blends would lean toward REM100 and would therefore show higher stiffness behavior than the mixture comprising of REM50. Hence, the relationship between stiffness and θ was almost linear for REM75 and REM100 compared to RPM50 and RPM100. This shows an acceptable mix range for the RPM in the mix. This observation also confirmed the sensitivity of RPM in the blends as the content increased.

This study further adopted Uzan's model to demonstrate a three-dimensional view plot of the stiffness behavior of the REM and RPM blends (Eq. 3) [85]. The model interpreted the resilient modulus by considering the shear loading effect [36]. Hence, the Uzan's model presents the relationship among three essential parameters, (i.e., $M_R$ θ and $\sigma_d$) [86].

$$M_R = k_1 \sigma_a \left(\frac{\theta}{\sigma_a}\right)^{k_2} \left(\frac{\sigma_d}{\sigma_a}\right)^{k_3}, \quad \text{(Eq. 3)}$$

where $\sigma_a$ is a reference pressure that is set as 100 kPa, and $k_1$, $k_2$, $k_3$ are regression parameters. In addition to these models, several others have been reported [36, 85]. From the three-dimensional view plot of Uzan's model, the response pattern of the materials is similar to that of Hicks and Monismith's modeled behavior. **Figure 5** shows the stiffness behavior obtained using Uzan's model.

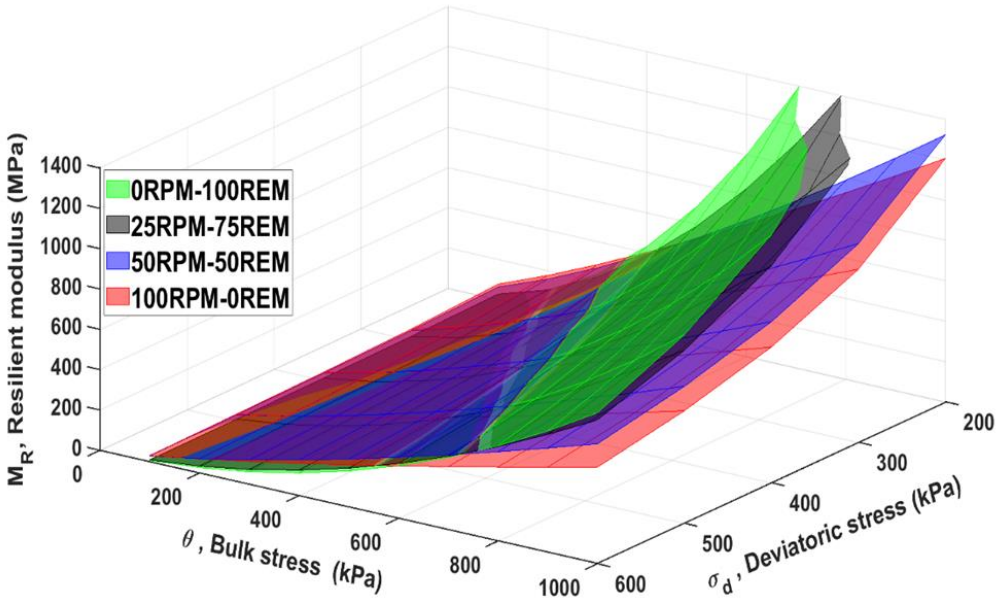


**Figure 5** Resilient modulus of pure REM and RPM and blended mixtures by Uzan's model.

## 4.2 Permanent deformation

The permanent deformation (PD) gradually develops with each load application and mainly occurs in the base and subbase layers [87, 88]. Compaction, crushing, and material migration cause PD [89], and are characterized in two phases: (a) an initial rapid increase in permanent strain with load applications, and (b) the deformation rate becomes constant but with a volume change [90]. Conceptually, predicting the PD allows the opportunity to limit the failure conditions [91], and several authors have modeled the characteristics of PD responses using analytical models, plasticity-based theory models, and shakedown theory [87, 88, 92-94]. The shakedown theory is compared with the Coulomb criterion, which uses the Mohr -Coulomb parameters [95].

In this study, the Coulomb criterion was adopted to investigate the behavior of the materials under consideration. The Coulomb approach presents the growth path of the PD in three different classifications (elastic, elasto-plastic, and failure) along with the loading cycles and stress conditions as shown in Figure 7 of **Paper**

**C**. The Coulomb criterion describes the mobilized shear strength for the development of PD and the maximum shear strength to failure [96].

The mobilized friction angle ρ(°) and incremental friction angle φ(°) express the degree of mobilized shear strength and maximum shear strength, respectively, and are expressed by two boundary lines. These boundary lines illustrate the elastic and failure limits and equations 4 and 5 of **Paper C** are used to compute them. In **Figure 6**, the ρ(°) and φ(°) of REM and RPM are shown.

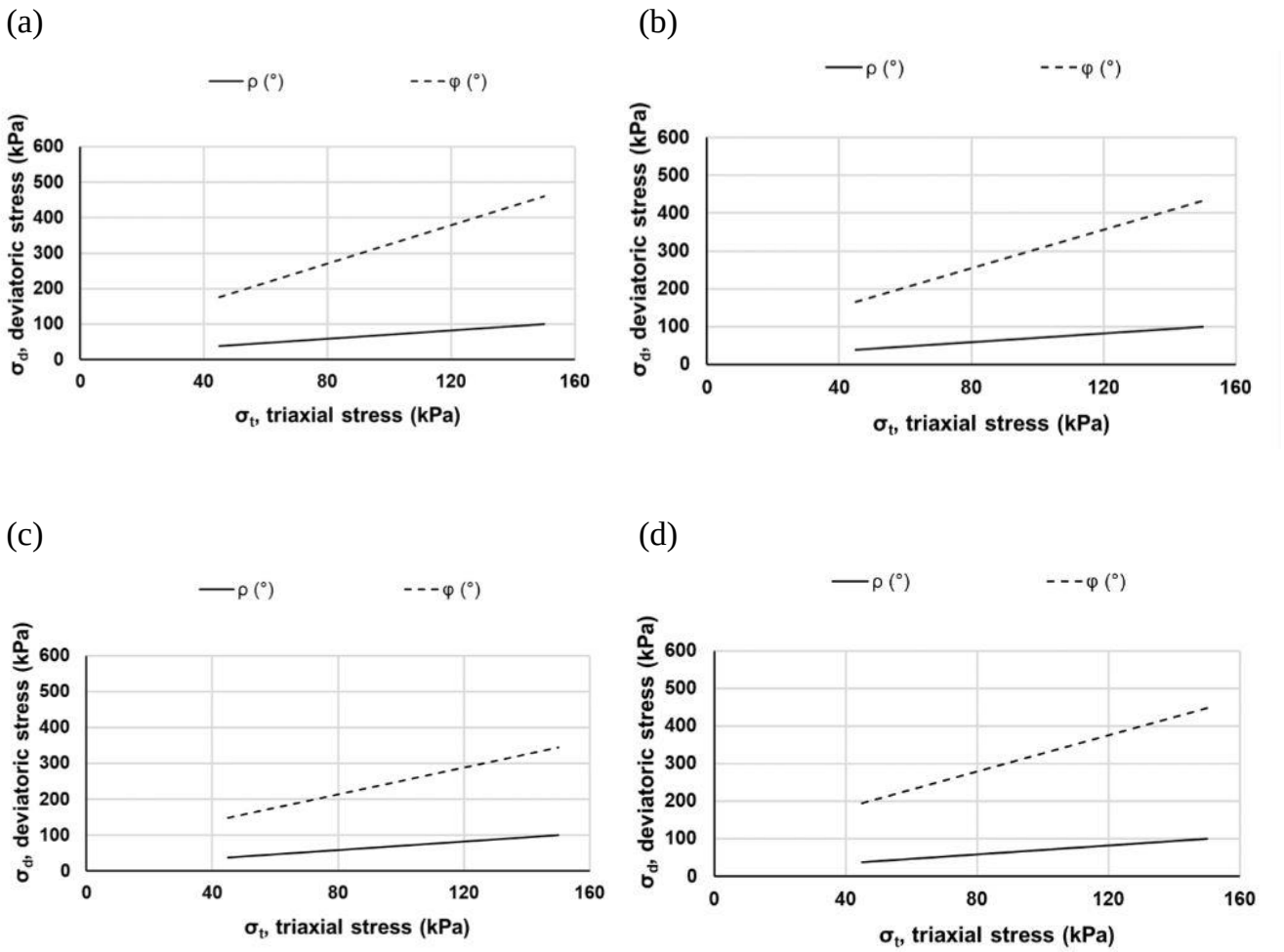


**Figure 6** Degree of mobilized shear strength ρ(°) and maximum shear strength φ(°) of (a) REM100, (b) REM75, (c) REM50, and (d) REM0.

The results clearly show no significant variation in the mobilization of shear strength, represented by ρ(°). However, some observations were made regarding the maximum shear to failure φ(°) for REM50 compared with the rest of the sam-

ples as the φ(°) was slightly lower. Although this was unexpected, it may be hypothesized that the particles underwent slight changes in the position and structure during the testing. Considering this, one study attributed poor packing and changes in gradation to differences in the performance of mixed materials compared with the materials in pure state (unmixed) [97]. Generally, the φ(°) value of REM50 was closer to that of REM75 than to that of REM0. The trends in the reported limit lines for REM100 and REM75 are almost the same, which is related to the stiffness previously mentioned. The values for ρ(°) and φ(°) angles of both the materials are shown in **Table 5**.

**Table 5** Mobilized angle of friction ρ(°) and incremental angle to failure φ(°) for REM and RPM

| Sample | Limit angles | |
|---|---|---|
| | ρ(°) | φ(°) |
| REM100 | 30.4 | 69.7 |
| REM75 | 30.4 | 68.5 |
| REM50 | 30.4 | 66.4 |
| REM0 | 30.4 | 71.4 |

## 4.3 Discussion

This study demonstrates the potential use of REM with a small amount of mechanically weak rocks in unbound construction (base and subbase layers). This approach is more profitable from an economic and environmental point of view compared to the use of conventional materials. The resilient modulus results indicate that only REM100 and REM75 exhibited higher elastic response, which was characterized by almost a linear trend as the θ increased. This behavior demonstrates the stability of the materials with an increased number of load applications and agrees well with similar observations highlighted in previous studies [98, 99]. A general decrease in performance was observed when the quantity of RPM in the mixture increased. Similar findings were also highlighted in **Paper B** regarding the effect of RPM, hence acceptable criteria for LA and MD values were established.

Despite the variation in stiffness shown by the two materials in pure conditions, the findings are in accordance with the results of previous studies [26, 34],

that analyzed the behavior of recycled materials from tunneling. In addition, the stiffness values obtained in this study were comparable to those values reported in the Netherlands for natural aggregates (100-400 MPa), mixed recycled aggregates (150-250 MPa), mixed recycled aggregates (400-600 MPa), and recycled concrete aggregates (600-800 MPa) [100]. Considering the values for recycled aggregates reported in the aforementioned study, the θ range within which the stiffness was calibrated was not provided. For similar considerations on the stiffness performance of REM in **Figure 4**, calibrating the stiffness values within 250-800 MPa would be within a θ range of 100-600 kPa.

In another study, the $M_R$ values of recycled concrete aggregates (RCA) was reported in the range of 239-357 MPa, 487-729 MPa and 575-769 MPa at different moisture contents [101]. The same study produced values for crushed brick and waste rock. After comparing the overall performance to quarry materials conclusions were reached that at 70% optimal moisture content, the peak performance of RCA with $M_R$ of 575-769 MPa was higher than 280-519 MPa for the crushed brick, 127-233 MPa for the waste rock, and 175-400 MPa for the quarry material [101]. Mixed recycled aggregates composed of concrete and mortar, ceramic and crushed rocks produced $M_R$ of 160-500 MPa within a θ range of 100-1000 kPa, and the authors mentioned that the performance is similar to that expected for crushed rock [102]. Furthermore, another study investigated the stiffness of two RCA and compared their performance to quartzite rocks and the results showed that the stiffness of RCA varied between 490-1010 MPa, and 480-685 MPa for quartzite rocks [103]. Generally, RCA yield considerably higher stiffness values than other aggregates as demonstrated in the aforementioned studies. This phenomenon has been attributed to the effect of self-cementing properties which are time dependent [104-106], and might be due to the further hydration of the unreacted inner parts of the cement grains.

In conclusion, the REM used in this study demonstrated appreciable stiffness and deformation responses comparable to those of RCA. This provides an opportunity to promote the increased use of REM and boost the confidence of end -users. In cases where REM comprises of mechanically weak rocks, such as RPM, this study has shown that an intermix of REM and RPM is feasible; however, considerable limitations on the content of RPM should be prioritized.

# 5. Developing recycled aggregates with Re-Con Zero Technology

## 5.1 Dry washing with two-component admixture

Re -Con Zero technology comprises of two-component admixture (i.e., high-water absorbing polymer and aluminum sulphate). Mixing the product with returned concrete (left over concrete in the drums of concrete trucks) facilitates hardened concrete which can easily be crushed into aggregates that can be used to dry wash the drums of concrete trucks [107]. The sizes of the dry-washing aggregates increased through agglomeration as the number of dry-washing cycles increased **(Paper D)**. The aggregates generated by this process are characterized by their mechanical and geometric properties, making them suitable for reuse in concrete and unbound applications. It is estimated that this approach saves approximately 40 times more $CO_2$ emissions than landfill disposal [108], and reduces concrete sludge by 80% [109]. In this study, recycled aggregates produced using the Re -Con Zero technology (RCZ) were used as feedstock for the wet recycling of excavation materials (EM), and the technical and environmental properties of final product were assessed. **Table 6** lists the mixing ratios of the materials fed into the recycling facility. A detailed description of the samples is provided in **Paper D**. This approach demonstrated the sustainable use of resources and broadened the scope of recycled materials under separate and mixed conditions for concrete and other civil engineering applications.

**Table 6** Samples collected with the mix ratio given in volume (%)

| Sample | Wet processing | RCZ | EM |
|---|---|---|---|
| RCZ-$F_0$ | No | - | - |
| RCZ-F | No | - | - |
| RCZ0 | Yes | 0 | 100 |
| RCZ50 | Yes | 50 | 50 |
| RCZ100 | Yes | 100 | 0 |

## 5.2 Physical and geometric properties

The composite layer of cement paste attached to the surface of the embedded aggregates was crucial for the gradation of the grain particles. The size distribution variations were observed to be dependent on the curing time of paste composite. This is because the recycling process, involving washing, scrubbing, eliminates the loose paste content. The particle -size distribution is shown in **Figure 7**. Some differences were observed between the feedstock RCZ-$F_0$ and RCZ-F from UiA. This variation may be related to the storage conditions in both cases. The wet -processed materials were fractionated at 4/16 mm from the production line.

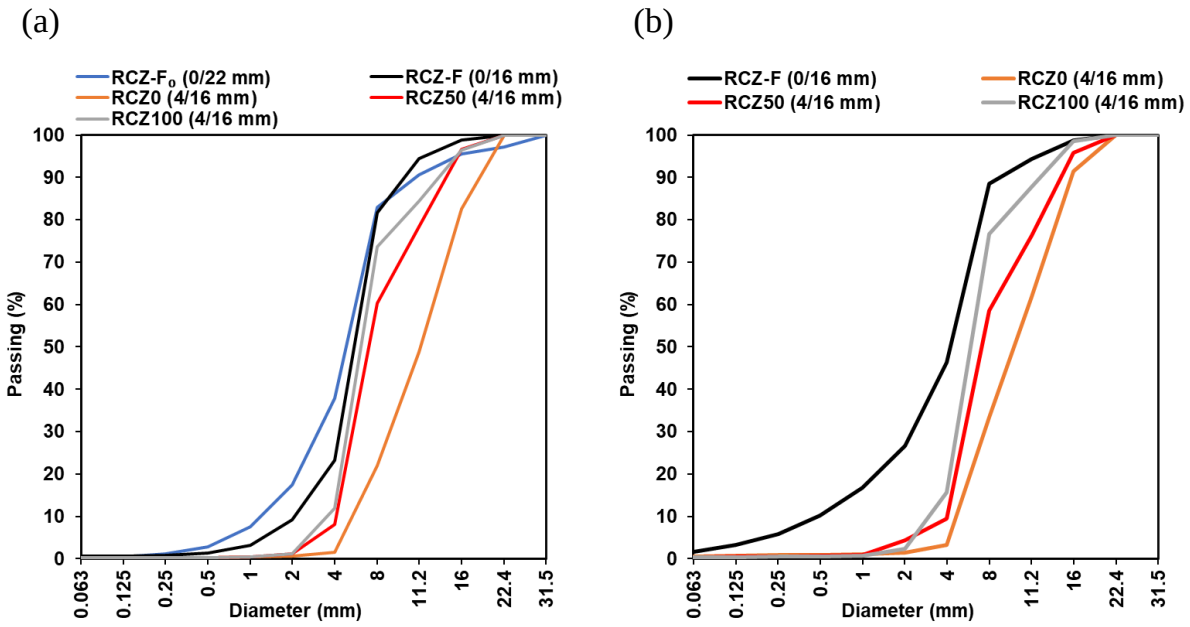


**Figure 7** Particle-size distribution of materials: UiA (a), and Velde (b).

This study further assessed the particle density and water absorption performance (see Table 2) of **Paper D**. Remarkable differences in water absorption values were observed. For the treated materials, lower values were recorded as RCZ increased. This was expected given the treatment efficiency of the wet technology which resulted in the removal of poorly cured paste from the grain particles. Regarding the feedstocks, the storage time also contributed to performance variation. Generally, although it is known that the paste content increases the water absorption of recycled aggregates from concrete waste [110, 111], the results obtained in

this study were optimal and comparable to those of other recycled aggregates from concrete sludge [112]. The particle density results demonstrate a similar trend of increasing density with increasing RCZ content. In this case, by comparing the values obtained from the two test sources UiA and Velde, the results did not significantly vary from each other. The values obtained for excavation materials are consistent with those results obtained in another study [113].

## 5.3 Mechanical characterization by Los Angeles and micro-Deval test

The applied technology is effective in transforming returned concrete sludge into recycled aggregates with excellent characteristics and properties. Considering the mechanical properties analyzed by the Los Angeles and micro-Deval tests and shown in **Table 7,** a clear trend of increased strength with increasing RCZ content can be observed. This demonstrates that RCZ is a high-quality material; hence its performance is comparable to typical values for natural aggregates found in Norway [113]. It is generally known that paste content significantly influences the mechanical strength of recycled aggregates from concrete waste [114-116]. In this case, the improved quality of the RCZ can be attributed to the application of the Re -Con Zero admixture, curing conditions and the applied treatment. In addition, it may be mentioned that the natural aggregates used in the parent concrete demonstrated excellent mechanical strength (i.e., resistance to crushing and wear). This observation was well reflected in the performance of the feedstocks where the amount of paste appeared to be the only variable that influenced the performance. Nevertheless, the pattern of the soluble content measured by the paste content in the materials demonstrated that a fraction of the well -cured paste was still present in the RCZ after processing, which was observed in the acid solubility results. In contrast, the slight difference in the performance of the feedstocks may be related to the positive effect of carbonation on improving the micro-structure of interfacial transition zone (i.e., the weakest region in concrete) [114, 117]. This may have slightly occurred in the materials tested at Velde, because they were stored in an open environment for a longer period. Calcium carbonate ($CaCO_3$) occupied the pore spaces within the paste to densify the open pores, thereby reducing the water absorption capacity [118]. Therefore, it is not surprising that the water absorption

values (as discussed in Section 5.2) were lower for the RCZ tested at Velde than for those tested at UiA. The study also demonstrated that a tolerable amount of high-quality RCZ could be mixed with excavation materials without compromising the overall strength. This is in support to the findings of a recent study in Norway that proposed composition criteria and requirements for recycled aggregates from both sources applied in road construction [39]. In this framework, LA and MD values of $\leq 35\%$ and $\leq 20\%$, and $\leq 40\%$ and $\leq 25\%$ are designed for mixtures of crushed concrete and excavation materials (Gjbn I), and concrete and brick (Gjb II), respectively.

**Table 7** Los Angeles and micro-Deval performance

| Sample | UiA | | Velde | |
|---|---|---|---|---|
| | LA | MD | LA | MD |
| RCZ-$F_0$ | 25 | 20 | 22 | 15 |
| RCZ-F | 23 | 18 | n.d.[a] | n.d.[a] |
| RCZ0 | 24 | 12 | 26 | 10 |
| RCZ50 | 22 | 10 | 24 | 11 |
| RCZ100 | 18 | 11 | 20 | 11 |

[a]Not determined

## 5.4 Solubility related to paste content in recycled aggregates

An acid solubility test was performed to assess the amount of paste in the materials and the related effects on the mechanical performance. The test was performed on samples before and after the Los Angeles test. Fine particles < 1.6 mm obtained after the Los Angeles test were used to identify the changing mechanism of calcium carbonates in the paste with respect to crushing. Details of the test can be found in Section 2.4 of **Paper D**. From the results shown in **Table 8**, the solubility is proportional to the amount of RCZ. This observation also confirmed some quantity of properly cured paste on the RCZ samples after the wet treatment. In addition, the increased concentration of paste fragments in the fines demonstrated that carbonate composites were one of the main minerals that disintegrated in high proportions during the crushing test (see x-ray diffraction analysis in Section 3.4 of **Paper D**). Regarding the feedstocks, almost the same solubility rate was reported, indicating the amount of paste in the original piles. These were higher

quantities than those of recycled materials. Hence, it was not surprising that the Los Angeles values obtained for the original feedstock were almost the same. The excavation material was found to be insoluble, which was not surprising considering its inherent composition and characteristics. Its increased solubility was prevalent in small fractions, as demonstrated in the samples denoted by $_{LA}$. A similar observation was made at the study that analyzed the effect of particle size on paste content [119]. Evidently, the paste content in the fine fractions was higher than that in the coarse fractions at the production line of the recycling facility. This relationship is crucial when considering the differences in paste content due to the particle size of the same material. Hence, increased fractions of cement paste can be expected in the accumulated fines at recycling facilities.

**Table 8** Acid soluble contents (wt.%) in the samples with various particle size given as arithmetic mean ± 1 standard deviation, (n = 3) and (n=4, $_{LA}$)

| Sample | Acid soluble part (%) | Standard deviation (%) | RSD (%) |
|---|---|---|---|
| RCZ-$F_0$ | 13.29 | 0.19 | 1.41 |
| RCZ-F | 13.80 | 0.05 | 0.35 |
| RCZ0 | 4.58 | 0.18 | 3.96 |
| RCZ50 | 8.27 | 0.41 | 4.96 |
| RCZ100 | 7.14 | 0.07 | 0.93 |
| $RCZ0_{LA}$ | 9.46 | 0.28 | 3.00 |
| $RCZ50_{LA}$ | 12.04 | 0.28 | 2.34 |
| $RCZ100_{LA}$ | 18.53 | 0.68 | 3.66 |

## 5.5 Environmental properties of recycled aggregates from concrete waste

A concern with the use of recycled aggregates sourced from concrete waste is the potential leaching of toxic chemicals into soil and groundwater. Environmental regulations and protocols have been designed to control the release from recycled aggregates. This study assessed the total chemical species present in the materials and compared their performance with the limit protocols established by the Norwegian Environmental Agency in **Table 9**. The applied test method is described in Section 2.4 of **Paper D**. In general, low levels of chemical species of potential concern (COPC) were found in the RCZ. Increased elevations of Cu, Cr,

and Zn were observed in excavation materials. However, in the intermixed phase, this pattern changed at lower concentrations. The changes were due to the introduction of the RCZ, which had previously recorded low values of these elements. Furthermore, feedstocks sourced from concrete sludge have low concentrations compared to excavation materials. Cr(VI) was consistently low in RCZ, indicating a low leaching response of Cr upon carbonation and a decrease in pH. In addition, it was observed that the recycling process played a significant role in reducing the amount of Cr(VI) in RCZ100 because slightly high levels were found in the original feedstock. Furthermore, the total concentrations in the fine fractions < 1.6 mm obtained from the materials were within an acceptable range. This indicated that the content of chemically active species in the paste content. Overall, although these results are promising, they demonstrate the environmental advantages of recycled materials under separate and blended conditions.

**Table 9** Content of COPC in the materials compared to Norwegian criteria for concrete waste. Concentrations are given in mg/kg.

| Element | RCZ-$AF_0$ | RCZ-AF | RCZ 0 | RCZ 50 | RCZ 100 | RCZ $0_{LA}$ | RCZ $50_{LA}$ | RCZ $100_{LA}$ | NEA limit[a] |
|---|---|---|---|---|---|---|---|---|---|
| As | <3 | <3 | <3 | <3 | <3 | <3 | <3 | <3 | 15 |
| Cd | <0.1 | <0.1 | <0.1 | <0.1 | <0.1 | <0.1 | <0.1 | <0.1 | 1.5 |
| Cr | 131 | 105 | 168 | 139 | 107 | 30.2 | 24.8 | 32.7 | 100 |
| $Cr^{6+}$ | 0.8 | 0.7 | <0.3 | <0.3 | <0.3 | 1.4 | 1.4 | 1.9 | 8 |
| Cu | 49 | 47.5 | 206 | 33.4 | 29 | 38.5 | 36.8 | 49.4 | 100 |
| Hg | <0.01 | <0.01 | <0.01 | <0.01 | <0.01 | <0.01 | <0.01 | <0.01 | 1 |
| Ni | 11.7 | 12.9 | 10.4 | 8.3 | 7.4 | 8.3 | 10.9 | 9.4 | 75 |
| Pb | 28.5 | 27.7 | 35.9 | 25.8 | 23.3 | 32.9 | 33.8 | 29.6 | 60 |
| Zn | 96.5 | 99 | 250 | 72.6 | 87.1 | 49 | 56.7 | 70.7 | 200 |

[a] Waste regulation limits for concrete waste developed and issued by Norwegian Environmental Agency.

Given the availability of returned concrete waste, it is possible to promote the use of special admixtures, which transform this waste into recycled aggregates with excellent mechanical and geometric properties. Thus, the produced recycled aggregates may replace conventional materials, which would reduce the depletion of aggregate reservoirs and the economic burden of acquiring virgin materials. This study contributes to the on-going discussions on the sustainability of the concrete industry.

# 6. Conclusions and future work

## 6.1 Main conclusions

Functional guidelines for broadening the knowledge and use of recycled aggregates from excavation and other sources will be key milestones in the sustainable management of resources in the construction industry. A significant feature in this case was the development of acceptance criteria based on mechanical and geometric properties in relation to geological variations. This thesis demonstrates a simplified procedure for establishing threshold values for the performance of aggregates recycled from excavation materials and other sources. End - users can formulate material mix -ratios based on the conditions of application by documenting the technical performance and inherent geological variations.

A comprehensive review of the impact of local geology on the mechanical performance of rocks by Los Angeles (LA) and micro-Deval (MD) tests broadens our understanding of the main aspects of geological influences. The parameters studied included mineralogy, grain and crystal size, grain shape, and porosity. Inferences made from diverse studies have demonstrated the scale of influence; hence, the relationship between the local geological parameters and mechanical strength should be simultaneously assessed. For instance, hard minerals (quartz and feldspar) contribute to the increased strength, whereas soft minerals (mica) reduce the rock strength. Other findings indicated otherwise regarding the influence of both minerals. Overall, these results indicate that establishing a synthesis of the effects of varying geological properties is critical for decision-making processes.

Furthermore, experimental validation of the properties of recycled excavation materials (REM) under separate and blended conditions with other materials was established. The mechanical performance was assessed by LA and MD, while X-ray diffraction and acid solubility tests were used to investigate the mineralogical and chemical changes in the fine fractions (< 1.6 mm). The LA performance of REM was stable and similar to that of recycled phyllite materials (RPM)- characterized by weak minerals. However, the MD varied significantly hence, a mix ratio of 40% RPM was found optimal for compliance with the acceptable application

criteria issued by Norwegian Public Roads Administration. The changes in mineralogy demonstrated that the weak minerals (i.e., mica and chlorite), were more abraded in MD than in LA, which indicated the aggressiveness of the test procedure on soft minerals.

The deformation properties of REM in systematic blends with 0%, 25%, 50%, and 100% was investigated using a repeated load triaxial test. The stiffness was assessed using Hicks and Monismith's model and Uzan's model and the Coulomb criterion was adopted to analyze the permanent deformation. REM demonstrated a stiffer response. Hence, the mix ratio denoted as REM75 produced stiffness pattern similar to that of REM100. This pattern changed as the quantity of REM reduced in the mix indicating that the performance was sensitive to the increased RPM. Regarding the permanent strain response, no differences were observed in the degree of mobilized friction angle $\rho(^0)$. The REM50 sample exhibited the lowest value of the incremental friction angle $\varphi(^0)$. However, the properties of the materials are believed to have significantly influence their performance. This phenomenon has been discussed.

This study investigated the extended performance of recycled aggregates (RCZ) derived from Re -Con Zero technology mixed with wet recycled excavation materials. The results demonstrated an increasing trend in LA and MD performances as the RCZ content increased. This study further assessed the potential concerns of the contents of chemical species in the materials and compared the findings with the pollution limit criteria established by the Norwegian Environmental Agency. Low levels of chemical species of potential concern were present. An increase in the concentrations of Cr, Cu, and Zn was observed in excavation materials, owing to variations in the local geology. The concentration of Cr(VI) was low, indicating that the potential leaching of Cr(VI) would be low upon carbonation with a decrease in pH. Overall, the chemical constituents present in the materials were acceptable which increases the chances of applying newly developed recycled materials from these sources under separate and mixed conditions in concrete and unbound applications without polluting the ecosystem.

## 6.2 Limitations and future work

This thesis expands the knowledge on the mechanical performance of recycled aggregates from excavation masses and other sources and promotes their application in unbound layers of road pavement. However, the following areas of improvement may be required to expand the scope of this study.

Given the wide range of geology and its effects on quality, further work should explore the impact of other geological factors on the general properties of recycled aggregates from the aforementioned sources. In addition, further testing frequencies should be explored to examine the impact of quality changes due to local geological parameters.

This study was primarily based on laboratory characterization of the materials. This may be expanded to the field to investigate the performance under external conditions. For example, on a small pilot scale, deflection and settlement measurements may be performed to investigate the behavior of materials.

In **Paper C**, the effects of the physical properties on the stiffness and deformation properties are discussed. Hence, further investigations of the impact of physical properties (i.e., morphological and shape parameters) on the deformation properties of recycled excavation materials premixed with other materials should be conducted.

Because this study only analyzed recycled excavation materials from one producer, it would be valuable to expand the investigation to include multiple producers across Norway to assess potential variations in performance and gain a deeper understanding of their behavior.

# Bibliography


[1] S. L. Huang, C.T. Yeh, and L. F. Chang, "The Transition to an Urbanizing World and the Demand for Natural Resources," *Current Opinion in Environmental Sustainability*, vol. (2), pp. 136-143, 2010.

[2] G. P. Peters, C. L. Weber, D. Guan, and K. Hubacek, "China's Growing $CO_2$ Emissions a Race between Increasing Consumption and Efficiency Gains," *Environmental Science & Technology*, vol. (41), pp. 5939-5944, 2007.

[3] S. Magnusson, K. Lundberg, B. Svedberg, and S. Knutsson, "Sustainable Management of Excavated Soil and Rock in Urban Areas–a Literature Review," *Journal of Cleaner Production*, vol. (93), pp. 18-25, 2015.

[4] S. Ritter, H. Einstein, and R. Galler, "Planning the Handling of Tunnel Excavation Material–a Process of Decision Making under Uncertainty," *Tunnelling and Underground Space Technology*, vol. (33), pp. 193-201, 2013.

[5] Euractiv, "Circular Economy- Excavated Soils: The Biggest Source of Waste You've Never Heard Of," https://www.euractiv.com/section/circular-economy/news/excavated-soils-the-biggest-source-of-waste-youve-never-heard-of/. Accessed: 24/11/2022.

[6] S. E. Hale, A. J. Roque, G. Okkenhaug, E. Sørmo, T. Lenoir, C. Carlsson, D. Kupryianchyk, P. Flyhammar, and B. Žlender, "The Reuse of Excavated Soils from Construction and Demolition Projects: Limitations and Possibilities," *Sustainability*, vol. (13), pp. 6083, 2021.

[7] M. Haas, R. Galler, L. Scibile, and M. Benedikt, "Waste or Valuable Resource–a Critical European Review on Re-Using and Managing Tunnel Excavation Material," *Resources, Conservation and Recycling*, vol. (162), pp. 105048, 2020.

[8] European Union "Circular Economy Action Plan: For a Cleaner and More Competitive Europe." https://ec.europa.eu/environment/circular-economy/pdf/new_circular_economy_action_plan.pdf. Accessed: 07/04/2022.

[9] United Nations “Transforming Our World: The 2030 Agenda for Sustainable Development.” https://sdgs.un.org/2030agenda. Accessed: 08/07/2022.

[10] R. Bellopede, and P. Marini, “Aggregates from Tunnel Muck Treatments. Properties and Uses,” *Physicochemical Problems of Mineral Processing*, vol. (47), pp. 259-266, 2011.

[11] R. H. Lieb, “Materials Management at the Gotthard Base Tunnel–Experience from 15 Years of Construction,” *Geomechanics and Tunnelling*, vol. (2), pp. 619-626, 2009.

[12] R. Simoni, “Gotthard Base Tunnel, Switzerland–the World’s Longest Railway Tunnel,” *In Proceedings of the Institution of Civil Engineers-Civil Engineering*, 2014.

[13] D. Walsh, I. McRae, R. Zirngibl, S. Chawla, H. Zhang, A. Alfieri, H. Moore, C. Bailey, A. Brooks, and T. Ostock, “Generation Rate and Fate of Surplus Soil Extracted in New York City,” *Science of the Total Environment*, vol. (650), pp. 3093-3100, 2019.

[14] Y. Moriguchi, and S. Hashimoto, “Material Flow Analysis and Waste Management,” *Taking Stock of Industrial Ecology*, pp. 247-262, 2016.

[15] P. Brunner, and H. Rechberger, “Practical Handbook of Material Flow Analysis: Boca Raton,” 2004.

[16] E. Van der Voet, “Substance Flow Analysis Methodology,” *A handbook of Industrial Ecology*, pp. 91-101, 2002.

[17] H. Bergsdal, R. A. Bohne, and H. Brattebø, “Projection of Construction and Demolition Waste in Norway,” *Journal of Industrial Ecology*, vol. (11), pp. 27-39, 2007.

[18] K. Cochran, and T. G. Townsend, “Estimating Construction and Demolition Debris Generation Using a Materials Flow Analysis Approach,” *Waste Management*, vol. (30), pp. 2247-2254, 2010.

[19] M. Hu, E. Van Der Voet, and G. Huppes, “Dynamic Material Flow Analysis for Strategic Construction and Demolition Waste Management in Beijing,” *Journal of Industrial Ecology*, vol. (14), pp. 440-456, 2010.

[20] T. Huang, F. Shi, H. Tanikawa, J. Fei, and J. Han, “Materials Demand and Environmental Impact of Buildings Construction and Demolition in China

Based on Dynamic Material Flow Analysis," *Resources, Conservation and Recycling*, vol. (72), pp. 91-101, 2013.

[21] F. Shi, T. Huang, H. Tanikawa, J. Han, S. Hashimoto, and Y. Moriguchi, "Toward a Low Carbon–Dematerialization Society: Measuring the Materials Demand and $CO_2$ Emissions of Building and Transport Infrastructure Construction in China," *Journal of Industrial Ecology*, vol. (16), pp. 493-505, 2012.

[22] A. Saeed, "Performance-Related Tests of Recycled Aggregates for Use in Unbound Pavement Layers," *Transportation Research Board*, vol. (598), 2008.

[23] R. Cardoso, R. V. Silva, J. de Brito, and R. Dhir, "Use of Recycled Aggregates from Construction and Demolition Waste in Geotechnical Applications: A Literature Review," *Waste management*, vol. (49), pp. 131-145, 2016.

[24] S. Erlingsson, and M. S. Rahman, "Evaluation of Permanent Deformation Characteristics of Unbound Granular Materials by Means of Multistage Repeated-Load Triaxial Tests," *Transportation Research Record*, vol. (2369), pp. 11-19, 2013.

[25] D. M. Barbieri, M. Tangerås, E. Kassa, I. Hoff, Z. Liu, and F. Wang, "Railway Ballast Stabilising Agents: Comparison of Mechanical Properties," *Construction and Building Materials*, vol. (252), pp. 119041, 2020.

[26] D. M. Barbieri, I. Hoff, and M. B. E. Mørk, "Organosilane and Lignosulfonate as Innovative Stabilization Techniques for Crushed Rocks Used in Road Unbound Layers," *Transportation Geotechnics*, vol. (22), pp. 100308, 2020.

[27] S. Adomako, C. J. Engelsen, R. T. Thorstensen, and D. M. Barbieri, "Repeated Load Triaxial Testing of Recycled Excavation Materials Blended with Recycled Phyllite Materials," *Materials*, vol. (15), pp. 621, 2022.

[28] A. Arulrajah, J. Piratheepan, and M. M. Disfani, "Reclaimed Asphalt Pavement and Recycled Concrete Aggregate Blends in Pavement Subbases: Laboratory and Field Evaluation," *Journal of Materials in Civil Engineering*, vol. (26), pp. 349-357, 2014.

[29] S. Mohsenian Hadad Amlashi, M. Vaillancourt, A. Carter, and J. P. Bilodeau, "Resilient Modulus of Pavement Unbound Granular Materials Containing Recycled Glass Aggregate," *Materials and Structures*, vol. (51), pp. 1-12, 2018.

[30] R. K. Rout, P. Ruttanapormakul, S. Valluru, and A. J. Puppala, "Resilient Moduli Behavior of Lime-Cement Treated Subgrade Soils," *In Geocongress 2012: State of the Art and Practice in Geotechnical Engineering*, pp. 1428-1437, 2012.

[31] M. Saberian, J. Li, and S. Setunge, "Evaluation of Permanent Deformation of a New Pavement Base and Subbase Containing Unbound Granular Materials, Crumb Rubber and Crushed Glass," *Journal of Cleaner Production*, vol. (230), pp. 38-45, 2019.

[32] A. Arulrajah, J. Piratheepan, M. Ali, and M. Bo, "Geotechnical Properties of Recycled Concrete Aggregate in Pavement Sub-Base Applications," *Geotechnical Testing Journal*, vol. (35), pp. 743-751, 2012.

[33] D. M. Barbieri, I. Hoff, and C.-H. Ho, "Crushed Rocks Stabilized with Organosilane and Lignosulfonate in Pavement Unbound Layers: Repeated Load Triaxial Tests," *Frontiers of Structural and Civil Engineering*, vol.(15), pp. 412-424, 2021.

[34] D. M. Barbieri, I. Hoff, and M. B. E. Mørk, "Innovative Stabilization Techniques for Weak Crushed Rocks Used in Road Unbound Layers: A Laboratory Investigation," *Transportation Geotechnics*, vol. (18), pp. 132-141, 2019.

[35] D. M. Barbieri, B. Lou, H. Chen, B. Shu, F. Wang, and I. Hoff, "Organosilane and Lignosulfonate Stabilization of Roads Unbound: Performance During a Two-Year Time Span," *Advances in Civil Engineering*, 2021.

[36] G. Cerni, A. Corradini, E. Pasquini, and F. Cardone, "Resilient Behaviour of Unbound Granular Materials through Repeated Load Triaxial Test: Influence of the Conditioning Stress," *Road Materials and Pavement Design*, vol. (16), pp. 70-88, 2015.

[37] F. Lekarp, U. Isacsson, and A. Dawson, "State of the Art II: Permanent Strain Response of Unbound Aggregates," *Journal of Transportation Engineering*, vol. (126), pp. 76-83, 2000.

[38] NPRA Håndbok N200 Vegbygging, Norway Vegdirektoratet, 2022.

[39] C. J. Engelsen, and K. R. Lysbakken, “Utnyttelse Av Resirkulert Tilslag N200 Vegbygging (REN 200): Kunnskap Og Erfaringer Med Resirkulerte Betong Og Gravemasser,” 2021.

[40] B. D. Prowell, J. Zhang, and E. R. Brown, "Aggregate Properties and the Performance of Superpave-Designed Hot Mix Asphalt," *Transportation Research Board*, 2005.

[41] R. Nålsund, “Railway Ballast Characteristics, Selection Criterion and Performance,” *Doctoral Thesis, Norwegian University of Science and Technology,* Norway, 2014.

[42] S. Benediktsson, “Effects of Particle Shape on Mechanical Properties of Aggregates,” *Master Thesis, Norwegian Norwegian of Science and Technology, Trondheim,* 2015.

[43] D. Wang, H. Wang, Y. Bu, C. Schulze, and M. Oeser, “Evaluation of Aggregate Resistance to Wear with Micro-Deval Test in Combination with Aggregate Imaging Techniques,” *Wear,* vol. (338), pp. 288-296, 2015.

[44] J. Richard, and J. Scarlett, “A Review and Evaluation of the Micro-Deval Test,” 1997.

[45] İ. Gökalp, V. E. Uz, and M. Saltan, “Testing the Abrasion Resistance of Aggregates Including by-Products by Using Micro Deval Apparatus with Different Standard Test Methods,” *Construction and Building Materials*, vol. (123), pp. 1-7, 2016.

[46] S. Senior, and C. Rogers, “Laboratory Tests for Predicting Coarse Aggregate Performance in Ontario,” *Transportation Research Record*, 1991.

[47] A. P. Pérez Fortes, S. Anastasio, E. Kuznetsova, and S. W. Danielsen, “Behaviour of Crushed Rock Aggregates Used in Asphalt Surface Layer Exposed to Cold Climate Conditions,” *Environmental Earth Sciences,* vol. (75), pp. 1-10, 2016.

[48] A. Hartley, “A Review of the Geological Factors Influencing the Mechanical Properties of Road Surface Aggregates,” *Quarterly Journal of Engineering Geology,* vol. (7), pp. 69-100, 1974.

[49] A. Kazi, and Z. R. Al-Mansour, “Influence of Geological Factors on Abrasion and Soundness Characteristics of Aggregates,” *Engineering Geology,* vol. (15), pp. 195-203, 1980.

[50] P. P. Giannakopoulou, P. Petrounias, A. Rogkala, B. Tsikouras, P. M. Stamatis, P. Pomonis, and K. Hatzipanagiotou, "The Influence of the Mineralogical Composition of Ultramafic Rocks on Their Engineering Performance: A Case Study from the Veria-Naousa and Gerania Ophiolite Complexes (Greece)," *Geosciences*, vol. (8), pp. 251, 2018.

[51] J. Majzlan, "Primary and Secondary Minerals of Antimony," pp. 17-47, 2021.

[52] W. Ajagbe, M. Tijani, and I. Oyediran, "Engineering and Geological Evaluation of Rocks for Concrete Production," *Lautech Journal of Engineering and Technology*, vol. (9), pp. 67-79, 2015.

[53] O. Ademila, "Engineering Geological Evaluation of Some Rocks from Akure, Southwestern Nigeria as Aggregates for Concrete and Pavement Construction," *Geology, Geophysics and Environment*, vol. (45), pp. 31-43, 2019.

[54] L. Afolagboye, A. Talabi, and O. Akinola, "Evaluation of Selected Basement Complex Rocks from Ado-Ekiti, Sw Nigeria, as Source of Road Construction Aggregates," *Bulletin of Engineering Geology and the Environment*, vol. (75), pp. 853-865, 2016.

[55] L. Pang, S. Wu, J. Zhu, and L. Wan, "Relationship between Retrographical and Physical Properties of Aggregates," *Journal of Wuhan University of Technology-Mater. Sci. Ed.*, vol. (25), pp. 678-681, 2010.

[56] M. Amrani, Y. Taha, A. Kchikach, M. Benzaazoua, and R. Hakkou, "Valorization of Phosphate Mine Waste Rocks as Materials for Road Construction," *Minerals*, vol. (9), pp. 237, 2019.

[57] L. M. Sousa, "The Influence of the Characteristics of Quartz and Mineral Deterioration on the Strength of Granitic Dimensional Stones," *Environmental Earth Sciences*, vol. (69), pp. 1333-1346, 2013.

[58] N. Yesiloglu-Gultekin, E. A. Sezer, C. Gokceoglu, and H. Bayhan, "An Application of Adaptive Neuro Fuzzy Inference System for Estimating the Uniaxial Compressive Strength of Certain Granitic Rocks from Their Mineral Contents," *Expert Systems with Applications*, vol. (40), pp. 921-928, 2013.

[59] T. Onodera, "Relation between Texture and Mechanical Properties of Crystalline Rock," *Congres Geologique International*, 1980.

[60] K. Du, Y. Sun, J. Zhou, M. Khandelwal, and F. Gong, "Mineral Composition and Grain Size Effects on the Fracture and Acoustic Emission (AE) Characteristics of Rocks under Compressive and Tensile Stress," *Rock Mechanics and Rock Engineering*, vol. (55), pp. 6445–6474, 2022.

[61] A. Hemmati, M. Ghafoori, H. Moomivand, and G. R. Lashkaripour, "The Effect of Mineralogy and Textural Characteristics on the Strength of Crystalline Igneous Rocks Using Image-Based Textural Quantification," *Engineering Geology*, vol. (266), pp. 105467, 2020.

[62] U. Åkesson, J. Stigh, J. E. Lindqvist, and M. Göransson, "The Influence of Foliation on the Fragility of Granitic Rocks, Image Analysis and Quantitative Microscopy," *Engineering Geology*, vol. (68), pp. 275-288, 2003.

[63] E. Kuznetsova, A. P. Pérez Fortes, S. Anastasio, and S. Willy Danielsen, "Behavior of Crushed Rock Aggregates Used in Road Construction Exposed to Cold Climate Conditions," *EGU General Assembly Conference Abstracts*, 2016.

[64] P. P. Giannakopoulou, P. Petrounias, B. Tsikouras, S. Kalaitzidis, A. Rogkala, K. Hatzipanagiotou, and S. F. Tombros, "Using Factor Analysis to Determine the Interrelationships between the Engineering Properties of Aggregates from Igneous Rocks in Greece," *Minerals*, vol. (8), pp. 580, 2018.

[65] P. Petrounias, P. P. Giannakopoulou, A. Rogkala, P. M. Stamatis, P. Lampropoulou, B. Tsikouras, and K. Hatzipanagiotou, "The Effect of Petrographic Characteristics and Physico-Mechanical Properties of Aggregates on the Quality of Concrete," *Minerals*, vol. (8), pp. 577, 2018.

[66] Ö. F. Apaydın, and M. Yılmaz, "Correlation of Petrographic and Chemical Characteristics with Strength and Durability of Basalts as Railway Aggregates Determined by Ballast Fouling," *Bulletin of Engineering Geology and the Environment*, vol. (80), pp. 4197-4205, 2021.

[67] S. Zhang, S. Qiu, P. Kou, S. Li, P. Li, and S. Yan, "Investigation of Damage Evolution in Heterogeneous Rock Based on the Grain-Based Finite-Discrete Element Model," *Materials*, vol. (14), pp. 3969, 2021.

[68] R. Ajalloeian, and M. Kamani, "An Investigation of the Relationship between Los Angeles Abrasion Loss and Rock Texture for Carbonate Aggregates," *Bulletin of Engineering Geology and the Environment*, vol. (78), pp. 1555-1563, 2019.

[69] M. Kamani, and R. Ajalloeian, "Evaluation of Engineering Properties of Some Carbonate Rocks Trough Corrected Texture Coefficient," *Geotechnical and Geological Engineering*, vol. (37), pp. 599-614, 2019.

[70] A. Gupta, B. Madhusudhan, A. Zervos, W. Powrie, J. Harkness, and L. Le Pen, "Grain Characterisation of Fresh and Used Railway Ballast," *Granular Matter*, vol. (24), pp. 1-9, 2022.

[71] M. Martinez-Echevarria, M. Lopez-Alonso, L. Garach, J. Alegre, C. Poon, F. Agrela, and M. Cabrera, "Crushing Treatment on Recycled Aggregates to Improve Their Mechanical Behaviour for Use in Unbound Road Layers," *Construction and Building Materials*, vol. (263), pp. 120517, 2020.

[72] L. Uthus, I. Hoff, and I. Horvli, "Evaluation of Grain Shape Characterization Methods for Unbound Aggregates," *In Proceedings of the International Conferences on the Bearing Capacity of Roads, Railways and Airfields*, Norway, 2005.

[73] Y. Guo, V. Markine, J. Song, and G. Jing, "Ballast Degradation: Effect of Particle Size and Shape Using Los Angeles Abrasion Test and Image Analysis," *Construction and Building Materials*, vol. (169), pp. 414-424, 2018.

[74] S. Adomako, R. Thorstensen, N. Akhtar, M. Norby, C. Engelsen, T. Danner, and D. Barbieri, "Evaluating the Effect of Mineralogy and Mechanical Stability of Recycled Excavation Materials by Los Angeles and Micro-Deval Test," *Eleventh International Conference on the Bearing Capacity of Roads, Railways and Airfields*, Norway, 2021.

[75] A. Abu Taqa, M. Al-Ansari, R. Taha, A. Senouci, G. M. Al-Zubi, and M. O. Mohsen, "Performance of Concrete Mixes Containing Tbm Muck as Partial Coarse Aggregate Replacements," *Materials*, vol. (14), pp. 6263, 2021.

[76] F. Agrela, A. Barbudo, A. Ramírez, J. Ayuso, M. D. Carvajal, and J. R. Jiménez, "Construction of Road Sections Using Mixed Recycled Aggregates Treated with Cement in Malaga, Spain," *Resources, Conservation and Recycling*, vol. (58), pp. 98-106, 2012.

[77] K. Voit, and E. Kuschel, "Rock Material Recycling in Tunnel Engineering," *Applied Sciences*, vol. (10), pp. 2722, 2020.

[78] M. Adom-Asamoah, and R. O. Afrifa, "A Study of Concrete Properties Using Phyllite as Coarse Aggregates," *Materials & Design*, vol. (31), pp. 4561-4566, 2010.

[79] K. Voit, "Application and Optimization of Tunnel Excavation Material of the Brenner Base Tunnel," *Doctoral Thesis, University of Natural Resources and Life Sciences Vienna*, Austria 2013.

[80] M. Norby, "Nytt Resirkulert Tilslag Produsert Fra Grave-Og Byggavfall," *Master Thesis, University of Agder*, Norway, 2020.

[81] H. Wang, D. Wang, P. Liu, J. Hu, C. Schulze, and M. Oeser, "Development of Morphological Properties of Road Surfacing Aggregates During the Polishing Process," *International Journal of Pavement Engineering*, vol. (18), pp. 367-380, 2017.

[82] M. Fladvad, "Optimal Utilisation of Unbound Crushed Aggregates for Road Construction," *Doctoral Thesis, Norwegian University of Science and Technology,* Norway, 2020.

[83] R. Hick, and C. Monismith, "Factors Influencing the Resilient Response of Granular Materials," *Highway Research Record*, vol. (345), pp. 15-31, 1971.

[84] A. J. Puppala, L. R. Hoyos, and A. K. Potturi, "Resilient Moduli Response of Moderately Cement-Treated Reclaimed Asphalt Pavement Aggregates," *Journal of Materials in Civil Engineering*, vol. (23), pp. 990-998, 2011.

[85] F. Lekarp, U. Isacsson, and A. Dawson, "State of the Art. I: Resilient Response of Unbound Aggregates," *Journal of Transportation Engineering*, vol. (126), pp. 66-75, 2000.

[86] J. Uzan, "Characterization of Granular Material," *Transportation Research Record,* vol. (1022), pp. 52-59, 1985.

[87] F. Lekarp, and A. Dawson, "Modelling Permanent Deformation Behaviour of Unbound Granular Materials," *Construction and Building Materials*, vol. (12), pp. 9-18, 1998.

[88] I. Pérez, L. Medina, and M. Romana, "Permanent Deformation Models for a Granular Material Used in Road Pavements," *Construction and Building Materials*, vol. (20), pp. 790-800, 2006.

[89] O. Tholen, “Falling Weight Deflectometer. A Device for Bearing Capacity Measurements: Properties and Performance,” 1980.

[90] S. Werkmeister, A. Dawson, and F. Wellner, “Pavement Design Model for Unbound Granular Materials,” *Journal of Transportation Engineering*, vol. (130), pp. 665-674, 2004.

[91] M. S. Rahman, and S. Erlingsson, “Predicting Permanent Deformation Behaviour of Unbound Granular Materials,” *International Journal of Pavement Engineering*, vol. (16), pp. 587-601, 2015.

[92] G. Cerni, F. Cardone, A. Virgili, and S. Camilli, “Characterisation of Permanent Deformation Behaviour of Unbound Granular Materials under Repeated Triaxial Loading,” *Construction and Building Materials*, vol. (28), pp. 79-87, 2012.

[93] S. Werkmeister, A. R. Dawson, and F. Wellner, “Permanent Deformation Behaviour of Granular Materials,” *Road Materials and Pavement Design*, vol. (6), pp. 31-51, 2005.

[94] P. Hornych, C. Chazallon, F. Allou, and A. El Abd, “Prediction of Permanent Deformations of Unbound Granular Materials in Low Traffic Pavements,” *Road Materials and Pavement Design*, vol. (8), pp. 643-666, 2007.

[95] I. Hoff, L. J. Bakløkk, and J. Aurstad, “Influence of Laboratory Compaction Method on Unbound Granular Materials,” *Proceedings of the 6th International Symposium on Pavements Unbound (UNBAR 6)*, UK, 2004.

[96] D. Barbieri, I. Hoff, and H. Mork, “Laboratory Investigation on Unbound Materials Used in a Highway with Premature Damage,” In *Bearing Capacity of Roads, Railways and Airfields*, pp. 101-108, 2017.

[97] H. Kazmee, E. Tutumluer, and D. Mishra, “Effects of Material Blending on Strength, Modulus and Deformation Characteristics of Recycled Concrete Aggregates,” *Transportation Research Board Meeting*, 2012.

[98] F. Gu, H. Sahin, X. Luo, R. Luo, and R. L. Lytton, “Estimation of Resilient Modulus of Unbound Aggregates Using Performance-Related Base Course Properties,” *Journal of Materials in Civil Engineering*, vol. (27), pp. 04014188, 2015.

[99] J. Zhang, F. Gu, and Y. Zhang, “Use of Building-Related Construction and Demolition Wastes in Highway Embankment: Laboratory and Field

Evaluations," *Journal of Cleaner Production*, vol. (230), pp. 1051-1060, 2019.

[100] BRBS Recycling, "Use of Recycled Aggregate - the Best Road Base Material on Earth," pp. 4, 2017.

[101] A. Arulrajah, J. Piratheepan, M. M. Disfani, and M. W. Bo, "Geotechnical and Geoenvironmental Properties of Recycled Construction and Demolition Materials in Pavement Subbase Applications," *Journal of Materials in Civil Engineering*, vol. (25), pp. 1077-1088, 2013.

[102] F. da Conceição Leite, R. dos Santos Motta, K. L. Vasconcelos, and L. Bernucci, "Laboratory Evaluation of Recycled Construction and Demolition Waste for Pavements," *Construction and Building Materials*, vol. (25), pp. 2972-2979, 2011.

[103] A. Gabr, and D. Cameron, "Properties of Recycled Concrete Aggregate for Unbound Pavement Construction," *Journal of Materials in Civil Engineering*, vol. (24), pp. 754-764, 2012.

[104] M. Arm, "Self-Cementing Properties of Crushed Demolished Concrete in Unbound Layers: Results from Triaxial Tests and Field Tests," *Waste Management*, vol. (21), pp. 235-239, 2001.

[105] B. J. Blankenagel, and W. S. Guthrie, "Laboratory Characterization of Recycled Concrete for Use as Pavement Base Material," *Transportation Research Record*, vol. (1952), pp. 21-27, 2006.

[106] R. Silva, J. De Brito, and R. Dhir, "Use of Recycled Aggregates Arising from Construction and Demolition Waste in New Construction Applications," *Journal of Cleaner Production*, vol. (236), pp. 117629, 2019.

[107] S.-H. Norman, "Mapei Technology Transforms Waste into a Resource Material, " *Concrete and Sustainability Special*, *RM International*, vol. 93. pp. 26-29, 2022.

[108] Re-Con Zero Evo: How Concrete Becomes Sustainable, "Re-Con Zero Evo: How Concrete Becomes Sustainable." https://www.mapei.com/it/en/realta-mapei/detail/re-con-zero-evo. Accessed: 09/01/2023.

[109] S. Adomako, A. Heimdal, and R. T. Thorstensen, "From Waste to Resource–Utilising Residue from Ready-Made Concrete as New Aggregate," *Nordic Concrete Research*, vol. (64), pp. 1-10, 2021.

[110] M. S. De Juan, and P. A. Gutiérrez, "Study on the Influence of Attached Mortar Content on the Properties of Recycled Concrete Aggregate," *Construction and Building Materials*, vol. (23), pp. 872-877, 2009.

[111] N. Kisku, H. Joshi, M. Ansari, S. Panda, S. Nayak, and S. C. Dutta, "A Critical Review and Assessment for Usage of Recycled Aggregate as Sustainable Construction Material," *Construction and Building Materials*, vol. (131), pp. 721-740, 2017.

[112] E. Anastasiou, M. Papachristoforou, D. Anesiadis, K. Zafeiridis, and E.-C. Tsardaka, "Investigation of the Use of Recycled Concrete Aggregates Originating from a Single Ready-Mix Concrete Plant," *Applied Sciences*, vol. (8), pp. 2149, 2018.

[113] S. Adomako, C. J. Engelsen, T. Danner, R. T. Thorstensen, and D. M. Barbieri, "Recycled Aggregates Derived from Excavation Materials—Mechanical Performance and Identification of Weak Minerals," *Bulletin of Engineering Geology and the Environment*, vol. (81), pp. 1-12, 2022.

[114] L. Li, J. Xiao, D. Xuan, and C. S. Poon, "Effect of Carbonation of Modeled Recycled Coarse Aggregate on the Mechanical Properties of Modeled Recycled Aggregate Concrete," *Cement and Concrete Composites*, vol. (89), pp. 169-180, 2018.

[115] D. Xuan, B. Zhan, and C. S. Poon, "Assessment of Mechanical Properties of Concrete Incorporating Carbonated Recycled Concrete Aggregates," *Cement and Concrete Composites*, vol. (65), pp. 67-74, 2016.

[116] S.-C. Kou, B.-j. Zhan, and C.-S. Poon, "Use of a Co2 Curing Step to Improve the Properties of Concrete Prepared with Recycled Aggregates," *Cement and Concrete Composites*, vol. (45), pp. 22-28, 2014.

[117] B. Lu, C. Shi, Z. Cao, M. Guo, and J. Zheng, "Effect of Carbonated Coarse Recycled Concrete Aggregate on the Properties and Microstructure of Recycled Concrete," *Journal of Cleaner Production*, vol. (233), pp. 421-428, 2019.

[118] E.-J. Moon, and Y. C. Choi, "Carbon Dioxide Fixation Via Accelerated Carbonation of Cement-Based Materials: Potential for Construction Materials Applications," *Construction and Building Materials*, vol. (199), pp. 676-687, 2019.

[119] C. J. Engelsen, H. A. van der Sloot, G. Wibetoe, G. Petkovic, E. Stoltenberg-Hansson, and W. Lund, “Release of Major Elements from Recycled Concrete Aggregates and Geochemical Modelling,” *Cement and Concrete Research*, vol. (39), pp. 446-459, 2009.

## Appended papers

The papers appended to this section have been published in or submitted to peer-reviewed journals.

# Paper A

**S. Adomako**, C. J. Engelsen, R. T. Thorstensen, and D. M. Barbieri, "Review of the Relationship between Aggregates Geology and Los Angeles and Micro-Deval Tests," *Bulletin of Engineering Geology and the Environment*, vol. (80), pp. 1963-1980, 2021. https://doi.org/10.1007/s10064-020-02097-y

Bulletin of Engineering Geology and the Environment (2021) 80:1963–1980
https://doi.org/10.1007/s10064-020-02097-y

REVIEW PAPER

# Review of the relationship between aggregates geology and Los Angeles and micro-Deval tests

Solomon Adomako[1] · Christian John Engelsen[2] · Rein Terje Thorstensen[1] · Diego Maria Barbieri[3]

Received: 5 October 2020 / Accepted: 28 December 2020 / Published online: 12 January 2021
© The Author(s) 2021

## Abstract

Rock aggregates constitute the enormous volume of inert construction material used around the globe. The petrologic description as igneous, sedimentary, and metamorphic types establishes the intrinsic formation pattern of the parent rock. The engineering properties of these rocks vary due to the differences in the transformation process (e.g. hydrothermal deposits) and weathering effect. The two most common mechanical tests used to investigate the performance of aggregates are the Los Angeles (LA) and micro-Deval (MD) tests. This study reviewed the geological parameters (including mineralogy, grain and crystal size, grain shape, and porosity) and the relationship to Los Angeles and micro-Deval tests. It was found that high content of primary minerals in rocks (e.g. quartz and feldspar) is a significant parameter for performance evaluation. Traces of secondary and accessory minerals also affect the performance of rocks, although in many cases it is based on the percentage. Furthermore, some studies showed that the effect of mineralogic composition on mechanical strength is not sufficient to draw final conclusions of mechanical performance; therefore, the impact of other textural characteristics should be considered. The disposition of grain size and crystal size (e.g. as result of lithification) showed that rocks composed of fine-grain textural composition of ≤ 1 mm enhanced fragmentation and wear resistance than medium and coarse grained (≥ 1 mm). The effect of grain shape was based on convex and concave shapes and flat and elongated apexes of tested samples. The equidimensional form descriptor of rocks somehow improved resistance to impact from LA than highly flat and elongated particles. Lastly, the distribution of pore space investigated by means of the saturation method mostly showed moderate ($R = 0.50$) to strong ($R = 0.90$) and positive correlations to LA and MD tests.

**Keywords** Los Angeles test · Micro-Deval test · Minerals · Grain and crystal size · Grain shape · Pore space

## Introduction

Studying the geological nature of rocks gives substantial information about the petrographic, mineralogic, and micro- and macro-structural composition. The relationship between geological features and the physical-mechanical performance of rocks is significant in a preliminary assessment and selection process as a construction material. In most cases, the focus is directed to the type of rock (e.g. porphyritic granite, limestone, amphibolite) and the underlying formation process (i.e. to investigate the effects of weathering). It is unequivocal that age cycle and the transition of rocks entail a significant alteration degree on the texture. Changes of textural configurations in geological time are due to weathering, which can be physical, chemical, and biological processes. In tropical and subtropical regions, severe climate causes high weathering profiles—often classified into geomorphic zones which promote the disintegration of rocks and result in variations of

✉ Solomon Adomako
Solomon.adomako@uia.no

Christian John Engelsen
ChristianJohn.Engelsen@sintef.no

Rein Terje Thorstensen
rein.t.thorstensen@uia.no

Diego Maria Barbieri
diego.barbieri@ntnu.no

[1] Department of Engineering and Science, University of Agder, 4879 Grimstad, Norway

[2] Department of Building and Infrastructure, SINTEF Community, v/ Arne Gunnar Brun, P.O. Box 124 Blindern, NO-0314 Oslo, Norway

[3] Department of Civil and Environmental Engineering, Norwegian University of Science and Technology, Høgskoleringen 7A, 7491 Trondheim, Trøndelag, Norway

mechanical strengths. Early discussions on the relationship between the physical-mechanical performance and the geological properties of rocks date back to the 1970s and 1980s (Hartley 1974; Kazi and Al-Mansour 1980).

Today, there is increased attention to the subject particularly because of the wide spectrum of technologies (e.g. digital image segmentation) used for the petrographic analysis and the several test protocols available, including Los Angeles (LA) and micro-Deval (MD) tests. The effects of void ratio, cracks, and weight loss on LA performance for several rock aggregates were investigated by Bahrami et al. (2019). Their study found that aggregates with high fragmentation resistance were due to changes in the morphology. The microtexture of rock aggregates resulted in high strength of frictional wear in an MD test (Török and Czinder 2017). Correlations existing between LA and other physical and mechanical properties have also shown the feasibility of estimating LA based on rock properties (Ugur et al. 2010; Esfahani et al. 2019). Furthermore, the LA performance can be connected to the mineral and chemical composition (Apaydın and Murat 2019). Sun et al. (2017) concluded that mineralogy and grain size have an influence on the mechanical performance of rocks. However, in their study, limited results on the relationship between the LA and geological parameters were found. In addition, no results on an MD test were reported. Geological quality assessment tests can be conducted to predict the performance of the material, and one frequently used method is the well-known Mohs mineral hardness scale (see Table 1). Hardness is determined by the scratch resistance against two minerals (Mohs 1825).

Despite numerous debates over precision and inconsistency due to non-linearity, some researchers (Rezaei et al. 2009; Anikoh et al. 2015; Banerjee and Melville 2015) have used it as a benchmark to calibrate and verify test specimens and other hardness scales.

The high demand of crushed rock aggregates for construction activities have resulted in increased depletion of natural bedrock reserves. Crushed rock aggregates account for almost 50% of aggregates production in Europe. The use of rock aggregates requires mechanical testing to ensure their suitability, which means that fragmentation and wear resistance should be assessed. For many decades, the LA and MD tests have been the most common methods and the frequent test protocols are EN-1097-2 and ASTM-C131, and EN-1097-1 and ASTM-D6928, respectively (see description of test methods below). Today, it is well known that geological composition significantly influences mechanical performance of aggregates. However, no comprehensive review of the relationship between geological parameters and Los Angeles and micro-Deval tests is conducted. In view of the many parameters that impact the performance of aggregates, a systematic review of the relationship between geological parameters and mechanical performance, i.e. LA and MD, has been conducted. The goal of this review is to create a comprehensive study and identify the relationships for the purpose of academic and scientific research. The study prioritizes mineralogy, grain size, crystal size, grain shape, and porosity. The study showed that unlike the MD test, the relationship between the LA test and geological parameters has received increased attention in the last few years.

**Table 1** Mohs mineral hardness scale (adapted from Bilan et al. (2018))

| Minerals of Mohs scale | Mohs hardness |
|---|---|
| Talc | 1 |
| Gypsum | 2 |
| Calcite | 3 |
| Fluorite | 4 |
| Apatite | 5 |
| Orthoclase | 6 |
| Quartz | 7 |
| Topaz | 8 |
| Corundum | 9 |
| Diamond | 10 |

## Description of the LA and MD test methods

Today, the LA test method in North America is standardized by AASHTO T-96 and ASTM-C131, and in Europe by EN-1097-2. This test measures the fragmentation resistance of rock aggregates (Fig. 1). The Norwegian National Railway Administration in the 1950s adopted the test to investigate the performance of railway ballast (Nålsund 2014). The EN-1097-2 requires a standardized particle size of 10/14 mm, from which a 5000-g mass is derived. In this method, eleven steel balls of diameter 45–49 mm are added to the test mass; the total amount of revolutions is equal to 500, running at 31–33 rotation per minute. The steel balls were dropped from a height to disintegrate the aggregate particles in a dry condition. After the test, aggregates are washed on 1.6-mm sieve, and the mass loss (%) is determined. Both ASTM-C131 and EN-1097-2 standards make provision for different particle gradings as an alternative, i.e. large and narrow particle range and classification. Typical LA values of aggregates with varying textural characteristics from the three rock classes are shown in Table 2.

The micro-Deval test is a wet test which requires filling the cylindrical steel drum with 2.5 l of water (Fig. 2). The current micro-Deval tests are standardized in both North America by ASTM-D6928 and AASHTO T327 and in Europe by EN-1097-1. In this test, aggregates of mass 500 g are moisturized together with 5000-g spherical steel balls in a hollow drum of internal diameter 200 ± 1 mm. Rotation of the steel drum is set

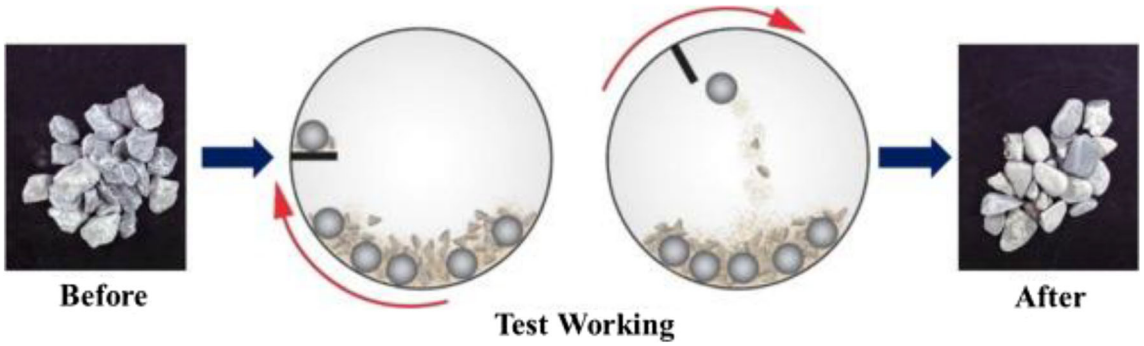


**Fig. 1** Diagram of the Los Angeles test setup and aggregates steel ball (crushing) interaction (adapted from Ge et al. (2018))

to 2000 revolutions running at a speed of 100 ± 5 rotation per minute. Afterwards, aggregates are washed on 1.6-mm sieve, and the average mass loss (%) of two test specimens is measured and calculated as the micro-Deval coefficient. It is also possible to perform micro-Deval tests on large and narrow particle range and classifications. In terms of test adequacy and performance, the micro-Deval test can properly determine the wear resistance of aggregates (Liu et al. 2017). Table 3 shows the MD coefficients of aggregates from igneous origin.

In terms of LA and MD, compliance to specific thresholds in road design manuals in connection to the performance of rock aggregates is important. In view of this, this review adopted the limit requirements of LA ≤ 30% for base and 35% for subbase courses and MD ≤ 15% for base and ≤ 15–20% for subbase courses, given in the Norwegian road construction handbook N200 (see Tables 4 and 5) to give concrete emphasis, clarity, and as reference to the resistant degree to both fragmentation and wear of the varying rock performances herein discussed in connection to their geological properties.

## Maximum MD and LA values reported in different standards

Both Tables 4 and 5 show the thresholds for MD and LA values for aggregates in varying applications.

## Influence of rock mineralogy

To assess the relationship between mineralogic composition and the fragmentation resistance, several parameters including cleavage plane, the content and type of minerals, the disposition, hardness, and fracture can be used. The identification of minerals requires a thorough analysis of the crystal features. Mineral density can be categorized into three main groups: light (< 3.0 g/cm$^3$), intermediate (3.0–4.0 g/cm$^3$), and heavy (> 4.0 g/cm$^3$) and the formation process can either be endogenic or exogenic according to Bilan et al. (2018). It is known that during the original crystallization of rocks, primary minerals are formed and, in most cases, they have a strong influence on the strength properties than secondary and accessory minerals.

## Dominance of primary minerals

The fundamental role of primary minerals such as quartz and feldspar in rock aggregates is based on the content and crystal size. Siliceous minerals (e.g. quartzo-feldspathic) are mainly composed of silicates, aluminates, and alkalis and have a relatively high hardness value ranging from 6 to 7 on Mohs mineral hardness scale. Quartz formation during diagenesis by biogenic action promotes authigenic microcrystalline quartz and as a result enhances the resistance to break easily (Liu et al. 2018a, b). There are conflicting findings on the role of primary minerals such as quartz and feldspar contents in determining the mechanical strength of rock aggregates.

Phosphate mine rocks of limestone, marl, and flintstone origin of varying mineral compositions showed that high amount of siliceous fraction of quartz and cristobalite content together with considerable amount of dolomite, and proportional fractions of calcite, fluorapatite, albite, anorthite, and illite influenced both fragmentation (i.e. LA > 53%) and wear

**Table 2** LA values of aggregates from different rock classes

| Rock type | Rock class | LA min value (%) | LA max value (%) | No. of samples | Average | Reference |
|---|---|---|---|---|---|---|
| Limestone | Sedimentary | 20.50 | 41.20 | 11 | 26.67 | Ozcelik (2011) |
| Marble | Metamorphic | 22.60 | 36.30 | 11 | 27.95 | |
| Andesite | Igneous | 15.40 | 18.90 | 10 | 16.82 | |


**Fig. 2** Diagram of micro-Deval setup (**a**) and standard 10/14-mm aggregates specimen, steel drum, and 5-kg spherical steel balls (**b**) (adapted from Durmeková et al. (2019))

(i.e. MD > 53%) resistance (Amrani et al. 2019). In the same study, fragmentation resistance increased for a fraction of these rocks with small content of cristobalite and illite, and high quartz content with LA < 48% (Amrani et al. 2019). The authors, however, suggested that the variation of performance was due to the presence of clay and flintstone. The study by Ajagbe et al. (2015) showed that the ratio of quartz and feldspar (QFR) is directly proportional to the LA. In their study, due to the proportional weights of quartz and feldspar content, the LA varied from 16 to 21%, and the presence of amphibole minerals in banded gneiss reduced the LA strength (Ajagbe et al. 2015). The ratio of quartz and feldspar together with small content of biotite, muscovite, and opaque minerals was found in granite gneiss and granite rock aggregates with average LA results of 26% each but quartzite with a relatively high composition of quartz; insignificant feldspar and similar content of biotite, opaque minerals, and muscovite showed LA > 30% (Ademila 2019). In the same study, although charnockite had a low content of quartz and feldspar, the presence of hornblende and hypersthene minerals must have contributed to the LA of 26% (Ademila 2019). Similar volume of quartz, feldspar, plagioclase, and mica was found for granite gneiss and biotite granite; however, LA coefficients were 27% and 22%, respectively (Egesi and Tse 2012). The same study found that increased content of muscovite in schist resulted in low resistance to fragmentation. The study by Pang et al. (2010) and Afolagboye et al. (2016) showed that high content of quartz or feldspar, or a combination of both, resulted in high fragmentation resistance; however, the overall performance also depends on other textural factors.

The lack of consistency existing between the content and disposition of minerals and how they influence strength parameters are linked to the metamorphosis process. However, one common concept of the metamorphosis of granite into granite gneiss is that both can have similar mineralogical compositions. The metamorphosis process of granite is believed to have a greater influence on the structural orientation (i.e. planar fabric and foliation) than on mineral transformation. Rocks of metamorphic origin with fine to very fine-grained felsic, and mica sparkle together with chlorite, epidote-zoisite, and calcite composition had a satisfactory LA of 30% but MD > 24% was reported (Barbieri et al. 2019). The same study found that igneous rocks which had been metamorphosed from coarse feldspar into fine epidote, with small content of chlorite and insignificant amount of calcite but a high content of quartz, fine feldspar, and amphibolization showed stronger resistance to both wear (MD of 10%) and fragmentation (LA of 17%). The LA and MD of two types of intrusive rocks (i.e. granitoid and gabbroid rocks) with varying mineralogical compositions have been analysed: quartz, feldspar, and mica minerals predominated the mineral composition of granitoid rocks while feldspar, mica, olivine, and pyroxene dominated gabbroid rocks. On average, mica content in gabbroid was small; thus, the small mica content together with other textural features had a positive influence on LA < 24% and MD < 11% (Johansson et al. 2016). In the study by Amuda et al. (2014), the high resistance to fragmentation of porphyritic granite was attributed to the low content of mica (biotite and muscovite).

Mica minerals (biotite and muscovite) are phyllosilicates, and they form in distinct layers in both intrusive and extrusive

**Table 3** MD values of aggregates from igneous origin

| Rock type | Rock class | MD min value (%) | MD max value (%) | No. of samples | Average | Reference |
|---|---|---|---|---|---|---|
| Basalt | Igneous | 7 | 13 | 9 | 9 | Apaydın and Murat (2019) |
| Granitoids | Igneous | 2 | 19 | 17 | 8 | Johansson et al. (2016) |
| Gabbroids | | 7 | 11 | 9 | 9 | |

**Table 4** Referenced micro-Deval limits for aggregates applications

| Application | Maximum micro-Deval abrasion loss (%) | Standard |
|---|---|---|
| Granular subbase | 30 | ASTM D6928-10 (2010) |
| Granular base | 25 | |
| Open-graded base course | 17 | |
| Structural concrete | 17–21 | |
| Concrete pavement | 13 | |
| Asphalt concrete base course and secondary road surface course | 21 | |
| Asphalt concrete surface course | 17–18 | |
| Base layer and subbase layer | 15 | NPRA. Håndbok N200 vegbygging. ( 2014) |
| Open-graded base and stone matrix asphalt | < 20 | General Directorate of Highway, Turkish Highway Technical Specifications, Ankara, Turkey ( 2013) |
| Bituminous base, surface coatings | < 25 | |

*ASTM*, American Society for Testing and Materials; *NPRA*, Norwegian Public Roads Administration

rocks. Increased content of mica reduces the mechanical strength. It was observed that about 15–20% of mica content in meta-greywacke aggregates did not compromise the fragmentation resistance (LA of 19%) while amphibolite aggregates with sparkle or no traces of mica content but high percentages of plagioclase and actinolite showed stronger resistance (LA of 9%) (Anastasio et al. 2016; Fortes et al. 2016). The detrimental effect by mica content is also connected to the distribution and structural formation of the grain boundaries (Fortes et al. 2016). Similar results were found by Nålsund (2010), where 20% of mica content had no damaging influence on the LA and MD performance. The rocks, however, had 65% of quartz and 15% of feldspar, i.e. QFR. The study by Petrounias et al. (2018a, b, c) also demonstrated that low content of phyllosilicate minerals have no detrimental effects on the engineering properties of rocks. This has been observed in a recent study (Solomon et al. 2020, manuscript in preparation).

The degree of weathering of plagioclase (solid solution of albite and anorthite) seems to have a significant effect on the mechanical performance. Plagioclase is mostly found in igneous and metamorphic rocks and sometimes in sedimentary rocks. Plagioclase has a hardness scale of 6–6.5. The study of ballast fouling by Apaydın and Murat (2019) of basalt rock aggregates from different sources showed that the LA (9–11%) increased with increased content of plagioclase mineral (10–28%) and opaque minerals (0.12–2.67%). This may indicate that the content of weathered plagioclase and opaque influences the resistance to fragmentation. Similar results were obtained in the study of the geotechnical performance of pyroclastic rocks by Okogbue and Aghamelu (2013). In their study, high content of weathered plagioclase ranging from 21 to 60% and other weathered minerals, including shale and lithic fragments ranging from 11 to 32%, and groundmass 11–36%, contributed to varying LA performances from 11 to 25%. The authors, however, claimed that these mineral properties would end up compromising the mechanical strength of pyroclastic rocks in a long term. Conversely, the study by Pomonis et al. (2007) showed that high content of plagioclase minerals 46–50% in dolerites and 68–71% in troctolites rocks

**Table 5** Maximum LA values reported in different standards

| Application | Maximum Los Angeles value (%) | Standard |
|---|---|---|
| Base layer | 30 | NPRA. Håndbok N200 vegbygging. ( 2014) |
| Subbase layer | 35 | |
| Aggregates for roads | 40 | ASTM C-131 (2008) |
| Surface treatment and porous asphalt | 30 | BS EN-13043 (2002) |
| Base layer | 50 | ASTM D-692 (2004) |
| Surface layer | 40 | |
| Aggregates (coarse) for concretes | 50 | ASTM C-33 (2013) |

*ASTM*, American Society for Testing and Materials; *BSI*, British Standard Institution; *NPRA*, Norwegian Public Roads Administration

has little effect on the LA performance of 10–13% and MD of 5–8%. It was however claimed that the plagioclase had suffered secondary weathering to form pockets of albite.

So far, the mixed findings on the effects of primary minerals in relation to both LA and MD show that it is important to study other textural properties to have a clearer overview of the behaviour and performance of rocks. However, most researchers claimed that the performance of rocks was based on the content of quartz or feldspar or the QFR and mica (biotite and muscovite). Overall, most of the rocks studied have good LA and MD performance based on the thresholds given in the Norwegian road construction handbook N200.

## Secondary and accessory minerals

Secondary minerals are formed by hydrothermal alteration and weathering of the Earth's crust. The transformation process involves environmental factors such as water, temperature, and other biological activities. Accessory minerals, on the other hand, mostly appear in small quantity and are therefore not regarded in the identification of rock type. Some examples include apatite, zircon, topaz, and magnetite.

The LA performance increased from 15 to 23% for pyroclastic rocks in the study by Aghamelu and Okogbue (2015), due to increased content of chlorite and glassy material. The authors claimed that the presence of these minerals could over a period of time cause strength failure. In the study by Pang et al. (2010) and Jayawardena (2017), the LA performance of 25% and 33–38%, respectively, of limestone showed that the strength depends on the content of calcite mineral. Both authors claimed that limestone may not be suitable for surface layer of road pavement. Calcite is a secondary mineral and is mainly found in marble and limestone. Calcite has a hardness value of 3 on Mohs scale. Similarly, in the study by Naeem et al. (2014), it was found that increased LA from 14 to 23% was based on increased content of calcite from 12 to 65%. The authors, however, found varying contents of bioclasts and micrite also in the limestone samples but concluded that rocks composed of small dolomitic content 5–15% in the matrix influenced the LA. In this case, emphasis was placed on the ratio of soft mineral (dolomite) in the matrix although other minerals, bioclast 5–20% and micrite 15–35%, may also have influenced the LA performance. Dolomite has a Mohs hardness value of 3.5–4, which is slightly higher than calcite.

The study by Petrounias et al. (2018a, b, c) showed that high serpentinization of ultramafic rocks resulted in LA value of 25–28%, whereas mafic and granodiorite rocks with LA of 7–20% had plagioclase and clinopyroxene, quartz, and hornblende in some of the rock components and albitite rocks with LA of 11–13% had quartz and clinopyroxene. In another study, Petrounias et al. (2018a, b, c) reported that serpentinization increased the LA values of serpentinite rocks from 17 to 25% and andesite rocks from 18 to 35%. The authors indicated that the presence of smectites in andesite rocks contributed to increasing the LA.

The research by Giannakopoulou et al. (2016) showed the effects of petrography on the LA performance of ultramafic rocks (dunite, harzburgite, and lherzolite). In their study, all rocks had been weathered and consisted of high amounts of secondary serpentine mineral. Forty-two percent of serpentine mineral constituted dunites together with small amounts of chlorite and talc, 12% was found in harzburgite which also had minor chlorite and chromite, and 12–17% was found in lherzolite with traces of batite. Among all rocks studied, harzburgite had a good LA of 15% (Giannakopoulou et al. 2016). This certainly was due to the low serpentinization. In the study by Giannakopoulou et al. (2018a, b), it was found that the variation of LA from 14 to 32% of ultramafic rocks was based on the ratio of secondary (serpentine) to primary (SEC/PR) minerals. This, however, suggests the effect of weathering on the mechanical performance of rocks. Conversely, the authors indicated that the presence of serpentine 30–40% did not influence the LA performance of dunite rocks compared to other ultramafic rocks which had the same degree of weathering. They claimed that the uniform formation of soft serpentine and hard olivine network enhanced serpentine to absorb stress and reduce crack propagation in dunites.

Clay minerals in rocks are formed by chemical weathering and are classified as weak minerals, with Mohs hardness of 2–2.5. The studies by Giannakopoulou et al. (2018a, b) and Esfahani et al. (2019) indicated that the presence of clay in rock aggregates has a significant impact on the LA performance. Hartley (1974) also indicated that soft mineral reduces the strength performance of rocks.

In Fig. 3, eight types of rocks showed different LA performances. It can be seen that the LA values are low for samples 4, 6, and 7. This is because these samples had no traces of amphiboles but they had high contents of quartz and good QFR. The performance of other samples is dependent on the amount of amphibole and mica (biotite and muscovite). Amphiboles have a hardness of 5–6 and biotite and muscovite are ranked 2.5–3 and 2–2.5, respectively, on Mohs hardness scale. Amphibole is an altered product of pyroxene, and therefore increased content of amphibole minerals in rocks results in low resistance to fragmentation and wear (Johansson et al. 2016). Feldspar, on the other hand, seemed to have no significant effect on the LA performance despite its hardness value on Mohs scale. In Fig. 3, the findings indicate that the assessment of other textural properties is necessary to fully describe the mechanical performance.

Statistical analyses for systematic evaluation of the variation and correlation between textural characteristics and technical performance have been reported in several studies (Wang et al. 2015; Johansson et al. 2016; Ajalloeian and Kamani 2019). The use of regression analysis permits the

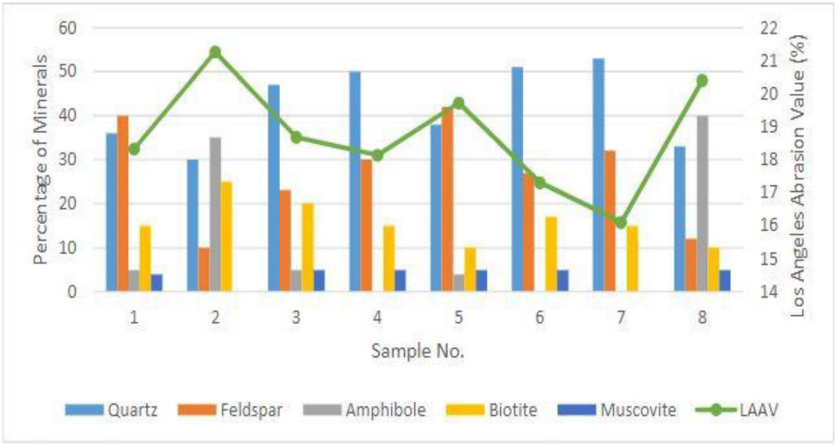


**Fig. 3** The relationship of Los Angeles abrasion value and mineral percentage of different types of rock (adapted from Ajagbe et al. (2015))

adoption of either Pearson or Spearman correlation coefficients to evaluate the relationship between two variables (Nagalli et al. 2016). In Table 6, linear, power, and polynomial regression equations are used to evaluate the effects between different mineralogic compositions, LA and MD. Zou et al. (2003) described Pearson correlation coefficients at 1, 0.8, 0.5, and 0.2, in strength directions as perfect, strong, moderate, and weakly positive, respectively, while −1, −0.8, −0.5, and −0.2 were described as perfect, strong, moderate, and weakly negative, respectively.

For ultramafic rocks, both equations showed almost strong and positive strength direction but the relationship of the influence of serpentine (SRP) mineral on LA is small compared to the ratio of secondary/primary (SEC/PR) minerals. Giannakopoulou et al. (2018a, b) indicated that increased contents of secondary minerals have a negative effect on the strength performance. Serpentinite is a product of ultramafic rock with serpentine minerals. The strength direction of the equation between SRP of serpentinite rock to LA can be described as close to strong and positive. Furthermore, the relationship between smectite and LA of andesite rock can be described as perfect and positive with much smaller influence on the LA compared to the relationship with serpentinite rock. In the study by Petrounias et al. (2018a, b, c), the LA increased with increased content of serpentine. The linear, second-, and third-order polynomial describes the relationship between quartz and LA of metamorphic rocks. The third-order equation described as strong and positive fits better the description of the relationship, which indicates that high quartz content results in high resistance to fragmentation.

The relationship between MD and mica content of granitoid rocks can be described as moderate and positive. The

**Table 6** Relationship between Los Angeles (LA) and micro-Deval (MD) tests and mineral content expressed in regression equation(s)

| Type of rock | Equation | Reference |
|---|---|---|
| Ultramafic rock | $LA = 0.141\ (SRP)^{a} + 16.343,\ R^2 = 0.65$ | Giannakopoulou et al. (2018a, b) |
| | $LA = 2.8042\ (SEC/PR)^{b} + 17.646,\ R^2 = 0.64$ | |
| Serpentinite rock | $SRP^{a} = 2.2156\ (LA) + 34.606,\ R^2 = 0.74$ | Petrounias et al. (2018a, b, c) |
| Andesite rock | $SM^{c} = 0.1688\ (LA) - 0.1194,\ R^2 = 0.99$ | |
| Metamorphic rock | $LA = -0.0006\ (Q^{d})^2 - 0.0674\ (Q^{d}) + 51.419,\ R^2 = 0.31$ | Dayarathna et al. (2017) |
| | $LA = -0.0002\ (Q^{d})^3 + 0.0366\ (Q^{d})^2 - 1.7955\ (Q^{d}) + 70.596,\ R^2 = 0.79$ | |
| | $LA = -0.1311\ (Q^{d}) + 52.812,\ R^2 = 0.30$ | |
| Granitoid rock | $MD = 2.843 + 0.384\ (M^{e}),\ R^2 = 0.50$ | Johansson et al. (2011) |
| | $MD = 3.601 + 0.413\ (M^{e}),\ R^2 = 0.57$ | |
| Basalt rock | $OP^{f} = 0.38\ (LA) - 3.01,\ R = 0.87$ | Apaydın and Murat (2019) |
| | $PL^{g} = 2.52\ (LA) - 7.99,\ R = 0.78$ | |
| Dolerites and troctolites | $PL^{g} = 10.78\ (MD) - 15.62,\ R^2 = 0.73$ | (Pomonis et al. 2007) |
| | $Q^{d} = 2E+17\ (MD)^{-21.574},\ R^2 = 0.91$ | |
| | $PL^{g} = 7.82\ (LA) - 36.02,\ R^2 = 0.47$ | |
| | $Q^{d} = 1E+17\ (LA)^{-15.945},\ R^2 = 0.85$ | |

[a] Percent of *SRP*, serpentine; [b] *SEC/PR*, ratio of secondary to primary minerals; [c] *SM*, smectite; [d] *Q*, quartz; [e] *M*, mica; [f] *OP*, opaque mineral; [g] *PL*, plagioclase

description of the equation of basaltic rocks and both opaque and plagioclase minerals showed to be strong and positive; however, the influence of opaque mineral on LA is small relative to plagioclase. In the case of both dolerites and troctolites, the description of the equation of quartz and MD relationship showed almost a perfect and positive strength direction while that of quartz and LA can be described as almost strong and positive. For MD and plagioclase of both rocks, the equation describing the relationship between the two yielded a much stronger and positive relationship compared with LA and plagioclase. In view of this, it can be mentioned that there is a greater effect of plagioclase on these rocks in MD than in LA.

## Influence of grain size and crystal size

Grain size and crystal size of rocks depend on the original formation and other transformation processes including weathering and hydrothermal alteration. The microstructure of different types of rocks appears in diverse composition and layer arrangements. Intragranular textures play a major role in the fragmentation and wear resistance of rocks. The relationship between compositional texture (crystal size, grain boundaries and sizes) and mechanical performance provides information about the behaviour and characteristics of materials in connection to their performance. The nature of these intrinsic properties is best quantified under microscopic investigations to obtain good approximations of the sizes (from μm to cm) and the interlocking boundaries.

Grain size is measured by the arrangement and composition of individual grains and they are often classified as fine, medium, and coarse. In contrast, crystal size constitutes individual crystals in a grain. The influence of these geological parameters on mechanical properties of rocks is widely investigated. Early studies include Kazi and Al-Mansour (1980) and Goswami (1984). Both authors found that pore volume and grain size significantly influenced the mechanical performance of acidic igneous rocks. In general, an increase in mean grain size (i.e. more than 1 mm) can result in a decrease of mechanical performance and vice versa. The dynamics of microstructure transformation (i.e. intragranular grain boundaries and arrangements) can give varying indications to the performance (Fortes et al. 2016; Johansson et al. 2016); therefore, textural grain and crystal size differences should also be connected to the ratio of fine to medium and coarse grain orientation in the matrix (Åkesson et al. 2001; Johansson et al. 2016). Furthermore, existing micro-fracture in a rock can promote rapid disintegration under impact test than others with no micro-fracture condition.

The effect of compositional texture (i.e. the matrix of groundmass and interlocking grain boundaries) gave variation of approximated LA performances for limestone (25%), granite (20%), gneiss (21%), and basalt (18%) (Pang et al. 2010). The spatial dispersion of fine-grained minerals investigated under cross-polarizer showed that hard minerals present in basalt, granite, and gneiss had strong interlocking grain boundaries and therefore enhanced the resistance to fragmentation compared to limestone with weak interlocking grains. Granite and basalt are of igneous sources and the formation of grain size and crystal size appear in different compositional textures. Basalt usually has a strong-grained interlocking texture and oftentimes leads to greater resistance to fragmentation and abrasion (Waltham et al. 1994). Granite, on the other hand, has varying granular textures and coarse-grained boundaries that increase brittleness (Anastasio et al. 2016).

The study by Aghamelu and Okogbue (2015) reported that the LA of pyroclastic rocks was 15–22%, despite the textural varieties of fine-grained to porphyritic in nature. The same study found that the changes of depositional action played a significant role since all the rocks had the presence of weak minerals; however, rocks of fine-grained texture but low glassy groundmass had LA of 15% (Aghamelu and Okogbue 2015). The micro-fabric (i.e. fine-porphyritic texture) of andesites contributed to the high resistance to MD of 7% compared to the coarse texture of porphyritic andesites which gave MD of 16% in the study by Török and Czinder (2017).

It is clear that the micro-fabric and fine-grained compositional textures have a good correlation to impact resistance from fragmentation. It is also worth considering that heterogenic textural characteristics (e.g. fine and medium, or medium and coarse) can be developed in some rock units during the transformation process. The performance of rocks with such microstructure feature can vary depending on the test method (i.e. LA and MD). The study by Lane et al. (2011) showed that under MD test, rocks of heterogenic grain textures (fine, medium, and coarse) can have worse performance due to poor interlock within and between the boundaries of the grain. Conversely, the resistance to disintegration in LA tests of porphyritic, fine-grained, and medium-grained granites did not vary significantly even though the photomicrographs of the rocks showed that fine-grained granites with an average LA of 22% was fine and equigranular in nature, the porphyritic granite gave average LA of 26–27% while medium-grained granites gave average LA of 23% (Afolagboye et al. 2016).

The effects of dispersion of grain size on the micro-macrostructure of granites from different locations are shown in Fig. 4. It can be observed that rock sample LTKWF-1, which is felsic in nature, has a strong dispersion of fine-grain sizes within the range 99% ≤ 1 mm and 79% ≤ 0.05 mm. The LA value of 16% shows that the interlock of the grain boundaries may have contributed to the resistance against fragmentation. FKNGRI-1 and FKNGR-2 are of the same origin but with different grain textures. FKNGRI-1 has a dominant amount of fine-grain (87% ≤ 1 mm) while FKNGR-2 has 81% ≤ 1 mm. KMSGR-1 and KMSTGR-2 were also collected from

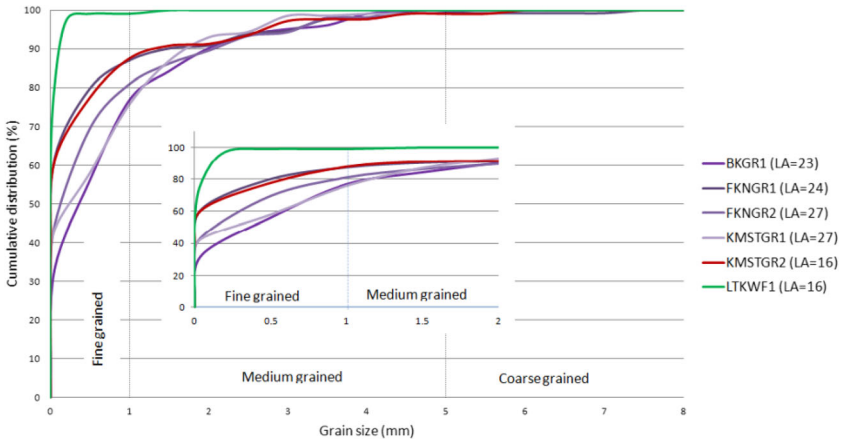


**Fig. 4** Distribution of grain size of granite samples with varying compositional textures, locations, and resistances against fragmentation (results) from LA tests. BKGRI-1 (medium-coarse grained), FKNGRI-1 and FKNGRI-2 (medium-grained), KMSTGR-1 (medium-grained), KMSTGR-2 (fine-grained microgranite), and LTKWF-I (fine-grained) (adapted from Jessica (2014))

the same source with considerable composition of fine-grained sizes, 76 ≤ 1 mm and 88 ≤ 1 mm, respectively. BKGR-1 has a composition of fine-grained sizes (77% ≤ 1 mm) and had a high resistance compared to FKNGRI-1, FKNGRI-2, and KMSGR-1. The reason for this could be due to the influence of other characteristics. Despite the difference in the texture, the performance of these granites is consistent with the LA values of granites reported to be 20.1–28.7% in the study by Afolagboye et al. (2016).

Figure 5 shows a strong and positive strength direction of the equation which describes the relationship between mean grain size and LA value for all granites. A similar relationship was also found between grain size and LA value for granitoid rocks which had been exposed to different degrees of crystallization (Johansson et al. 2011). Conversely, meta-sandstone, meta-greywacke, meta-gabbro, and greywacke with varying compositional textures and mineral grain sizes had no relationship to the LA performance (Anastasio et al. 2017). This means that the relationship of the LA test and geological composition of rocks from either one or multiple parent source could be different due to other textural characteristics; therefore, it is important to assess related genetical parameters simultaneously.

## The texture coefficient principle

One feasible approach to estimate the mechanical performance of rocks based on multiple geological factors is the use of texture coefficient (Howarth and Rowlands 1986; Howarth and Rowlands 1987; Ozturk and Nasuf 2013; Ajalloeian and Kamani 2019). The texture coefficient (TC) quantitatively analyses the orientation of grain shape, interlocking grain boundaries, and the parking density of the matrix by thin section image analyses and quantifies different components including form factor (FF), aspect ratio (AR), angle factor (AF), and area weighting (AW) of the grains (Ajalloeian and Kamani 2019), and the relationship to basic geometric data is given by the following equations.

$$\mathrm{FF} = \frac{4\pi.A}{P^2} \tag{1}$$

$$\mathrm{AR} = \frac{L}{W} \tag{2}$$

$$\mathrm{AW} = \frac{\sum(\text{Grain areas within the reference area boundary})}{(\text{Area boundary by the reference area})} \tag{3}$$

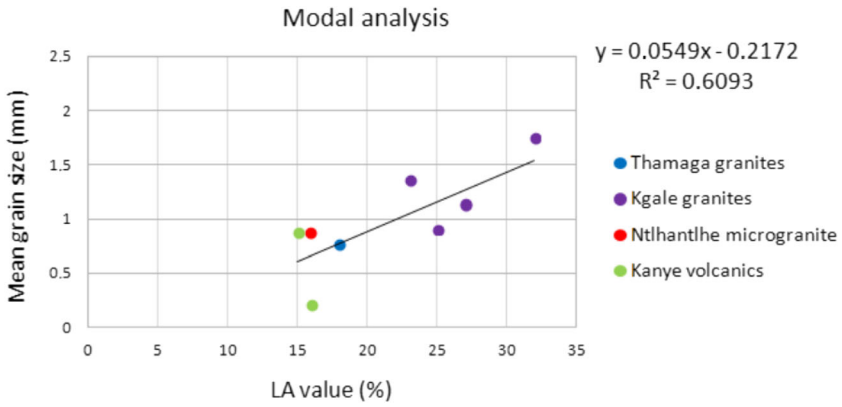


**Fig. 5** Distribution of mean grain size and LA value of granites in a modal analysis (adapted from Jessica (2014))

$$\mathrm{AF} = \sum_{i=1}^{9} \left\{ \frac{x_i}{\frac{N(N-1)}{2}} \right\} \times i \quad (4)$$

where $x_i$ is the number of angular differences in each class and N denotes the total number of elongated particles.

Form factor measures the deviation from the circularity of the grain cross section; the aspect ratio is simply the ratio of length to width. Angle factor determines the angularity of the grain and area weighting (AW) is the parking density of the matrix. In the case of $N_0$, $N_1$, AR, and AF, numerical values are assigned to regulate the precision and classification of the parameters when applied. TC is a parameter used in previous years, but it has been used in recent studies to evaluate the total effects of rock texture on the mechanical performance of rocks (Ozturk and Nasuf 2013; Esmailzadeh et al. 2017; Ajalloeian and Kamani 2019)

$$\mathrm{TC} = \mathrm{AW}\left[\left(\frac{N_0}{N_0+1} \times \frac{1}{\mathrm{FF}_0}\right) + \left(\frac{N_1}{N_0+N_1} \times \mathrm{AR}_1 \times \mathrm{AF}_1\right)\right] \quad (5)$$

where

| | |
|---|---|
| TC | texture coefficient |
| AW | grain packing weighting |
| $N_0$ | number of grains whose aspect ratio is below a pre-set discrimination level of 2.0 |
| $N_1$ | number of grains whose aspect ratio is above a pre-set discrimination level of 2.0 |
| $\mathrm{FF}_0$ | arithmetic mean of discriminated form factors for $N_0$ grains |
| $\mathrm{AR}_1$ | arithmetic mean of discriminated aspect ratios for $N_1$ grains |
| $\mathrm{AF}_1$ | angle factor, quantifying grain orientation for $N_1$ grains |

The weak bivariate statistical relationship between single components ($\mathrm{FF}_0$, $\mathrm{AR}_1$, $\mathrm{AF}_1$, $N_0$, $N_1$) and LA value showed the inefficient predictive capability of LA value using individual geological and geometrical components such as form factor, aspect ratio, angle factor, and area weighting: on the other hand, a strong and positive correlation ($R^2$ =0.64) was achieved for TC and LA (Ajalloeian and Kamani 2019). Furthermore, a strong and positive correlation coefficient ($R^2$ = 0.86) was achieved between TC and LA in polynomial regression analysis in the same study. At least, this gives conclusive evidence of the predictive capacity of LA value using TC. Despite the breakthrough with the use of TC, there are some limitations. One argument is that factors such as weathering and altered minerals, matrix type, mineralogical composition, and micro-cracks are not covered in the TC equation (Kamani and Ajalloeian 2019); therefore, in cases where the low correlation between TC and mechanical performance occurs, the reason could be due to failure in expanding the TC equation to include the aforementioned factors. The relationship between TC and LA and MD values are not well covered in the literature. This limits the opportunity to make a comprehensive case about the use of TC in the context of Los Angeles and micro-Deval tests.

## Morphology (grain shape) change in LA and MD tests

The continuous evolution of shape deterioration at the macro-scale leads to the loss of internal cohesion and destabilizes the skeletal framework for effective load transfer. The shape parameter (see Fig. 6) is categorized into three independent dimensions, i.e. surface texture, form, and angularity (Al-Rousan et al. 2007), which may also be called scale dependencies.

The form scale is a measure of the total boundary length or perimeter which could be quantified by flat and elongation, roundness, or sphericity index. Surface texture measures surface topography (e.g. surface micro-irregularities) and it can be analysed following the principles by the wavelet technique, spherical harmonic analysis, or Fourier series while angularity is a measure of the sharp edges or corners of the particle. Surface texture is a complex property: The characteristics of roughness could affect the resistance to friction between particles. Due to heterogeneity of surface morphological features, most used advanced methods such as three-dimensional (3D) laser scanners, optical interferometry, and X-ray micro-computed tomography (μXCT) are used to quantify true surface texture. In view of this, a brief overview of two aforementioned methods are described below.

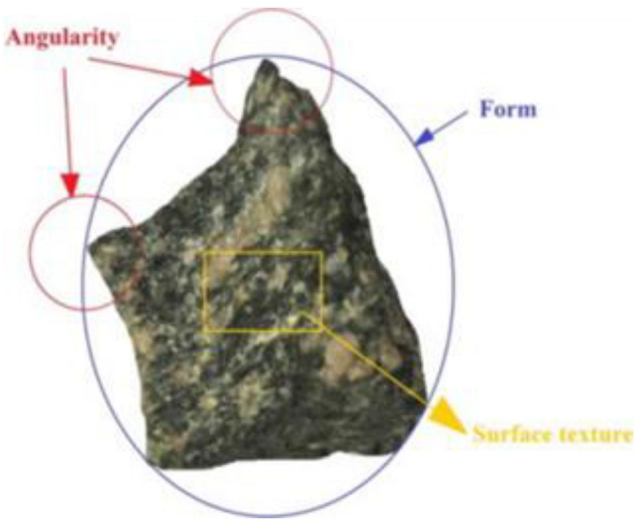


**Fig. 6** The shape properties of a coarse sample. Blue represents form, yellow denotes surface texture, and red indicates angularity (adapted from Guo et al. (2018))

## Methods for measuring surface texture

### 3D laser scanning

3D laser scanning techniques reflect a significant step in the advancement of measurements of volume and surface texture of rocks. This approach has been used by several researchers (Yang et al. 2019; Anochie-Boateng et al. 2012) to describe and to evaluate surface micro-irregularities, and to characterize other morphological properties (Guo et al. 2018). Furthermore, compared with other methods such as optical interferometry and X-ray micro-computed tomography (μXCT), 3D laser scanners are cost-effective, portable, and user-friendly. The 3D system provides adequate spatial coordinates of the points laying on the rock surface; moreover, the technology offers the possibility to make projections of polar coordinates on a Cartesian coordinate system to describe the characteristics of micro-irregularities (Asahina and Taylor 2011). In the same study, the authors adopted two sets of principles to define the coordinate system: axes in the Cartesian coordinate and the origin which is situated at the centre of the object.

This work adopted the techniques and processes outlined in Liu et al. (2018a, b) to demonstrate a typical 3D laser scanning of a rock particle (Fig. 7).

A rock sample of appropriate size is attached to a turntable and the required stages of rotational scans are taken at a high resolution, i.e. 0.02 mm in this case. A total of *n* scans covering all sides of the material are taken. The device throws a triangular laser beam on the spotted particle to capture the textural area and volume. While most 3D laser scanners have an integrated computerized software which automatically measures the morphological details of the captured region (i.e. surface area and volume), Liu et al. (2018a, b) developed a MATLAB to measure the morphological details of the captured images. Considering the capacity of X-ray micro-computed tomography (μXCT) and 3D laser scanners to measure small scale and large scale, respectively (Asahina and Taylor 2011), the measurements performed with the two technologies seem to be consistent. Furthermore, it was found that 3D laser scanners cannot penetrate the internal structure of solid particles (Liu et al. 2018a, b), and therefore only a 3D reconstruction on the surface can be created; on the other hand, μXCT does not suffer from this limitation.

### X-ray micro-computed tomography

X-ray micro-computed tomography (μXCT) is a rapid and non-destructive test which applies X-ray attenuation to investigate the internal structure of solid particles. The μXCT is very effective and has therefore been applied in a wide range of material investigations (i.e. soil and rocks) and in different fields.

The process involves the transmission of an X-ray beam through a fixed sample (e.g. rock particle) and a collection of radiograph projections as the sample continuously rotates or at defined scan intervals. Each projection captures a cross section (slice) of the fixed sample and all of them are eventually superimposed to produce the true three-dimensional volume. According to Liu et al. (2018a, b), the highest resolution of the captured images reported in Fig. 8 was 5 μm at 1024 × 1024 pixels and the greyscale images obtained after the process were analysed for surface area and volumes using the VGStudio MAX software.

One dilemma is that some researchers have raised concern that both LA and MD do not give reliable estimates of the long-term influence of morphology due to short test durations. These researchers claim that the constant cycles of aggregate-steel ball interaction are not a significant representation of the dynamics and frequency of vehicular fragmentation and wear

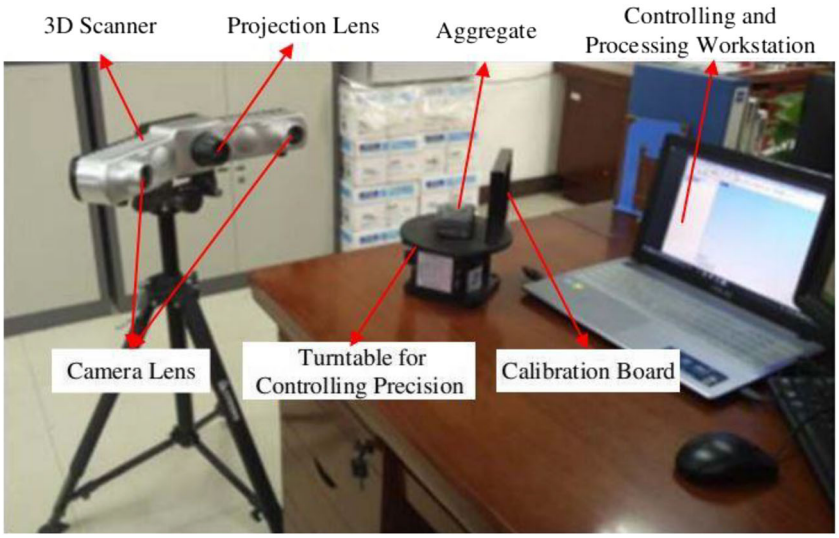


**Fig. 7** Setup of the 3D laser scanner to rock particle (adapted from Liu et al. (2018a, b))

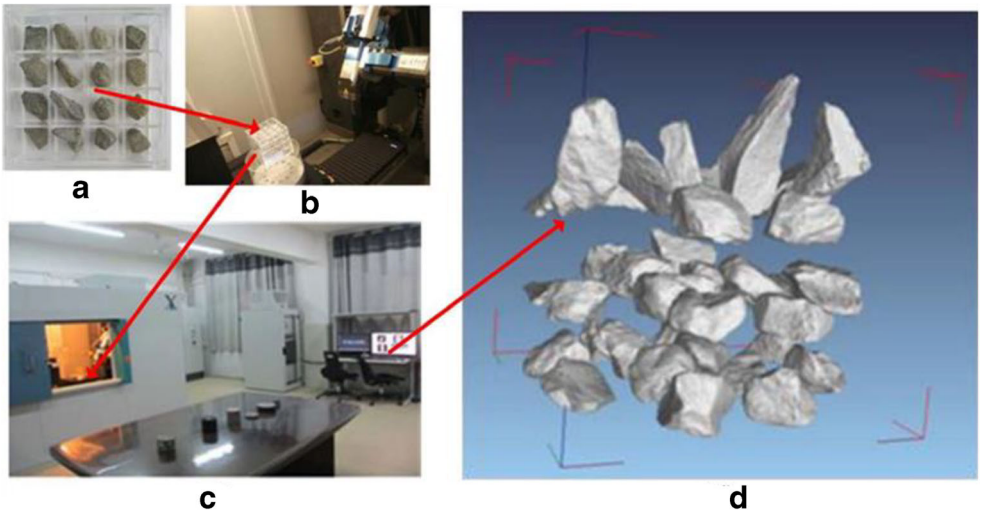


**Fig. 8** X-ray CT aggregates scanning process (images courtesy of Dr. Fangyuan Gong): (**a**) aggregates; (**b**) scanning sample; (**c**) X-ray CT setup; (**d**) 3D models from X-ray technology (adapted from Liu et al. (2018a, b))

impact; therefore, these cycles do not give any information about long-term durability.

## Morphology change in MD test

In the MD test, the surface texture, grain vertices, and sharp edges wear off while the LA test disintegrates the complete shape. Elongated, flat, and sharp edges generally tend to show weak resistance to continuous fragmentation and wear impact. However, the frequency and deformation behaviour also depends on the duration of the test. To understand the evolution of grain erosion, the use of 3D image analysis instead of 2D in connection to numerical simulations is described as effective methods to study the morphological behaviour before and after impact (Wu et al. 2018; Quintanilla et al. 2019). The issue of frequency and increased rotation cycles of modified MD as opposed to standard test cycle could result in unresponsive morphological changes (Wang et al. 2015). On the other hand, increased rotation cycles of LA could significantly decrease the steepest apex of particles and worsen the interlocking property. One reason could be connected to the development of larger, rounded, and stronger convex bands which enhances wear resistance (Quintanilla et al. 2017; Quintanilla et al. 2019). In the same study, the standard MD test was observed to have little influence on the form morphological descriptor of ballast granite while surface texture and angularity suffered rapid wear. Similarly, the morphological properties of varying aggregates and MD test cycle revealed that increased deterioration of angularity after the test contributes highly to the loss of mass than the wear of surface texture and sphericity (Lane et al. 2011; Wang et al. 2017).

The obvious reason for the rapid and increased eroding of angularity is connected to the interaction between the steepest apex of particles and other test particles, steel balls, and inner hard surface of the steel cylindrical mould for the MD test. Further possible explanation given to the variation of the degree of deterioration between the morphological properties in relation to MD test cycle is that both MD test and morphological parameters have a relationship to other mineralogic properties including Mohs mineral hardness value; therefore, high Mohs hardness value leads to low wear on the particle (Wang et al. 2017).

Figure 9 shows the modelled effects on morphological parameters in a standard MD test. The apex of the ballast particle and other grain vertices progresses into a round shape along with the MD test. The concave and rough topography of the surface texture have been smoothened, while the erosion of the perimeter (form) may result in loss of mass.

## Morphology change in the LA test

The measuring orientations of LA on particle morphology make it possible to use digital image and estimation chart (e.g. Krumbein chart) for the sphericity and roundness index. The study by Okonta (2015) found that the ability of ballast quartzites to abrade after three to four cycles of LA by the chart method gave a consistent rating scale of progressive disintegration measured by the image analysis. The quartzites, however, appeared to be more rounded when abraded to 20% LA to failure (Okonta 2015). The LA abrades larger shapes into small particles over several turns; therefore, digital image gives effective estimation of morphological changes. Using digital image to quantify morphology, Qian et al. (2014) made two observations after several turns of LA: (1) increased rotations of LA largely disintegrates the form descriptor of the aggregates and (2) small particles generated during the test experience little or no damage on angularity, surface texture, and form descriptors since these particles are mostly shielded from the impact by the steel balls.

The loss of angularity of granite (25%), limestone (27%), tuff (21%), and diabase (20%) was consistent to the LA values (i.e. 21%, 25%, 20%, 16%), respectively (Zhang et al. 2020).

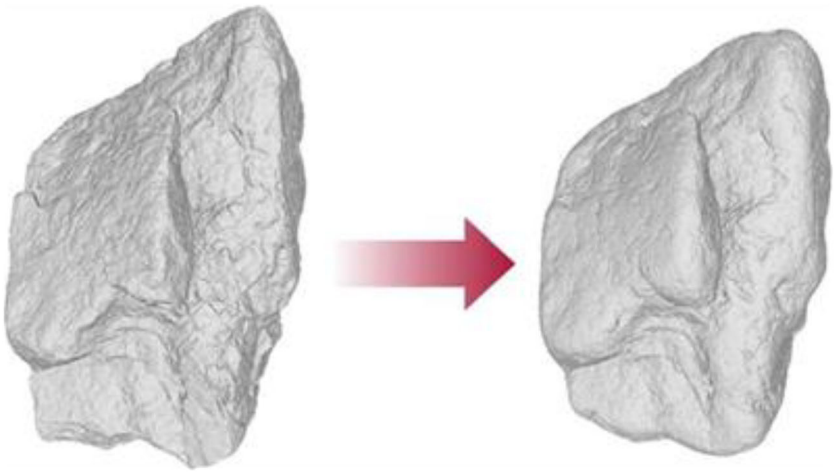

**Fig. 9** Changes in the modelled morphology of ballast before and after the standard micro-Deval test (adapted from Quintanilla et al. (2019))

The gradual loss to angularity during the LA test is connected to the ratio of flakiness and elongation index of coarser specimens. This means aggregates that record high mass loss have a high ratio of flakiness and elongation index and hence become susceptible to break under impact test. By this, it is important to respect flakiness and elongation index for test specimens. A simple validation of the loss of steep apex of ballast grains was demonstrated by Guo and Jing (2017) and Guo et al. (2018), where the average abrasion depth (AAD) and maximum abrasion depth (MAD) were designed to quantify the individual abrasion degradation and loss of steep apexes after an LA test. With simple numerical expressions, their study showed that flat and elongated particles have the highest deterioration at the apex regions than cubic particles. The production of coarse particles of quality morphological parameters depends on the crushing stages and mechanisms. The study by Rajan and Singh (2020) mentioned that the two- and three-stage crushing is reasonable to produce basaltic aggregates of standard morphological parameters. Their investigations showed that up to three-stage crushing was sufficient to produce aggregates of quality interlocking and textural properties which could be used in asphalt mixes. To this extent, the shape distribution of coarse particles must be proportional to the sizes in which they appear.

## Influence of porosity

Porosity is the pore volume of a rock. The variation of pore volume in each type of rock depends on the transformation and development process. Porosity is classified into two groups following the transformation process: primary porosity, which refers to existing pore space and its distribution between the grains and matrix before deposition, and secondary porosity, which occurs after the deposition process as a result of fracturing, recrystallization, and weathering.

The effects of porosity on mechanical performance are widely discussed in the literature (Hartley 1974; Kazi and Al-Mansour 1980; Kahraman and Fener 2007; Ugur et al. 2010; Esfahani et al. 2019) in connection to a variety of aggregates and several numerical cut-offs to differentiate the cluster of less or more porous volume on aggregates. With regard to LA, the effect becomes obvious due to the impact nature from the steel balls compared to MD. Aggregates of high porosity disintegrate more rapidly than those with low porous nature (Kahraman and Fener 2007). The estimate on what appears to be less or more porous nature is also based on the type of rock and grain arrangement together with the applied technique since different test techniques (e.g. water absorption and porosimetry tests) produce different coefficients given in percentage or decimal and micrometre (μm). In this review, the distribution of porosity is primarily based on water absorption and porosity tests.

The relationship between porosity and mechanical performance is commonly demonstrated using statistical regression equations. However, remarkable differences exist between the collective assessment of porosity and LA and MD of aggregates from all three rock units compared to each single unit. These differences show different correlations in regression functions. Igneous rocks with almost perfect and positive coefficient ($R$ = 0.93) in a power equation compared with sedimentary ($R$ = 0.44) and metamorphic ($R$ = 0.35) showed high sensitivity to the strength direction of the equation: which describes the relationship between LA performance and porosity for igneous rocks (Ozcelik 2011). In this case, although the igneous rocks had good LA values (15–19%), it recorded the highest margin of porosity index from 3.10 to 4.97%, compared to sedimentary (0.20–5.15%) and metamorphic (0.16–0.41%). Conversely, Esfahani et al. (2019) correlated porosity to LA of 273 rock datasets from igneous, sedimentary, and metamorphic origin: the relationship of porosity to LA showed weak and positive coefficient correlations in linear ($R$ = 0.34) and almost moderate and positive correlations in a

quadratic function ($R = 0.41$). The same study found that the multiple correlation of water absorption, porosity, and density to LA gave almost strong and positive coefficient ($R = 0.85$) and therefore for such assessment, multiple regression analysis is suitable (Esfahani et al. 2019).

Petrounias et al. (2018a, b, c) found that the large LA variation (7–58%) of igneous rocks (ultramafic, mafic, and intermediate-acidic volcanic) was due to variation of total porosity 0.48–11.93% with coefficient of $R^2 = 0.76$ to LA and $R^2 = 0.65$ of water absorption 0.14–2.13% to LA. Linear function suitably expressed the relationship between porosity and LA while exponential function was used to express the relationship between water absorption and LA. Mafic rocks with good total porosity and water absorption values showed greater resistances to LA (Petrounias et al. 2018a, b, c). In a similar study by Rigopoulos et al. (2013), the linear function between LA 10 and 43% of varying aggregates in the trachyte, mafic, and ultramafic group showed almost strong and positive correlation coefficient of $R^2 = 0.76$ to water absorption. The linear correlation between water absorption 0.52–1.36% and LA 14–25% of limestone yielded a strong and positive coefficient of $R = 0.81$, while that of total porosity of 2–8% and LA was also strong and positive ($R = 0.88$) in the study by Naeem et al. (2014). Similar results are reported in the study by Ioannou et al. (2010) where the coefficient ($R^2 = 0.76$) was found between the water absorption 1.6–5.6% and LA > 23% of limestone. The authors indicated that weathering activities influenced the distribution of pore size and performance.

Table 7 gives a summary of the relationships between porosity, water absorption, and LA. The strength direction of the equations describing the relationships is largely characterized by moderate to strong correlation coefficients and few equations which are close to perfect correlations. These may give the indication of the effects of porosity on the mechanical performance of rocks.

## Conclusions

A comprehensive literature review study has been conducted to establish the relationship between geological parameters (mineralogy, grain size, crystal size, grain shape, and porosity) of rocks and two most common tests: the Los Angeles (LA) test and micro-Deval (MD) test. The geological make-up of rocks comprise of a wide range of properties that influence the physical-mechanical performance. In view of the findings, Table 8 gives a summary following the chronological structure of thematic concepts discussed in the paper, i.e. geological factors as type, and their effects on LA/MD.

The findings of the review study prove that it is not sufficient to draw final conclusion regarding the mechanical

**Table 7** Summary of the relationship between LA and porosity, water absorption given in regression equations

| Type of rock | Equation | Reference |
|---|---|---|
| Igneous, sedimentary, and metamorphic | $LA = 1.293P^a + 27.472$, $R = 0.342$ | Esfahani et al. (2019) |
| | $LA = 3.057WA^b + 21.463$, $R = 0.596$ | |
| | $LA = 30.371 - 0.901P^a + 0.162\ P^2$, $R = 0.418$ | |
| | $LA = 20.032 + 4.673WA^b - 0.13WA^{b2}$, $R = 0.607$ | |
| Limestone | $LA = 1.8744WA^b + 20.489$, $R^2 = 0.76$ | Ioannou et al. (2010) |
| Limestone | $LA = 5.906\ (n_t{}^a) + 1.5039$, $R = 0.88$ | Naeem et al. (2014) |
| | $Wa^b = 0.0577LAV - 0.2856$, $R = 0.81$ | |
| Mafic | $LA = 3.3336n_t{}^a + 10.303$, $R^2 = 0.76$ | Petrounias et al. (2018a, b, c) |
| Ultramafic | $LA = 9.9902e^{0.7445w(b)}$, $R^2 = 0.65$ | |
| Intermediate-acidic volcanic | | |
| Trachyte | $LA = 10.0294W_a{}^b + 12.1085$, $R^2 = 0.76$ | Rigopoulos et al. (2013) |
| Mafic | | |
| Ultramafic | | |
| Metamorphic | $LA = 33.894\ (AP^a)^{0.1473}$, $R = 0.35$ | Ozcelik (2011) |
| Sedimentary | $LA = 13{,}164\ (UVW^b)^{-6.2501}$, $R = 0.54$ | |
| Igneous | $LA = 27.069\ (AP^a)^{0.08}$, $R = 0.44$ | |
| | $LA = 35{,}175\ (UVW^b)^{-7.3541}$, $R = 0.60$ | |
| | $LA = 9.974\ (AP^a)^{0.3937}$, $R = 0.93$ | |
| | $LA = 44.661\ (UVW^b)^{-1.1609}$, $R = 0.94$ | |

[a] (P, $n_t$, AP), porosity; [b] (WA,W, Wa, UVW), water absorption

**Table 8** Summary of major factors affecting LA and MD (types and effects)

| Type | Major findings on effects |
|---|---|
| Primary minerals and disposition<br>1. Quartz<br>2. Feldspar<br>3. Mica | -A larger content of quartz and feldspar increases the resistance to LA and MD.<br>-A mica content up to 15–20% in rocks does not compromise the overall strength property.<br>-The intragranular matrix of these minerals also contributes to the degree of disintegration and wear a rock experiences under the test regimes. |
| Secondary and accessory minerals and disposition<br>1. Serpentine<br>2. Chlorite group of minerals | -LA and MD performance largely depends on the content, and disposition of secondary and accessory minerals present in tested rock sample. |
| Textural composition<br>1. Grain size<br>2. Crystal size | -The size, shape, and spatial dispersion of mineral grains are mainly affected by foliation and subsequently influence the textural description and performance of rocks.<br>-Some authors mentioned that the grain size smaller than 1 mm coupled with fine-grained compositional texture also contributed to fragmentation and wear resistance. They argued that a grain size larger than 1 mm or medium- and coarse-grained fabric in some case enhances disintegration of rocks under impact from LA.<br>-Some rocks also develop heterogenic textural grain feature (i.e. fine, medium, and coarse or a combination of fine and medium, medium, and coarse). Rocks composed of such feature have poor grain interlock within the boundaries which in turn reduces resistance to LA and MD.<br>-The texture coefficient (TC) principle appears to be a feasible approach to analyse multiple textural parameters of the microstructure in relation to LA, in spite of its limitations. Furthermore, few studies have sought to adopt this approach and to establish the relationship with LA. |
| Textural composition<br>1. Grain shape | -Morphological description of rocks is based on three parameters, namely, form descriptor, surface texture descriptor, and angularity descriptor which all have independent influence on the performance of rocks by LA/MD test.<br>-Rocks composed of steep apex (angular) morphological features experience rapid disintegration/wear under LA/MD test.<br>-Rock surface texture is most likely to experience wear under MD test.<br>-Disintegration and wear of form descriptor enhance mass loss. |
| Textural composition<br>1. Porosity | -Most papers report moderate and strong positive correlation coefficients between porosity and LA. This means that highly porous rocks experience rapid disintegration under LA. |

performance based on one textural factor; thus, a simultaneous consideration of all the relevant factors is necessary. The relationship/correlation between MD and geological parameters is not widely considered compared to LA; therefore, research efforts in this area are needed. Furthermore, the relationship between LA, MD and micro-cracks, mineral spatial distribution, and mineral shape should be further investigated.

**Acknowledgements** Open Access funding provided by University of Agder.The work presented in this paper is part of the ongoing project MEERC (More Efficient and Environmentally Friendly Road Construction), partly funded by the Research Council of Norway (NFR) (project number 273700) and Sorlandets Kompetansefond.

## C - ompliance with ethical standards

**Conflict of interest** The authors declare that they have no conflict of interest.

**Open Access** This article is licensed under a Creative Commons Attribution 4.0 International License, which permits use, sharing, adaptation, distribution and reproduction in any medium or format, as long as you give appropriate credit to the original author(s) and the source, provide a link to the Creative Commons licence, and indicate if changes were made. The images or other third party material in this article are included in the article's Creative Commons licence, unless indicated otherwise in a credit line to the material. If material is not included in the article's Creative Commons licence and your intended use is not permitted by statutory regulation or exceeds the permitted use, you will need to obtain permission directly from the copyright holder. To view a copy of this licence, visit http://creativecommons.org/licenses/by/4.0/.

## References


Ademila O (2019) Engineering geological evaluation of some rocks from Akure, Southwestern Nigeria as aggregates for concrete and pavement construction. Geology Geophysics and Environment 45(1): 31–43. https://doi.org/10.7494/geol.2019.45.1.31

Afolagboye LO, Talabi AO, Akinola OO (2016) Evaluation of selected basement complex rocks from Ado-Ekiti, SW Nigeria, as source of road construction aggregates. Bulletin of Engineering Geology and the Environment 75(2):853–865. https://doi.org/10.1007/s10064-015-0766-1

Aghamelu OP, Okogbue CO (2015) Usability of pyroclastic rocks as construction materials; example from Nigeria. https://doi.org/10.1007/978-3-319-09048-1_240

Ajagbe WO, Tijani MA, Oyediran IA (2015) Engineering and geological evaluation of rocks for concrete production. Lautech Journal of Engineering and Technology 9(2):67–79 Retrieved from https://laujet.com/index.php/laujet/article/view/85

Ajalloeian R, Kamani M (2019) An investigation of the relationship between Los Angeles abrasion loss and rock texture for carbonate aggregates. Bulletin of Engineering Geology and the Environment 78(3):1555–1563. https://doi.org/10.1007/s10064-017-1209-y

Åkesson U, Lindqvist J, Göransson M, Stigh J (2001) Relationship between texture and mechanical properties of granites, central Sweden, by use of image-analysing techniques. Bulletin of Engineering Geology and the Environment 60(4):277–284. https://doi.org/10.1007/s100640100105

Al-Rousan T, Eyad M, Erol T, Tongyan P (2007) Evaluation of image analysis techniques for quantifying aggregate shape characteristics. Construction and Building Materials 21(5):978–990. https://doi.org/10.1016/j.conbuildmat.2006.03.005

American Society for Testing and Materials (2004) ASTM D692: standard specification for coarse aggregate for bituminous paving mixtures

American Society for Testing and Materials (2008) ASTM C131/C131M: standard test method for resistance to degradation of small-size coarse aggregate by abrasion and impact in the Los Angeles machine

American Society for Testing and Materials (2010) ASTM D6928: standard test method for resistance of coarse aggregate to degradation by abrasion in the micro-Deval apparatus

American Society for Testing and Materials (2013) ASTM C 33/C 33M: standard specification for concrete aggregates

Amrani M, Taha Y, Kchikach A, Benzaazoua M, Hakkou R (2019) Valorization of phosphate mine waste rocks as materials for road construction. Minerals 9(4):237. https://doi.org/10.3390/min9040237

Amuda AG, Uche OAU, Amuda AK (2014) Physicomechanical characterization of basement rocks for construction aggregate: a case study of Kajuru area, Kaduna, Nigeria. IOSR Journal of Mechanical and Civil Engineering 11(6):46–51

Anastasio S, Fortes APP, Kuznetsova E, Danielsen SW (2016) Relevant petrological properties and their repercussions on the final use of aggregates. Energy Procedia 97:546–553. https://doi.org/10.1016/j.egypro.2016.10.073

Anastasio S, Fortes APP, Hoff I (2017) Effect of aggregate petrology on the durability of asphalt pavements. Construction and Building Materials 146:652–657. https://doi.org/10.1016/j.conbuildmat.2017.04.126

Anikoh GA, Adesida PA, Afolabi OC (2015) Investigation of physical and mechanical properties of selected rock types in Kogi State using hardness tests. Journal of Mining World Express (MWE) Volume 4 https://doi.org/10.14355/mwe.2015.04.004

Anochie-Boateng JK, Komba J, Tutumluer E (2012) Aggregate surface areas quantified through laser measurements for South African asphalt mixtures. Journal of Transportation Engineering 138(8): 1006–1015. https://doi.org/10.1061/(ASCE)TE.1943-5436.000041

Apaydın ÖF, Murat Y (2019) Correlation of petrographic and chemical characteristics with strength and durability of basalts as railway aggregates determined by ballast fouling. Bulletin of Engineering Geology and the Environment: 1–9. https://doi.org/10.1007/s10064-019-01654-4

Asahina D, Taylor MA (2011) Geometry of irregular particles: direct surface measurements by 3-D laser scanner. Powder Technology 213(1–3):70–78. https://doi.org/10.1016/j.powtec.2011.07.008

Bahrami K, Aghda SMF, Noorzad A, Talkhablou M (2019) Investigation of abrasion and impact resistance of aggregates in different environments in Direh, Kermanshah, Iran. Geotechnical and Geological Engineering 37(3):2015–2028. https://doi.org/10.1007/s10706-018-0741-2

Banerjee KS, Melville RS (2015) Preliminary investigation of geotechnical properties of the rock aggregates commonly used for civil engineering construction in Trinidad and Tobago. West Indian Journal of Engineering 38(1)

Barbieri DM, Hoff I, Mork MBE (2019) Innovative stabilization techniques for weak crushed rocks used in road unbound layers: a laboratory investigation. Transportation Geotechnics 18:132–141. https://doi.org/10.1016/j.trgeo.2018.12.002

Bilan NV, Nikitenko IS, Tereshkova OA, Khazova OV (2018) Geology. Laboratory operations manual. Study of the Material Composition os the Earth's Crust

British Standard Institution (BSI) (2002) CEN 13043: aggregates for bituminous mixtures and surface treatments for roads, airfields, and other trafficked areas. European Committee for Standardization

Dayarathna IWTP, Puswewala UGA, Abeysinghe AMKB, Rohitha LPS (2017) Relationship between Los Angeles abrasion value and mineral content of metamorphic rocks

Durmeková T, Grega D, Tornyai R (2019) A high potential of the micro-Deval test in rock quality assessment. Acta Geologica Slovaca 11(1):1–9

Egesi N, Tse AC (2012) Engineering-geological evaluation of rock materials from Bansara, Bamenda Massif Southeastern Nigeria, as aggregates for pavement construction. Geosciences 2(5):107–111

Esfahani MK, Kamani M, Ajalloeian R (2019) An investigation of the general relationships between abrasion resistance of aggregates and rock aggregate properties. Bulletin of Engineering Geology and the Environment 78(6):3959–3968. https://doi.org/10.1007/s10064-018-1366-7

Esmailzadeh A, Behnam S, Mikaeil R, Naghadehi MZ, Saei S (2017) Relationship between texture and uniaxial compressive strength of rocks. Civil Engineering Journal 3(7):480–486. https://doi.org/10.28991/cej-2017-00000106

Fortes APP, Anastasio S, Kuznetsova E, Danielsen SW (2016) Behaviour of crushed rock aggregates used in asphalt surface layer exposed to cold climate conditions. Environmental Earth Sciences 75(21):1414. https://doi.org/10.1007/s12665-016-6191-3

GDH, Turkish Highway Technical Specifications (2013). General Directorate of Highway, Ankara, Turkey

Ge H, Sha A, Han Z, Xiong X (2018) Three-dimensional characterization of morphology and abrasion decay laws for coarse aggregates. Construction and Building Materials 188:58–67. https://doi.org/10.1016/j.conbuildmat.2018.08.110

Giannakopoulou PP, Tsikouras B, Hatzipanagiotou K (2016) The interdependence of mechanical properties and petrographic characteristics of ultramafic rocks from gerania ophiolitic complex. Bulletin of the Geological Society of Greece 50(4): 1829–1837. https://doi.org/10.12681/bgsg.11922

Giannakopoulou P, Petrounias P, Rogkala A, Tsikouras B, Stamatis P, Pomonis P, Hatzipanagiotou K (2018a) The influence of the mineralogical composition of ultramafic rocks on their engineering performance: a case study from the Veria-Naousa and Gerania ophiolite

complexes (Greece). Geosciences 8(7):251. https://doi.org/10.3390/geosciences8070251

Giannakopoulou PP, Petrounias P, Tsikouras B, Kalaitzidis S, Rogkala A, Hatzipanagiotou K, Tombros SF (2018b) Using factor analysis to determine the interrelationships between the engineering properties of aggregates from igneous rocks in Greece. Minerals 8(12):580. https://doi.org/10.3390/min8120580

Goswami SC (1984) Influence of geological factors on soundness and abrasion resistance of road surface aggregates: a case study. Bulletin of the International Association of Engineering Geology-Bulletin de l'Association Internationale de Géologie de l'Ingénieur 30(1):59–61. https://doi.org/10.1007/BF02594279

Guo YL, Jing GQ (2017) Ballast degradation analysis by Los Angeles abrasion test and image analysis method. The 10th International Conference on the Bearing Capacity of Roads, Railways and Airfields (BCRRA 2017), Athens

Guo Y, Markine V, Song J, Jing G (2018) Ballast degradation: effect of particle size and shape using Los Angeles abrasion test and image analysis. Construction and Building Materials 169:414–424. https://doi.org/10.1016/j.conbuildmat.2018.02.170

Hartley A (1974) A review of the geological factors influencing the mechanical properties of road surface aggregates. Quarterly Journal of Engineering Geology 7(1):69–100. https://doi.org/10.1144/GSL.QJEG.1974.007.01.05

Howarth DF, Rowlands JC (1986) Development of an index to quantify rock texture for qualitative assessment of intact rock properties. Geotechnical Testing Journal 9(4):169–179. https://doi.org/10.1007/BF01019511

Howarth DF, Rowlands JC (1987) Quantitative assessment of rock texture and correlation with drillability and strength properties. Rock Mechanics and Rock Engineering 20(1):57–85. https://doi.org/10.1007/BF01019511

Ioannou I, Petrou MF, Fournari R, Andreou A, Hadjigeorgiou C, Tsikouras B, Hatzipanagiotou K (2010) Crushed limestone as an aggregate in concrete production: the Cyprus case. Geological Soc Publishing House. 331:127–135. https://doi.org/10.1144/SP331.11

Jayawardena US (2017) Laboratory studies of Miocene limestone in Sri Lanka. Quarterly Journal of Engineering Geology and Hydrogeology 50(4):422–425. https://doi.org/10.1144/qjegh2016-106

Jessica S (2014) Comparative study of established test methods for aggregate strength and durability of Archean rocks from Botswana. Dissertation, Uppsala University

Johansson E, Lukschová Š,Miškovský K (2011) Petrographic characteristics of granitoid and gabbroid intrusive rocks as a tool for evaluation of mechanical properties. Technological properties of rock aggregates. Dissertation, Luleå University of Technology

Johansson E, Miškovský K, Bergknut M, Šachlová Š (2016) Petrographic characteristics of intrusive rocks as an evaluation tool of their technical properties. Geological Society, London, Special Publications 416(1):217–227. https://doi.org/10.1144/SP416.19

Kahraman S, Fener M (2007) Predicting the Los Angeles abrasion loss of rock aggregates from the uniaxial compressive strength. Materials Letters 61(26):4861–4865. https://doi.org/10.1016/j.matlet.2007.06.003

Kamani M, Ajalloeian R (2019) Evaluation of engineering properties of some carbonate rocks trough corrected texture coefficient. Geotechnical and Geological Engineering 37(2):599–614. https://doi.org/10.1007/s10706-018-0630-8

Kazi A, Al-Mansour ZR (1980) Influence of geological factors on abrasion and soundness characteristics of aggregates. Engineering Geology 15(3–4):195–203. https://doi.org/10.1016/0013-7952(80)90034-4

Lane DS, Druta C, Wang LB, Xue WJ (2011) Modified micro-Deval procedure for evaluating the polishing tendency of coarse aggregates. Transportation Research Record(2232): 34–43. https://doi.org/10.3141/2232-04

Liu J, Zhao S, Mullin A (2017) Laboratory assessment of Alaska aggregates using micro-Deval test. Frontiers of Structural and Civil Engineering 11(1):27–34. https://doi.org/10.1007/s11709-016-0359-5

Liu H, Guo W, Liu D, Zhou S, Deng J (2018a) Authigenic embrittlement of marine shale in the process of diagenesis. Natural Gas Industry B 5(6):575–582. https://doi.org/10.1016/j.ngib.2018.11.005

Liu Y, Gong F, You Z, Wang H (2018b) Aggregate morphological characterization with 3D optical scanner versus X-ray computed tomography. Journal of Materials in Civil Engineering 30(1):04017248. https://doi.org/10.1061/(ASCE)MT.1943-5533.0002091

Mohs F (1825). Treatise on mineralogy: or, the natural history of the mineral kingdom, A. Constable and Company, Edinburgh, and Hurst, Robinson, and Company, London

Naeem M, Khalid P, Sanaullah M, Din ZU (2014) Physio-mechanical and aggregate properties of limestones from Pakistan. Acta Geodaetica et Geophysica 49(3): 369–380. http:// https://doi.org/10.1007/s40328-014-0054-8.org

Nagalli B, Vasconcellos EMG, Nagalli A (2016) Correlation between petrographic and physico-mechanical variables of basalts of the Parana magmatic province. Electronic Journal of Geotechnical Engineering 21(1):363–374

Nålsund R (2010) Effect of grading on degradation of crushed-rock railway ballast and on permanent axial deformation. Transportation Research Record 2154(1):149–155. https://doi.org/10.3141/2154-15

Nålsund R (2014) Railway ballast characteristics, selection criterion and performance. Dissertation, Norwegian Univeristy of Science and Technology (NTNU)

Norwegian Public Roads Administration (NPRA) (2014) Håndbok N200 vegbygging. Norway, Vegdirektoratet

Okogbue CO, Aghamelu OP (2013) Performance of pyroclastic rocks from Abakaliki Metropolis (southeastern Nigeria) in road construction projects. Bulletin of Engineering Geology and the Environment 72(3–4):433–446. https://doi.org/10.1007/s10064-013-0489-0

Okonta FN (2015) Effect of grading category on the roundness of degraded and abraded railway quartzites. Engineering Geology 193:231–242. https://doi.org/10.1016/j.enggeo.2015.03.018

Ozcelik Y (2011) Predicting Los Angeles abrasion of rocks from some physical and mechanical properties. Scientific Research and Essays 6(7):1612–1619

Ozturk CA, Nasuf E (2013) Strength classification of rock material based on textural properties. Tunnelling and Underground Space Technology 37:45–54. https://doi.org/10.1016/j.tust.2013.03.005

Pang L, Wu S, Zhu J, Wan L (2010) Relationship between retrographical and physical properties of aggregates. Journal of Wuhan University of Technology-Mater. Sci. Ed. 25(4):678–681. https://doi.org/10.1007/s11595-010-0069-0

Petrounias P, Giannakopoulou PP, Rogkala A, Lampropoulou P, Koutsopoulou E, Papoulis D, Tsikouras B,Hatzipanagiotou K (2018a) The impact of secondary phyllosilicate minerals on the engineering properties of various igneous aggregates from Greece. Minerals 8(8). https://doi.org/10.3390/min8080329

Petrounias P, Giannakopoulou PP, Rogkala A, Stamatis PM, Lampropoulou P, Tsikouras B, Hatzipanagiotou K (2018b) The effect of petrographic characteristics and physico-mechanical properties of aggregates on the quality of concrete. Minerals 8(12):577. https://doi.org/10.3390/min8120577

Petrounias P, Giannakopoulou P, Rogkala A, Stamatis P, Tsikouras B, Papoulis D, Lampropoulou P, Hatzipanagiotou K (2018c) The influence of alteration of aggregates on the quality of the concrete: a case study from serpentinites and andesites from central Macedonia (North Greece). Geosciences 8(4):115. https://doi.org/10.3390/geosciences8040115

Pomonis P, Rigopoulos I, Tsikouras B, Hatzipanagiotou K (2007) Relationships between petrographic and physicomechanical properties of basic igneous rocks from the Pindos ophiolitic complex, NW Greece. Bulletin of the Geological Society of Greece 40(2): 947–958. https://doi.org/10.12681/bgsg.16778

Qian Y, Boler H, Moaveni M, Tutumluer E, Hashash YMA, Ghaboussi J. (2014) Characterizing ballast degradation through Los Angeles abrasion test and image analysis. Transportation Research Record(2448): 142–151. https://doi.org/10.3141/2448-17

Quintanilla ID, Combe G, Emeriault F, Toni JB, Voivret C, Ferellec JF (2017) Wear of sharp aggregates in a rotating drum. EPJ Web of Conferences, EDP Sciences. https://doi.org/10.1051/epjconf/201714007009

Quintanilla ID, Combe G, Emeriault F, Voivret C, Ferellec JF (2019) X-ray CT analysis of the evolution of ballast grain morphology along a micro-Deval test: key role of the asperity scale. Granular Matter 21(2):30. https://doi.org/10.1007/s10035-019-0881-y

Rajan B, Singh D (2020) Investigation on effects of different crushing stages on morphology of coarse and fine aggregates. International Journal of Pavement Engineering 21(2):177–195. https://doi.org/10.1080/10298436.2018.1449951

Rezaei A, Masad E, Chowdhury A, Harris P (2009) Predicting asphalt mixture skid resistance by aggregate characteristics and gradation. Transportation Research Record(2104): 24–33. https://doi.org/10.3141/2104-03

Rigopoulos I, Tsikouras B, Pomonis P, Hatzipanagiotou K (2013) Determination of the interrelations between the engineering parameters of construction aggregates from ophiolite complexes of Greece using factor analysis. Construction and Building Materials 49:747–757. https://doi.org/10.1016/j.conbuildmat.2013.08.065

Sun W, Wang L, Wang Y (2017) Mechanical properties of rock materials with related to mineralogical characteristics and grain size through experimental investigation: a comprehensive review. Frontiers of Structural and Civil Engineering 11(3):322–328. https://doi.org/10.1007/s11709-017-0387-9

Török A, Czinder B (2017) Relationship between density, compressive strength, tensile strength and aggregate properties of andesites from Hungary. Environmental Earth Sciences 76(18):639. https://doi.org/10.1007/s12665-017-6977-y

Ugur I, Demirdag S, Yavuz H (2010) Effect of rock properties on the Los Angeles abrasion and impact test characteristics of the aggregates. Materials characterization 61(1):90–96. https://doi.org/10.1016/j.matchar.2009.10.014

Waltham T, Bell F, Culshaw M (1994) Engineering geology for society and territory–Volume 5

Wang D, Wang H, Bu Y, Schulze C, Oeser M (2015) Evaluation of aggregate resistance to wear with micro-Deval test in combination with aggregate imaging techniques. Wear 338–339:288–296. https://doi.org/10.1016/j.wear.2015.07.002

Wang HN, Wang DW, Liu PF, Hu J, Schulze C, Oeser M (2017) Development of morphological properties of road surfacing aggregates during the polishing process. International Journal of Pavement Engineering 18(4):367–380. https://doi.org/10.1080/10298436.2015.1088153

Wu JF, Wang LB, Hou Y, Qian ZY, Meng LJ, Zhao Q (2018) Simulation on the micro-Deval test for the aggregate wear properties measurement. Construction and Building Materials 180:445–454. https://doi.org/10.1016/j.conbuildmat.2018.03.264

Yang, H. W., Lourenço, S. D., Baudet, B. A., Choi, C. E., Ng, C. W (2019) 3D analysis of gravel surface texture. Powder Technology, 346, 414–424. https://doi.org/10.1016/j.powtec.2019.01.074

Zhang S, Jianzhong P, Li R, Wen Y, Zhang J (2020) Investigation on comparison of morphological characteristics of various coarse aggregates before and after abrasion test. Materials 13(2):492. https://doi.org/10.3390/ma13020492

Zou KH, Tuncali K, Silverman SG (2003) Correlation and simple linear regression, RSNA . Published online. Radiology 227:617–628. https://doi.org/10.1148/radiol.2273011499

## Paper B

**S. Adomako**, C. J. Engelsen, T. Danner, R. T. Thorstensen, and D. M. Barbieri, "Recycled aggregates derived from excavation materials– Mechanical performance and identification of weak minerals,"*Bulletin of Engineering Geology and the Environment*, vol. (81), no. 8, pp. 1-12, 2022. https://doi.org/10.1007/s10064-022-02817-6

Bulletin of Engineering Geology and the Environment (2022) 81: 340
https://doi.org/10.1007/s10064-022-02817-6

ORIGINAL PAPER

# Recycled aggregates derived from excavation materials—mechanical performance and identification of weak minerals

Solomon Adomako[1] · Christian John Engelsen[2] · Tobias Danner[3] · Rein Terje Thorstensen[1] · Diego Maria Barbieri[4]

Received: 25 January 2022 / Accepted: 4 July 2022 / Published online: 30 July 2022
© The Author(s) 2022

## Abstract

The present study investigates the mechanical performance of recycled aggregates derived from excavation materials (REM). REM is blended with different quantities of recycled phyllite materials (RPM) and is investigated by Los Angeles (LA) and micro-Deval (MD) tests. X-ray diffraction (XRD) and acid solubility test are performed on the pulverized fractions < 1.6 mm obtained from the LA and MD tests to assess the respective degree of fragmentation and wear of mineral components. The results of the materials in unblended conditions showed considerable difference between MD performance while similar performance was found for LA. Furthermore, about 40% of RPM was sufficient to blend with REM without disturbing the required performance for blended mixtures. Mechanically weak minerals, i.e., phyllosilicates in RPM, significantly influenced the MD performance in blended and unblended varieties, and limestone minerals seem to disintegrate when mixed with amphibolite -which has the potential to dissolve in acidic environments.

**Keywords** Recycled excavation materials · Recycled phyllite materials · Los Angeles · Micro-Deval · Phyllosilicates

## Introduction

Recycled materials are receiving global attention thanks to the significant attainable environmental and economic benefits (Wang et al. 2018). However, large quantities of recycled materials (e.g., produced from construction and demolition waste (CDW), etc.) require significant management planning (Ritter et al. 2013). Given this, stringent legislative policies and regulations enforce the potential value. In Europe, for instance, one of the legal and action plan initiative for waste management is the Waste Framework Directive 2008/98/EC which present basic guidelines toward recycling and reuse (European Commission 2008). This initiative promotes resource efficiency by supporting recycle operations and the market value of recycled materials for construction activities (Haas et al. 2020).

Considering CDW, the European waste catalogue (EWC) specifies mineral waste that constitutes typical CDW in a table of sequence, where excavated soil, stones, and dredging spoil are listed. Hence, some countries consider excavated soil and land leveling materials as CDW (Ng and Engelsen 2018). The management of excavation materials particularly from construction activities has not received enough attention due to socio-economic and political reasons (Crawford et al. 2017; Dahlbo et al. 2015; Huang et al. 2018). This has made it almost difficult to trace and track global volume generated annually. Consequently, data on handling and use of excavation materials is under-reported (Magnusson et al. 2015). So far, readily accessible recycling technologies for CDW focuses more on other waste products such as wood, concrete,

✉ Solomon Adomako
solomon.adomako@uia.no

Christian John Engelsen
christianJohn.engelsen@sintef.no

Tobias Danner
tobias.danner@sintef.no

Rein Terje Thorstensen
rein.t.thorstensen@uia.no

Diego Maria Barbieri
diegomb271@gmail.com

1 Department of Engineering and Science, University of Agder, 4879 Grimstad, Norway

2 Department of Building and Infrastructure, SINTEF Community, Blindern, P.O.Box 124, NO-0314 Oslo, Norway

3 Department of Architecture, Materials and Structures, SINTEF Community, Postboks 4760 Torgarden, 7465 Trondheim, Norway

4 Department of Civil and Environmental Engineering, Norwegian University of Science and Technology, Høgskoleringen 7A, 7491 Trondheim, Norway

masonry, glass, etc. (Menegaki and Damigos 2018; Ng and Engelsen 2018; Tam and Tam 2006), than excavated soil. Nevertheless, a few countries such as France, Italy, Austria, and Switzerland have implemented national legislative and recycling guidelines to promote excavation materials, mainly from tunnel construction (Magnusson et al. 2015). Similarly, in Norway, national projects such as Kortreist stein (short-travelled aggregates) and RESGRAM (recycled aggregates from excavation masses) are designed to develop technological processing solutions for sustainable use of high-quality excavation materials. Norway has a long tradition of adopting national policies and regulations, economic incentives, and extended producer responsibility to promote recycle operations and to create a market for high-quality waste materials (Karstensen et al. 2020).

Currently in Western Norway, the production of recycled excavation materials (REM) using a modernized wet processing recycling technology is practiced. This technology may be regarded as one of the best processing methods when it comes to recycling large and complex stream of waste materials. It effectively produces quality products through its washing steps and separation efficiency. In addition, the technology balances processing, material quality and market performance. Given that recycled aggregates derived from REM vary from source to source in geology, and they constitute a significant amount of fine fraction with potential organic and clay contaminated particles, its management is complex. Hence, the technology operated in Norway is an ideal choice. The recurring challenge is that subsequent physical, mechanical, and chemical properties of processed REM are not consistent and stabilized. This is because the REM produced are occasionally constituted by phyllites in the stockpile (Norby 2020). Phyllites are characterized by layered silicates and have low strength properties (Dengg et al. 2018); hence in this context, this could contribute to the performance variation observed in processed REM. In the USA, New York City faces the challenge of enacting policies which may open for complete use of REM (Walsh et al. 2019). These developments increase the skepticisms about the service performance and overall use of REM. Nevertheless, some studies have demonstrated the feasible use of REM in other applications (Dengg et al. 2018; Lieb 2011; Voit and Kuschel 2020).

In general, the mechanical performance of recycled aggregates produced from excavation materials may be intrinsically linked to mineralogical constituents. In a recent study, the Los Angeles (LA) and micro-Deval (MD) performance of REM was studied (Norby 2020). The LA values were found to be in the region 25–28%, while the MD varied considerably from 7 to 20%. In another study, the LA of REM increased from 17–30% and 10–26% for MD (Barbieri et al. 2019). Both studies demonstrated in an X-ray diffraction (XRD) analysis that REM comprised of a significant amount of phyllosilicates (i.e., mica and chlorite minerals) (Barbieri et al. 2019; Norby 2020). Furthermore, a comprehensive review study of the influence of mineralogy and other geological parameters on the LA and MD performance of different rock aggregates has recently been published (Adomako et al. 2021). The study found that quartz and feldspar had a good correlation to LA and MD performance and that rock aggregates containing approximately 20% of mechanically weak minerals such as phyllosilicates show satisfactory mechanical properties. The study further identified some textural features such as spatial distribution, grain shape and size, morphology, etc. as influential factors (Adomako et al. 2021). In another study, recycled phosphate aggregates of sedimentary origin composed of limestone, marl, and flintstone from a single location showed a significant variation of 46–67% for LA and 50–70% for MD due to the presence of clay and flintstone (Amrani et al. 2019). At this point, conclusions may be reached that the influence of mineralogy on the performance of excavation materials is fundamental.

It is also essential to emphasize that some authors have generally reported satisfactory performance values for excavation materials. In one particular case involving recycled andesite and marble aggregates from the same source, the LA of both materials reached permissible strengths of 25% and 27%, respectively, and therefore the authors implied that both materials could be applied in asphalt pavements characterized by light to medium traffic (Akbulut and Gürer 2007). The LA performance of recycled basalt aggregates was reported to be 13% and was incorporated into stone mastic asphalt (Karakuş 2011). The LA of recycled crushed basaltic aggregates was reported to be satisfactory at a value of 21% in the study by Arulrajah et al. (2012). In specific cases where the performance is compromised, it has been suggested by some authors that these materials (e.g., recycled basaltic aggregates) may be blended with other materials to achieve higher workability and strengths (Ali et al. 2011; Arulrajah et al. 2013). Speaking of blending recycled materials to achieve optimum performance, a function-based investigation by repeated load triaxial test was performed on REM which had been partially replaced by phyllite materials in different quantities (Adomako et al. 2022). The result first showed considerable stiffness variation between REM and phyllites in unblended condition, and phyllites substituted at 25% and 50% in REM confirmed a decrease in stiffness with increased content of RPM. Regarding the deformation behavior, both materials performed similarly. Conclusions reached by the authors were that the performance of the materials typically compares to other recycled materials despite the stiffness variation.

From the above review, it is clear that a few studies have extensively researched on the implications of mechanically weak rocks constituted in excavation materials. Questions

related to which production level of REM may be expedient considering the presence of weak materials, and how the masses may be mixed to achieve satisfactory mechanical performance has not been studied in detail. Given this, the purpose of the present study is to investigate the LA and MD performance of REM mixed with mechanically weak materials in different quantities to establish the limit thresholds while maintaining acceptable performance. The study aims at establishing performance relationships based on the content of recycled phyllite materials (RPM) in REM and potential applications in unbound layers of road pavement. This approach may promote the use of REM in quantities significantly higher than current production levels and may serve as quality control guide in matters of REM and other mixtures. The last part of the study was to examine changing mineral assembly in the fine fractions extracted from blended mixtures in order to identify and understand which minerals abrade in both tests as indication of the effect of weak minerals. The study also compares the performance of other rock aggregates derived from different production sites across Norway.

## Materials and methods

### Sample preparation

In this study, the production of REM and RPM at Velde AS in Sandnes (Norway) is shown in Fig. 1. The facility uses wet recycling technology (CDE, Northern Ireland) to process excavation materials and construction waste. The facility has a 350 tons per hour processing capacity. The processing steps begins with transporting the feedstock of excavation material onto a 100 mm grizzly feeder which is further transported to the scrubbing and washing units of the recycling facility. An over band magnet separator removes ferrous metals from the materials. Lightweight floatation materials are dewatered and separated through another chamber, and the rest of the feedstock are dewatered and fractionated before passing through secondary magnetic separation. The final products then comprise of fractionated fine and coarse size particles. The fraction obtained for investigation in the study is 4/16 mm. This is one of the standard fractions currently produced by the facility for road and concrete applications. The lithology of REM comprise of gneiss, granite, feldspathic rock, and occasional presence of phyllites (Norby 2020). The materials were sourced from the north Jæren region in Norway. On the other hand, RPM (320 tons) was obtained from a surplus material which had been collected after cable trench blasting operations in Stavanger city. The processing of both REM and RPM through the recycling plant followed the same production protocol.

Other rock materials were included in the experimental study for a useful comparison to the performance with REM and RPM in blended and unblended conditions. This was to broaden the scope of materials likely to be found in excavation materials. These rocks were conventionally produced as they were mechanically crushed and separated into various sizes and are for commercial use. Table 1 shows the characteristics including the processing technique, and source of materials used in the study.

### Mix design of RPM in REM and PGr

Blended and unblended mixtures of RPM, REM and PGr, and the different fractions obtained for X-ray diffraction analysis (XRD) is as shown in Table 2. As mentioned already, REM was blended with other rock aggregates including PGr. The reason for generating such mixture was to understand to effect of hard and durable rock in REM. The fractions obtained after the LA test were separated using a 1.6 mm sieve; hence, fractions denoted by 4/16 in Table 2 represent a batch of materials before LA and MD tests. Obtaining fine fractions after the MD test was challenging; therefore, the process involved pouring the tested specimen onto a 1.6 mm sieve, and the liquid residue passing through the 1.6 mm was collected and oven-dried at a temperature of 80 °C for 24–48 h.

### Physical and mechanical tests

The particle-size distribution of the samples was determined following the procedure described in (CEN 933-1

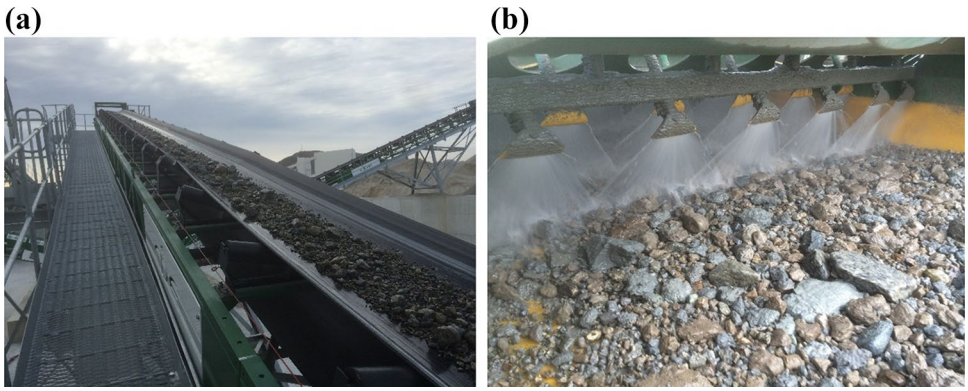


**Fig. 1** Production of REM and RPM from Velde Pukk: **a** transport of materials on a conveyor belt and **b** washing process

**Table 1** Description of the samples studied

| Sample name | Material type | Process type/ technology | Composition | Producer | Source of material | Particle-size (mm) |
|---|---|---|---|---|---|---|
| REM | Excavation material | Wet processing | Gneiss, Granite, and Feldspatic rock | Velde | North Jæren | 4/16 |
| RPM | Excavation material | Wet processing | Phyllite | Velde | Stavanger | 4/16 |
| CrR | Rock material | Crushed | Gneiss, Granite, Feldspar, and quartzite | Reddal Sand | Kristiansand | 8/16 |
| Lim | Rock material | Crushed | Limestone | Franzefoss minerals | Nordland | 10/20 |
| PGr | Rock material | Crushed | Porphyritic Granite | Ringknuten | Kristiansand | 8/16 |
| Amp | Rock material | Crushed | Amphibolite | Ringknuten | Kristiansand | 8/16 |

2012a) by mechanical sieving. The flakiness index (FI) was evaluated based on the techniques described in (CEN 933-3 2012b). In addition, the particle density (oven-dried) and water absorption were determined according to (CEN 1097-6 2013) on aggregates passing 31.5 mm and retained on 4 mm sieves.

Regarding the LA and MD, the procedures described in (CEN 1097-2 2010) and (CEN 1097-1 2011), respectively, were followed. The particle size for the LA test was 10/14 mm, and a 5000 ± 5 g test portion was derived from the laboratory sample. Eleven steel balls were added to the test mass. The test duration completes at 500 revolutions, i.e., 15 min. After the test, the aggregates are washed on a 1.6 mm sieve, dried, and the mass loss (%) is determined. The MD test involved 2.5 ± 0.5 L of water. The particle size for MD was 10/14 mm, and the test portion was 500 g. Spherical balls amounting to 5000 g was added to the test mass and soaked in the cylindrical steel drum. The test cycle is up to 2 h, and after the test, the aggregates are washed on a 1.6 mm sieve, and the retained fraction is dried. The average mass loss (%) of two test specimens is calculated as the micro-Deval coefficient. In both tests, low coefficients imply strong resistance.

**Table 2** Intermix of RPM in REM and PGr and fractions used for XRD analysis

| Sample name | Mix proportion RPM (%) | The fraction used for XRD |
|---|---|---|
| RPM(4/16) | 100 | 4/16 mm |
| RPM100 | 100 | < 1.6 mm after LA |
| RPM100(> 1.6) | 100 | > 1.6 mm after LA |
| RPM100 MD | 100 | < 1.6 mm after MD |
| PGr100 | 100 | < 1.6 mm after LA |
| RPM80-REM20 | 80 | < 1.6 mm after LA |
| RPM60-REM40 | 60 | < 1.6 mm after LA |
| RPM40-REM60 | 40 | < 1.6 mm after LA |
| RPM20-REM80 | 20 | < 1.6 mm after LA |
| RPM80-PGr20 | 80 | < 1.6 mm after LA |
| RPM60-PGr40 | 60 | < 1.6 mm after LA |
| RPM40-PGr60 | 40 | < 1.6 mm after LA |
| RPM20-PGr80 | 20 | < 1.6 mm after LA |
| REM(4/16) | 0 | 4/16 mm |
| REM100 | 0 | < 1.6 mm after LA |
| REM100(> 1.6) | 0 | > 1.6 mm after LA |
| REM100 MD | 0 | < 1.6 mm after MD |

## Chemical and mineralogical analysis

The pulverized fraction of REM, RPM, and PGr was initially selected, and the mineral composition was determined by Bruker D8 Focus X-ray diffractometer in Bragg–Brentano geometry (θ/2θ), equipped with a LynxEye superspeed detector. Generator settings were 40 kV, and 40 mA and diffractograms were recorded with Cu-Kα radiation (λ = 1.54060 Å), a step size of 0.02° and a fixed divergence slit of 0.2 mm. The measurements were taken from 5 to 60° 2θ. The specimens were prepared by a combination of front- and side-loading to reduce particle orientation effects. First, the specimen was carefully pressed into the specimen holder (front-loading), and the surface was flattened with a glass plate. While holding the glass plate on the surface, the holder was laterally knocked on the table to compact the powder to reduce the orientation of particles (side-loading). Potential free space in the holder was then filled, and the procedure was repeated. Excess material was stripped off with a glass plate.

In the blended mixture of Lim and Amp, fractions < 1.6 mm deriving from the LA tests were used for the acid-solubility tests. The test was performed based on NT Build 437 (1995). First, the sample was milled and then reduced to a test portion. Next, a sample mass of 4 g was transferred into a 250 ml beaker fixed onto a magnetic stirrer. Next, 3 ml ethanol, 150 ml of denoised water, and 10 ml of concentrated nitric acid were added into the beaker and mixed using a magnetic stirrer plate. After 30 min of agitation, the beaker rested for some hours and the insoluble part was gravimetrically calculated and used to determine the acid solubility.

## Results and discussion

### Physical properties

The water absorption (WA), particle density ($\rho_{density}$), and FI performance of studied materials is shown in.

Table 3. These are essential parameters for selecting rock aggregates for road construction and concrete. The WA coefficients obtained in the study was 0.3–0.6%. Martinez-Echevarria et al. (2020) reported the WA values of natural and recycled aggregates at 1% and 4–9%, respectively. Generally, high-quality rock aggregates tend to have low WA coefficients due to their small pore space and the tight intergrowth of the grain boundaries. In this study, it may be claimed that such less porous response, particularly for recycled materials, shows the potential to reduce the effects of ice and salt crystallization within the voids (Hartley 1974). The $\rho_{density}$ values obtained in this study ranged from 2.5 to 2.7 g/ml, which agrees well with similar measurements performed on other aggregates. For example, a study reported 2.8 and 2.4 g/ml $\rho_{density}$ for natural and recycled concrete aggregates, respectively (Martinez-Echevarria et al. 2020). Furthermore, a study in India reported $\rho_{density}$ of 2.2–2.3 g/ml for excavation mass (10/20 mm) produced by wet processing technology (Engelsen et al. 2020).

Regarding the FI, the Norwegian pavement design code N200 sets the FI threshold equal to 20–25% for bound and unbound layers based on the actual or anticipated annual average daily traffic (Norwegian Public Roads Administration 2018). Therefore, particles with high FI are not recommended for construction. In this study, Lim and RPM recorded 38% and 31%, respectively, which is higher than the cut off specified in N200. The FI of REM was 13%, consistent with the range 7–18% of recycled aggregates (Martinez-Echevarria et al. 2020). Both CrR and Amp had an FI of 10%, and PGr had 14%. Overall, the materials used in this study showed good physical properties except for Lim and RPM with high FI.

The particle-size distribution of the materials is shown in Fig. 2. For RPM 4/16, approximately 7% of the fraction was less than 2 mm, making it significantly finer than the others, except amphibolite which had about 8% < 2 mm. In addition,

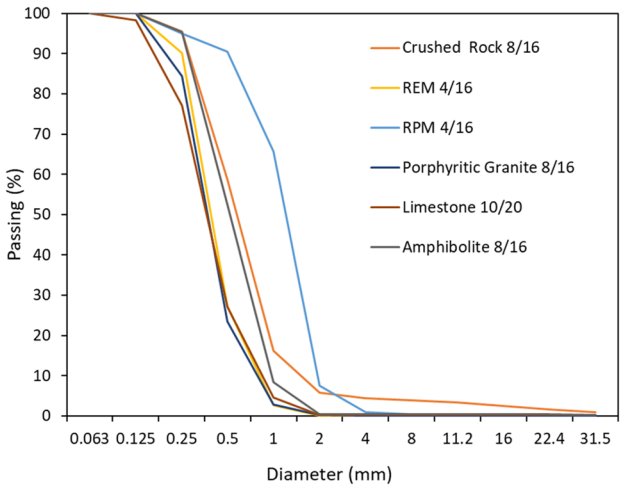


**Fig. 2** Particle-size distribution of tested materials

around 3% of CrR 8/16 fraction was less than 4 mm. The gradations shown in Fig. 2 is consistent with industrial production of all materials. Based on visual inspection, the texture of mechanically crushed materials appeared to have sharp angular grain shapes. Considering the sliding and interlocking effect between the contact surface of the particles during handling and transportation, this could be the reason for the fine fraction obtained in some of the samples.

### Mechanical performance of REM blended with RPM and PGr

The LA and MD performance related to blended mixtures of REM with RPM and PGr, and respective combinations is shown in Fig. 3. To define the maximum intermixing level of the weakest material, the performance was compared to the Norwegian LA and MD criteria for aggregates used in the sub-base and base layers. These are MD ≤ 15% for base and ≤ 20% for subbase course and LA for base and subbase at ≤ 35% (NPRA 2018).

**Table 3** Physical properties of the samples specified as arithmetic mean ± 1 standard deviation, $n = 3$, and limit threshold for bound and unbound application in N200

| Sample name | WA (%) EN 1097-6 | NPRA (2018) | $\rho_{density}$(g/ml) EN 1097-6 | NPRA (2018) | FI (%) EN 933-3 | NPRA (2018) |
|---|---|---|---|---|---|---|
| REM | 0.3 ± 0.2 | Values must be declared | 2.5 ± 0.1 | Values must be declared | 12.6 ± 2.5 | ≤ 20–25 |
| CrR | 0.3 ± 0.9 | | 2.7 ± 0.1 | | 10.1 ± 1.7 | |
| Lim | 0.3 ± 0.4 | | 2.6 ± 0.2 | | 38.5 ± 0.2 | |
| PGr | 0.3 ± 0.5 | | 2.5 ± 0.1 | | 14.7 ± 2.3 | |
| RPM | 0.6 ± 0.1 | | 2.5 ± 0.1 | | 31.1 ± 1.3 | |
| Amp | 0.3 ± 0.5 | | 2.7 ± 0.3 | | 10.6 ± 0.3 | |

Considering the LA performance of REM blended with RPM (Fig. 3a), the results show that all blends produced in the study was below the upper LA limit of 35%. This was expected since the LA values of the materials in unblended state were 28% and 26% for REM and RPM, respectively. Other LA values for phyllite and quartz phyllite have been reported to be 17% and 26%, respectively (Adom-Asamoah and Afrifa 2010; Voit and Kuschel 2020) which clearly shows the extent of performance variation within the same material. According to Voit and Kuschel (2020), the quartz phyllites had a significant schistosity textural characteristics, hence this may have contributed to the low resistance to LA.

Regarding the MD performance of REM which had been partially blended with RPM, the results show some changes (Fig. 3a). The MD values of unblended REM and RPM was 6% and 26%, respectively. In this case, MD was the critical parameter in RPM; hence, it was observed that increased content of RPM in REM reduced the wear resistance. Figure 4 present the LA and MD of selected rock materials in Norway (Norwegian Geological Survey (NGU) 2019). Based on reported LA and MD performance, it could be mentioned that the LA of both REM and RPM are satisfactory. Regarding the MD, although the MD of RPM is significantly higher which indicates low resistance, our study demonstrates that 40% replacement ratio of RPM in REM gives a competitive baseline of the maximum quantity of RPM in REM. In view of this, the performance is comparable with natural rock materials shown in Fig. 4.

The PGr was found to be a hard and durable material in this study, as shown in Fig. 3b. The LA and MD of PGr was found to be 18% and 9%, respectively. The effect of blending PGr in REM resulted in improved resistance to the LA. This was expected given the performance of PGr. The MD performance of both materials did not significantly differ from each other. Compared to other studies, Afolagboye et al. (2016) reported the LA performance of PGr in the region 25–28%. In addition, the performance of PGr is comparable to the values obtained from other hard rocks such as gneiss, gabbro, basalt, and amphibolite in Fig. 4. From the conclusions reached in the review by Adomako et al. (2021), that hard minerals, strong interlock boundaries, and morphological features contribute to resistance to crushing and wearing of rocks; it may equally be said of PGr, and other rocks reported in Fig. 4, given the good performance. RPM was also blended with PGr to assess the performance (see Fig. 3c). Again, the critical factor is the MD performance of RPM, as increased content decreased the MD performance of the mixture. In view of this, RPM's maximum content for optimal performance of the mixture was observed in the region of 20–30%.

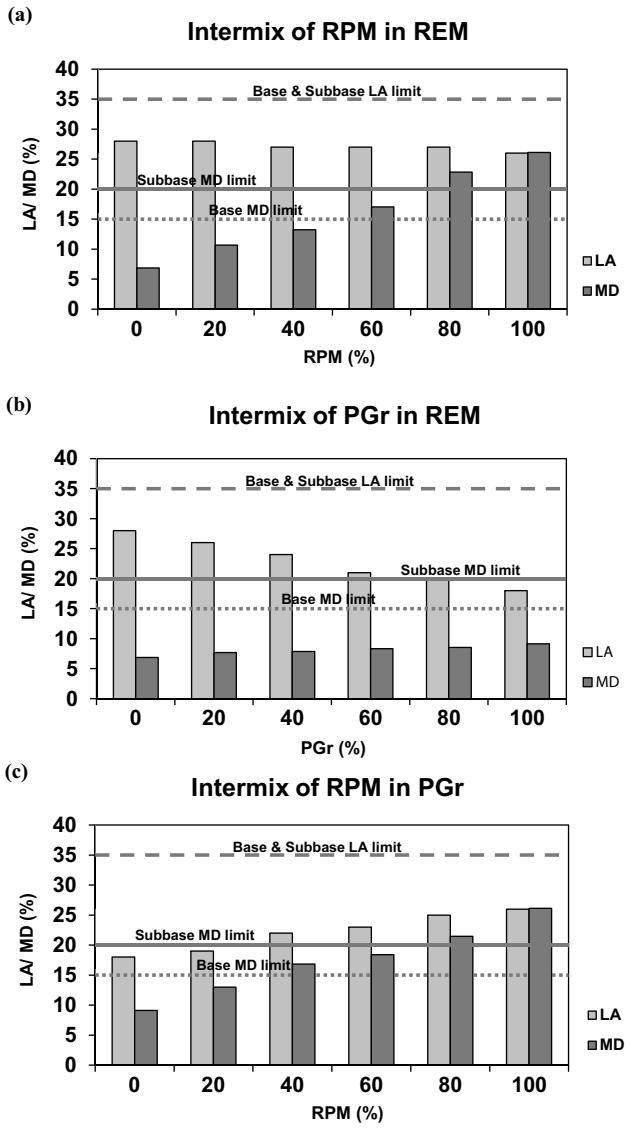


**Fig. 3** LA and MD performance of **a** Intermix of RPM in REM, **b** PGr in REM, and **c** RPM in PGr

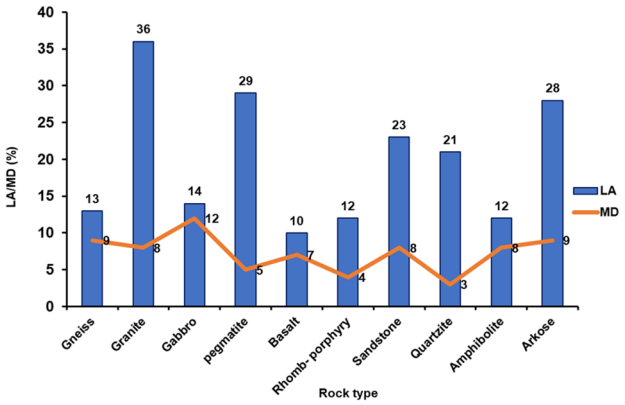


**Fig. 4** The LA and MD of different rock materials found in Norway

Concrete rubbles often appear in excavation materials. They are often crushed to recycled concrete aggregates (RCA) in different grain sizes for use in road construction or production of new concrete. RCA often contain varying amounts of calcium carbonate ($CaCO_3$) due to the well-known carbonation process occurring in the concrete service life (Engelsen et al. 2017). In crushed conditions, the $CaCO_3$ may increase due to the higher surface area for carbonation. Generally, research has demonstrated the effect carbonation in recycled materials (e.g., RCA) (Dongxing et al. 2017; Engelsen et al. 2017). A recent study has investigated the performance of concrete using excavation materials and concrete rubble as feedstock to produce recycled aggregate (Mujica et al. 2019). Given that carbonation is likely to influence the performance of RCA in REM, this study utilizes limestone to replace RCA. Limestone contains a significant amount of $CaCO_3$. Hence, the effect of mixing limestone (Lim) representing crushed concrete rubble in REM is essential. Figure 5a–c shows the performance of Lim blended with REM and Amp, and CrR and REM. Altered pyroxene results in Amp and in some cases, Amp is also shown to have low resistance to wear and crushing (Johansson et al. 2016; Ajagbe et al. 2015). In addition, it has been found that Amp dissolves in acidic environments at low to medium temperatures and forms clay like minerals such as chlorite and griffithite (Yongli et al. 2019). Given this, mixing Lim with Amp was essential to establish a baseline criteria and to further investigate potential solubility of both materials in acidic environment.

The LA and MD performance of Lim was 33% and 29%, respectively. The maximum intermixing level of Lim in REM was below 40%, where the MD was the weakest parameter in comparison to other rock materials. Both the LA and MD performance can be seen in Fig. 5a. Other study report the LA values of Lim in the region of 25–38% (Jayawarden 2017; Pang et al. 2010). To establish a baseline mix criteria for Lim if blended with Amp (amphibolite)—a product of pyroxene, the result in Fig. 5b shows that the Amp used in the study was also hard and durable. Hence, an intermix level of Lim up to 20% was sufficient to comply with the MD requirement. The LA and MD of Amp was 16% and 12%, respectively. This is comparable to the LA and MD performance of other hard rocks shown in Fig. 4.

Furthermore, the crushed rock material (CrR) which was used in this study comprised of sharp-grained granite, gneiss, feldspathic rock, and quartzite and the results showed lower LA and MD strength compared to REM (see Fig. 5c). The LA and MD of CrR was 36% and 15%, respectively. Although the composition of different lithotypes in CrR was not quantified in this study, the authors

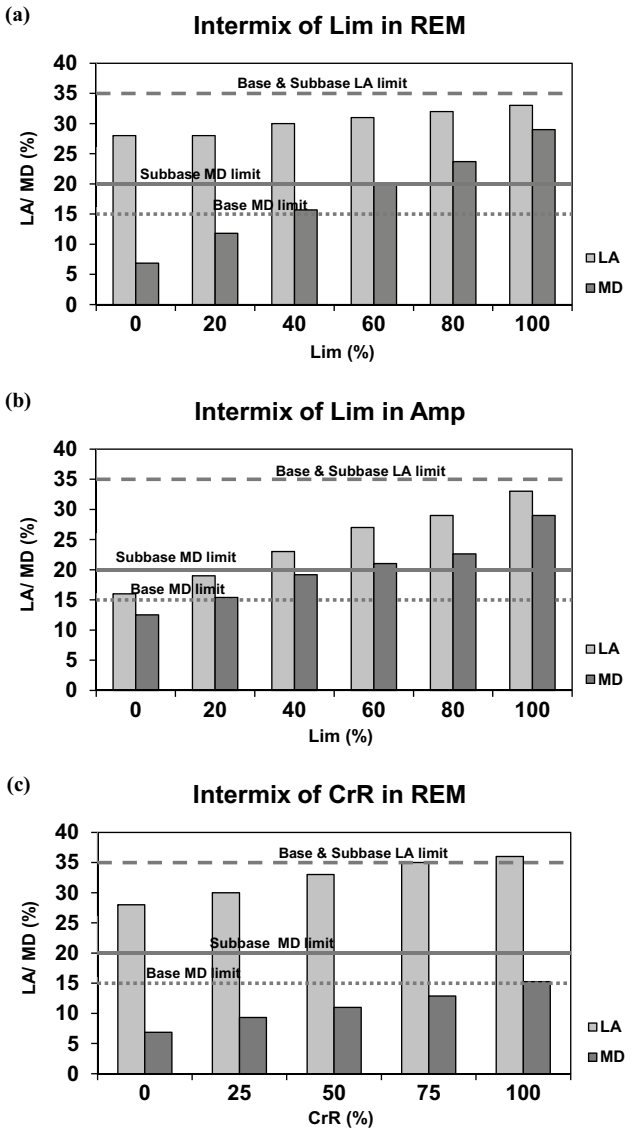


**Fig. 5** LA and MD performance of intermix of **a** Lim in REM, **b** Lim in Amp, and **c** CrR in REM

believe that other textural features may have contributed to the low resistance in LA. Given the presence of quartz dominant materials and feldspar, the concept of proportionality of quartz to feldspar (QFR) as established in the review by Adomako et al. (2021) seem to have very little influence in this case. In Fig. 6, example of the narrative of QFR is shown. It can be seen that QFR was the main influential mineral. The LA parameter of CrR was not significantly over the cut-off. Nevertheless, the maximum mixing level of CrR in REM was 75% to meet the base/subbase criteria from a technical viewpoint.

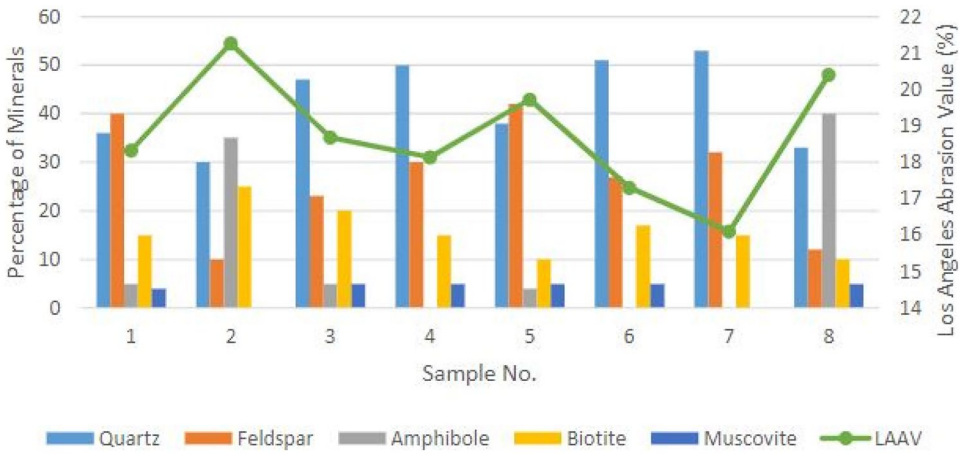


**Fig. 6** The influence of minerals on the LA performance of different rocks (adapted from Ajagbe et al. 2015)

## Identification of weak mineral assembly

The crushing and wearing effect of the LA and MD tests reduce the particle size and changes the state of textural features. Hence, determining the mineralogy of the fine fraction (< 1.6 mm) provides essential information on the intermixing effect. The fine fractions from the Lim-Amp and RPM-REM mixes were therefore analyzed. Considering that Lim is mainly composed of $CaCO_3$, acid solubility of the fine fraction was investigated. This approach could indicate the primary mineral types pulverized and compounded in < 1.6 mm fraction after the LA test. The results of acid solubility of the fine fractions (< 1.6 mm) are shown in Fig. 7. In unblended condition, the acid solubility of Lim and Amp was 100% and 7%, respectively. Since the acid-soluble part of amphibolite is only 7%, the soluble carbonates (mostly $CaCO_3$) in Lim dominate at increased intermix levels; hence, it was apparent that the carbonate minerals in Lim were the major minerals in the fine fraction. The nonlinearity may relate to a slight increase in the acid solubility of Amp upon increased mixing content of Lim.

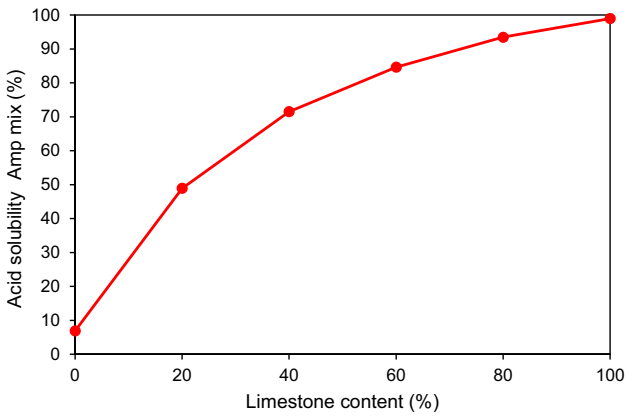


**Fig. 7** Effect of acid solubility on the intermix of Lim in Amp

Since the mineral assembly present in the fine fractions of RPM-REM cannot be assessed with the acid-soluble test, XRD test was performed, and the results are shown in Fig. 8. The mineral compositions of RPM and REM before LA are denoted by RPM (4/16) and REM (4/16). In addition, RPM100 (< 1.6) and REM (< 1.6) depicts the mineral assembly which accumulated in the fine fraction < 1.6 mm sieve and RPM100 (> 1.6) and REM (> 1.6) represent minerals retained on 1.6 mm sieve after the LA tests.

The main minerals identified in RPM are microcline/orthoclase and traces of anorthite from the feldspar group, quartz, biotite, muscovite, and chlorite. The mineral composition of REM is microcline/orthoclase and plagioclase from the feldspar group, quartz, muscovite, biotite, and a small quantity of clinochlore. The diffractograms of mica and chlorite in RPM showed high peak intensities in the fine fraction (4/16) given as the reference material, i.e., before LA testing. This indicated the crushing effect occurring at the expense of these soft minerals. Conversely, the diffractograms of the pulverized trace of REM showed insignificant intensity of weak minerals. This development relates to the low presence of weak minerals and shows that the REM used in the study was a good material.

Furthermore, XRD analysis was performed on the blended mixtures composed of RPM and REM (Fig. 9a) and PGr and RPM (Fig. 9b). The diffractograms show the fractions < 1.6 mm after the LA tests. Both cases found a good correlation between increased intensities (amount) of mica and chlorite peaks with increased RPM content. This was expected because RPM contained a significant amount of phyllosilicate minerals; therefore, these were the main minerals that were significantly pulverised in the LA and MD tests. However, a moderate presence of phyllosilicate minerals (about 15–20%) is reported to have no influence in the LA and MD performance in phyllites (Norby 2020). In this case, this means that the influence of weak mineral depends on the quantity present. Similar conclusions were reached

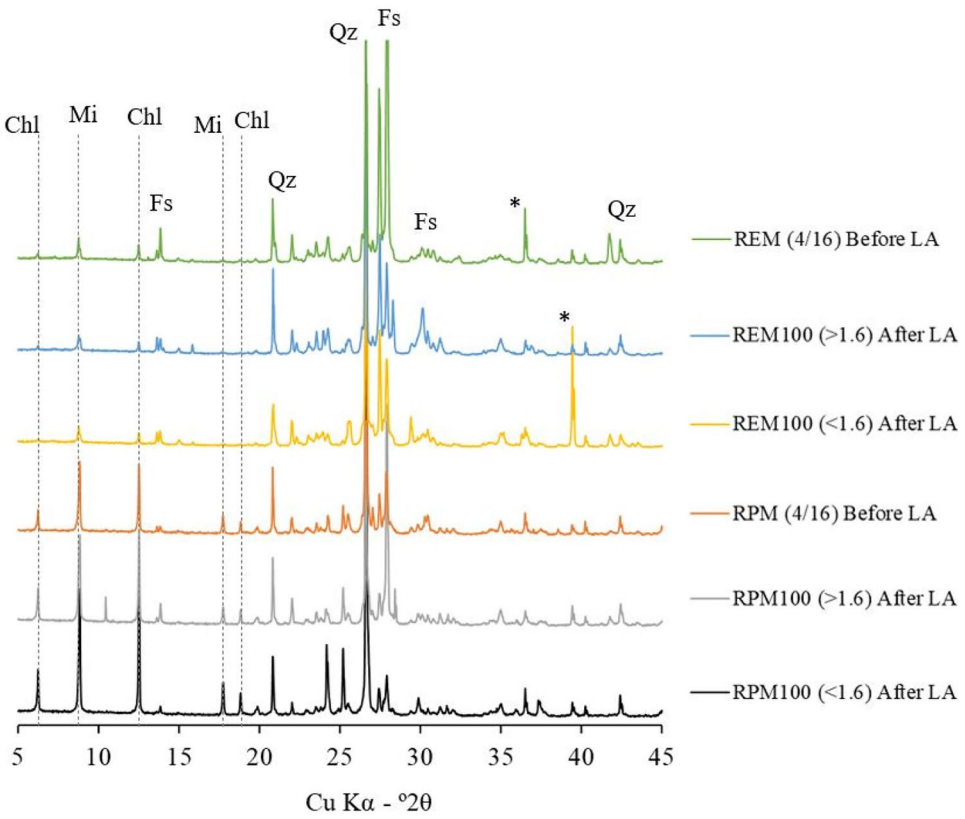


**Fig. 8** X-ray diffractograms pattern of RPM and REM, marked with the prominent peaks of the main mineral phases (Chl = chlorite, Mi = mica, Fs = feldspar, Qz = quartz). * indicates an artefact ("the spottiness") caused by abnormal high intensity of a large grain in diffraction position (here quartz)

in other studies (Anastasio et al. 2016; Nålsund 2010) for different types of rocks. Although no quantitative estimates of mineral components in percentages were determined in this study, it is evident that the performance of PGr was not influenced by the peak of mica in the diffractogram. Furthermore, it is claimed that the effect of mica minerals on the strength property also depends on its structural formation and distribution of the grain boundaries (Fortes et al. 2016). From this standpoint, it may be appropriate to mention the importance of reaching conclusion based on global geological nature, as mentioned by Adomako et al. (2021).

The relationship between the test method and mineralogy was studied to compare the effect of both LA and MD on the degree of wear of minerals present in RPM and REM. In Fig. 10, the results of the diffractograms in connection to the test methods are displayed. REM100LA and REM100 MD represent the diffractograms taken on fine fractions after both LA and MD tests, respectively. The same classification occurs for RPM100LA and RPM100 MD. Generally, the investigation highlighted a high wearing tendency of mechanically soft minerals (mica and chlorite) in the MD test compared to the disintegration or crushing effect

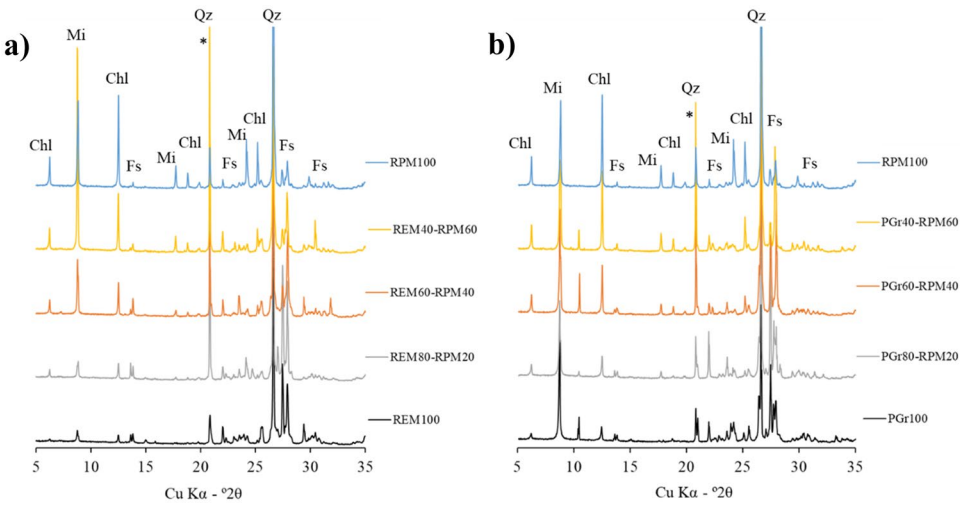


**Fig. 9** X-ray diffraction results showing mineral accumulation and changes in the fine fraction (< 1.6 mm) after the LA test of **a** RPM-REM and **b** RPM-PGr blends, marked with the prominent peaks of the main mineral phases (Chl = chlorite, Mi = mica, Fs = feldspar, Qz = quartz).* indicates an artefact ("spottiness") caused by abnormal high intensity of a large grain in diffraction position (here quartz). Peaks around 11° 2θ observed in some diffractograms might be associated with cyclosilicate minerals (e.g., cordierite/indialite)

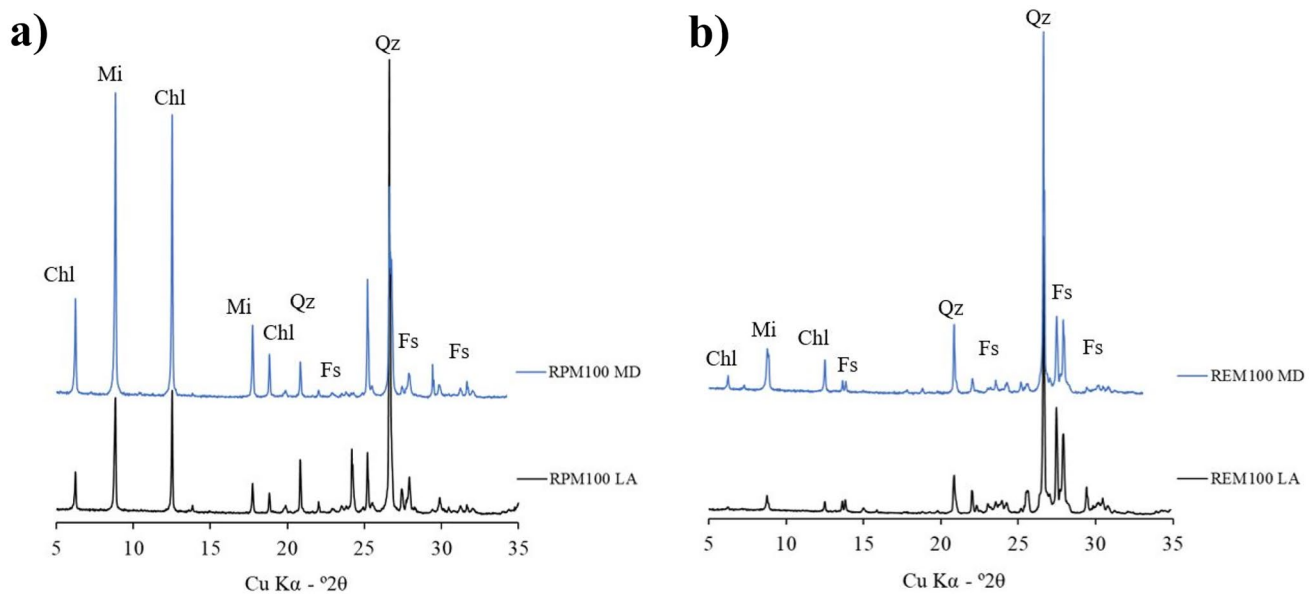


**Fig. 10** Diffractograms showing the relationship between LA and MD test and the minerals present in **a** RPM and **b** REM

associated with LA testing. This development is shown in the peak intensities of the minerals. The findings are consistent with the claim that the degree of degradation by MD on rock aggregates is connected to mineral hardness, defined by the Mohs hardness scale (Wang et al. 2017). Some studies (Apaydın and Yılmaz 2019; Johansson 2011) have also reported that reliable relationships exist between the content of mica and MD on granitoid and basaltic rocks. Given this, it may be concluded that the amount of mica and chlorite in RPM may have contributed to the weak MD performance. This also shows the importance of assessing both parameters (LA and MD), particularly for mixed recycled aggregates.

## Conclusions

This study has presented the results of the mechanical performance of recycled aggregates derived from excavation materials (REM) which is mixed with recycled phyllite materials (RPM). The Los Angeles (LA) and micro-Deval (MD) tests were used in the investigation. In addition, X-ray diffraction (XRD) and acid solubility tests were performed to identify mechanically weak minerals accumulated in the fine fraction, after the tests.

The results have shown that RPM and REM had similar and satisfactory LA of 28% and 26%, respectively, but a significant difference in MD performance of 26% for RPM and 6% for REM was found. At the intermix level, it was found that REM could tolerate up to 40% of RPM before it exceeded the MD limit of 15–20% defined in N200 by the Norwegian Road Public Administration. Blending REM with the hard rock PGr (Porphyritic granite) indicated that a higher content of PGr in this combination showed increased resistance to LA. Furthermore, the maximum intermix level of RPM in PGr was only 20%. Regarding the use of limestone (Lim) in REM blends, Lim's maximum blending ratio should be less than 40% to satisfy the MD limit. The LA was the critical parameter of mixtures generated from local crushed rock material (CrR) and REM; hence, approximately 75% of CrR was the maximum tolerable content to reach the base course and subbase criteria.

Consistency was found when the mineralogy of the fine fractions (< 1.6 mm) from the LA and MD tests were assessed. Limestone minerals mainly seem to disintegrate when mixed with amphibolite—a product of pyroxene which also is characterized by soluble components when exposed to acidic environment. The XRD analyses of pure and blended mixes of RPM in REM and RPM in PGr showed a good relationship between increased intensities of mica and chlorite with increased RPM. Regarding the relationship encompassing LA and MD, and mineralogy, it was observed that the wearing of weak minerals (mica and chlorite) was high in the MD test compared to the disintegration effect by LA. This may be attributed to the conditions of MD test, namely (a) the wear nature of the test method, and (b) the moisturized condition of the test. The less effect to mineral wear in LA may be due to reasons such as the dry method of the test and expected cushioning effect by pulverized fraction which prevents large particles to further disintegrate during the test.

Given the study's overall findings, it may be concluded that the REM used in this study present excellent mechanical properties due to the low presence of weak minerals and may be used for construction purposes. Furthermore, foreign rock materials (e.g., phyllite) in REM can be tolerable in

quantities significantly higher than the average levels found in today's production. The authors are of the opinion that the findings of the study may be applicable in other scenarios where excavation is characterized by satisfactory LA and MD performance and a low content of mechanically weak minerals.

**Acknowledgements** The work presented in this paper is part of the ongoing project MEERC (More Efficient and Environmentally friendly Road Construction), partly funded by the Research Council of Norway (NFR) [project number 273700] and Sorlandets Kompetansefond.

**Funding** Open access funding provided by University of Agder.

## Declarations

**Competing interests** The authors declare no competing interests.

**Open Access** This article is licensed under a Creative Commons Attribution 4.0 International License, which permits use, sharing, adaptation, distribution and reproduction in any medium or format, as long as you give appropriate credit to the original author(s) and the source, provide a link to the Creative Commons licence, and indicate if changes were made. The images or other third party material in this article are included in the article's Creative Commons licence, unless indicated otherwise in a credit line to the material. If material is not included in the article's Creative Commons licence and your intended use is not permitted by statutory regulation or exceeds the permitted use, you will need to obtain permission directly from the copyright holder. To view a copy of this licence, visit http://creativecommons.org/licenses/by/4.0/.

## References

Adom-Asamoah M, Afrifa RO (2010) A study of concrete properties using phyllite as coarse aggregates. Mater Des 31(9):4561–4566. https://doi.org/10.1016/j.matdes.2010.03.041

Adomako S, Engelsen CJ, Thorstensen RT, Barbieri DM (2021) Review of the relationship between aggregates geology and Los Angeles and Micro-Deval tests. Bull Eng Geol Env 80:1–18. https://doi.org/10.1007/s10064-020-02097-y

Adomako S, Engelsen CJ, Thorstensen RT, Barbieri DM (2022) Repeated load triaxial testing of recycled excavation materials blended with recycled phyllite materials. Materials 15(2):621. https://doi.org/10.3390/ma15020621

Afolagboye L, Talabi A, Akinola O (2016) Evaluation of selected basement complex rocks from Ado-Ekiti, SW Nigeria, as source of road construction aggregates. Bull Eng Geol Environ 75:853–865. https://doi.org/10.1007/s10064-015-0766-1

Ajagbe WO, Tijani MA, Oyediran IA (2015) Engineering and geological evaluation of rocks for concrete production. Lautech J Eng Technol 9(2):67–79. Retrieved from https://laujet.com/index.php/laujet/article/view/85

Akbulut H, Gürer C (2007) Use of aggregates produced from marble quarry waste in asphalt pavements. Build Environ 42(5):1921–1930. https://doi.org/10.1016/j.buildenv.2006.03.012

Ali M, Arulrajah A, Disfani M, Piratheepan J (2011) Suitability of using recycled glass-crushed rock blends for pavement subbase applications. Geo-Front: Adv Geotech Eng 1325–1334. https://doi.org/10.1061/41165(397)136

Amrani M, Taha Y, Kchikach A, Benzaazoua M, Hakkou R (2019) Valorization of phosphate mine waste rocks as materials for road construction. Minerals 9(4):237. https://doi.org/10.3390/min9040237

Anastasio S, Fortes A, Kuznetsova E, Danielsen SW (2016) Relevant petrological properties and their repercussions on the final use of aggregates. Energy Procedia 97:546–553. https://doi.org/10.1016/j.egypro.2016.10.073

Apaydın ÖF, Yılmaz M (2019) Correlation of petrographic and chemical characteristics with strength and durability of basalts as railway aggregates determined by ballast fouling. Bull Eng Geol Env 1–9. https://doi.org/10.1007/s10064-019-01654-4

Arulrajah A, Ali M, Disfani MM, Piratheepan J, Bo M (2013) Geotechnical performance of recycled glass-waste rock blends in footpath bases. J Mater Civ Eng 25:653–661. https://doi.org/10.1061/(ASCE)MT.1943-5533.0000617

Arulrajah A, Ali M, Piratheepan J, Bo M (2012) Geotechnical properties of waste excavation rock in pavement subbase applications. J Mater Civ Eng 24:924–932. https://doi.org/10.1061/(ASCE)MT.1943-5533.0000419

Barbieri DM, Hoff I, Mørk MBE (2019) Innovative stabilization techniques for weak crushed rocks used in road unbound layers: a laboratory investigation. Transport Geotech 18:132–141. https://doi.org/10.1016/j.trgeo.2018.12.002

Crawford RH, Mathur D, Gerritsen R (2017) Barriers to improving the environmental performance of construction waste management in remote communities. Procedia Eng 196:830–837. https://doi.org/10.1016/j.proeng.2017.08.014

Dahlbo H, Bachér J, Lähtinen K, Jouttijärvi T, Suoheimo P, Mattila T, Sironen S, Myllymaa T, Saramäki K (2015) Construction and demolition waste management—a holistic evaluation of environmental performance. J Clean Prod 107:333–341. https://doi.org/10.1016/j.jclepro.2015.02.073

Dengg F, Zeman O, Voit K, Bergmeister K (2018) Fastening application in concrete using recycled tunnel excavation material. Struct Concr 19:374–386. https://doi.org/10.1002/suco.201600200

Dongxing X, Zhan B, Poon CS (2017) Durability of recycled aggregate concrete prepared with carbonated recycled concrete aggregates. Cement Concr Compos 84:214–221. https://doi.org/10.1016/j.cemconcomp.2017.09.015

Engelsen CJ, Malhotra SK, Bhatiani G, Nath K (2020) Detailed assessment of the technical properties of recycled aggregates from mixed C&D waste. Indian Concr J 94:32–39

Engelsen CJ, Van Der Sloot HA, Petkovic G (2017) Long-term leaching from recycled concrete aggregates applied as sub-base material in road construction. Sci Total Environ 587:94–101. https://doi.org/10.1016/j.scitotenv.2017.02.052

European Commission (2008) Directive 2008/98/EC on waste (waste framework directive). https://www.eea.europa.eu/policy-documents/waste-framework-directive-2008-98-ec. Accessed 21 Dec 2021

European Committee for Standardization (2010) CEN: Tests for mechanical and physical properties of aggregates. Part 2: Methods for the determination of resistance to fragmentation

European Committee for Standardization (2011) CEN: Tests for mechanical and physical properties of aggregates. Part 1: Determination of the resistance to wear (micro-Deval)

European Committee for Standardization (2012a) CEN: Tests for geometrical properties of aggregates. Part 1: Determination of particle size distribution–sieving method

European Committee for Standardization (2012b) CEN: Tests for mechanical and physical properties of aggregates. Part 3: Determination of particle shape–flakiness index

European Committee for Standardization (2013) CEN: Tests for mechanical and physical properties of aggregates part 6: Determination of particle density and water absorption

Fortes APP, Anastasio S, Kuznetsova E, Danielsen SW (2016) Behaviour of crushed rock aggregates used in asphalt surface layer exposed to cold climate conditions. Environ Earth Sci 75:1414. https://doi.org/10.1007/s12665-016-6191-3

Haas M, Galler R, Scibile L, Benedikt M (2020) Waste or valuable resource—a critical European review on re-using and managing tunnel excavation material. Resour Conserv Recycl 162:105048. https://doi.org/10.1016/j.resconrec.2020.105048

Hartley A (1974) A review of the geological factors influencing the mechanical properties of road surface aggregates. Q J Eng Geol 7:69–100. https://doi.org/10.1144/GSL.QJEG.1974.007.01.05

Huang B, Wang X, Kua H, Geng Y, Bleischwitz R, Ren J (2018) Construction and demolition waste management in China through the 3R principle. Resour Conserv Recycl 129:36–44. https://doi.org/10.1016/j.resconrec.2017.09.029

Johansson E, Miškovský K, Bergknut M, Šachlová Š (2016) Petrographic characteristics of intrusive rocks as an evaluation tool of their technical properties. Geol Soc (london, Special Publications) 416(1):217–227. https://doi.org/10.1144/SP416.19

Jayawarden US (2017) Laboratory studies of Miocene limestone in Sri Lanka. Q J Eng GeolHydrogeol 50:422–425. https://doi.org/10.1144/qjegh2016-106

Johansson E (2011)Technological properties of rock aggregates. PhD Thesis, Luleå Tekniska Universitet

Karakuş A (2011) Investigating on possible use of Diyarbakir basalt waste in Stone Mastic Asphalt. Constr Build Mater 25:3502–3507. https://doi.org/10.1016/j.conbuildmat.2011.03.043

Karstensen KH, Engelsen CJ, Saha PK (2020) Circular economy initiatives in Norway. Circular Economy: Global Perspective, pp 299–316

Lieb R (2011) Experience in spoil management on conclusion of excavations for the Gotthard base tunnel. Tagung der italienischen Tunnelbaugesellschaft Convegno SIG (Società Italiana Gallerie), Samoter, VeronaFiere

Magnusson S, Lundberg K, Svedberg B, Knutsson S (2015) Sustainable management of excavated soil and rock in urban areas–a literature review. J Clean Prod 93:18–25. https://doi.org/10.1016/j.jclepro.2015.01.010

Martinez-Echevarria M, Lopez-Alonso M, Garach L, Alegre J, Poon C, Agrela F, Cabrera M (2020) Crushing treatment on recycled aggregates to improve their mechanical behaviour for use in unbound road layers. Constr Build Mater 263:120517. https://doi.org/10.1016/j.conbuildmat.2020.120517

Menegaki M, Damigos D (2018) A review on current situation and challenges of construction and demolition waste management. Curr Opin Green Sustain Chem 13:8–15. https://doi.org/10.1016/j.cogsc.2018.02.010

Mujica EVH, Engelsen CJ, Nodland MS (2019) Recycled aggregates produced from two different feedstock materials—applied in ready-mixed concrete. In Proceedings of the International Conference on Sustainable Materials, Systems and Structures, Rovinj, Croatia, pp 272–279

Nålsund R (2010) Effect of grading on degradation of crushed-rock railway ballast and on permanent axial deformation. Transp Res Rec 2154:149–155. https://doi.org/10.3141/2154-15

Ng S, Engelsen CJ (2018) Construction and demolition wastes. Waste Supplement Cementitious Mater Concrete 229–255. https://doi.org/10.1016/B978-0-08-102156-9.00008-0

Norby M (2020) Nytt Resirkulert Tilslag Produsert fra Grave-og Byggavfall. Master Thesis, University of Agder

Norwegian Public Roads Administration (NPRA) (2018) Håndbok N200 Vgbygging; NPRA: Vejdirektoratet

Norwegian Geological Survey (NGU) (2019)- Rock database.

NT Build 437 (1995) Concrete, hardened and mortar; calcium oxide and soluble silica contents, Nordtest method

Pang L, Wu S, Zhu J, Wan L (2010) Relationship between retrographical and physical properties of aggregates. J Wuhan Univ Technol Mater 25:678–681. https://doi.org/10.1007/s11595-010-0069-0

Ritter S, Einstein H, Galler R (2013) Planning the handling of tunnel excavation material—a process of decision making under uncertainty. Tunn Undergr Space Technol 33:193–201. https://doi.org/10.1016/j.tust.2012.08.009

Tam VW, Tam CM (2006) A review on the viable technology for construction waste recycling. Resour Conserv Recycl 47:209–221. https://doi.org/10.1016/j.resconrec.2005.12.002

Voit K, Kuschel E (2020) Rock material recycling in tunnel engineering. Appl Sci 10:2722. https://doi.org/10.3390/app10082722

Walsh D, Mcrae I, Zirngibl R, Chawla S, Zhang H, Alfieri A, Moore H, Bailey C, Brooks A, Ostock T (2019) Generation rate and fate of surplus soil extracted in New York City. Sci Total Environ 650:3093–3100. https://doi.org/10.1016/j.scitotenv.2018.09.284

Wang H, Wang D, Liu P, Hu J, Schulze C, Oeser M (2017) Development of morphological properties of road surfacing aggregates during the polishing process. Int J Pavement Eng 18:367–380. https://doi.org/10.1080/10298436.2015.1088153

Wang L, Chen L, Tsang DC, Li JS, Baek K, Hou D, Ding S, Poon CS (2018) Recycling dredged sediment into fill materials, partition blocks, and paving blocks: Technical and economic assessment. J Clean Prod 199:69–76. https://doi.org/10.1016/j.jclepro.2018.07.165

Yongli L, Huang F, Gao W, Tang X, Ren Y, Meng L, Zhang Z (2019) Experimental study of dissolution-alteration of amphibole in a hydrothermal environment. Acta Geologica Sinica-English Edition 93(6):1933–1946. https://doi.org/10.1111/1755-6724.14368

## Paper C

**S. Adomako**, C. J. Engelsen, R. T. Thorstensen, and D. M. Barbieri, “Repeated Load Triaxial Testing of Recycled Excavation Materials Blended with Recycled Phyllite Materials,” *Materials*, vol. (15), no. 2, pp. 621, 2022.
https://doi.org/10.3390/ma15020621

*materials*

MDPI

*Article*

# Repeated Load Triaxial Testing of Recycled Excavation Materials Blended with Recycled Phyllite Materials

**Solomon Adomako [1,*], Christian John Engelsen [2], Rein Terje Thorstensen [1] and Diego Maria Barbieri [3]**

[1] Department of Engineering and Science, University of Agder, 4879 Grimstad, Norway; rein.t.thorstensen@uia.no
[2] Department of Building and Infrastructure, SINTEF Community, 0314 Oslo, Norway; christianjohn.engelsen@sintef.no
[3] Department of Civil and Environmental Engineering, Norwegian University of Science and Technology (NTNU), 7491 Trondheim, Norway; diego.barbieri@ntnu.no
* Correspondence: solomon.adomako@uia.no

**Abstract:** Recycled Excavation Materials (REM) are becoming viable alternative construction resources due to their economic benefits. However, REM may be composed of weak rocks, e.g., phyllites, limiting the use in a base layer. The present paper attempts to further the knowledge of the mechanical performance of REM by performing Repeated Load Triaxial Tests (RLTT). REM are mixed with Recycled Phyllite Materials (RPM) in systematic blends of 0%, 25%, 50%, and 100%. The batches' resilient modulus ($M_R$) and permanent deformation (PD) characteristics were assessed to establish the maximum RPM allowed into REM while maintaining the required performance. Hicks and Monismith's and Uzan's models were used to characterize the stiffness behavior. A wide variation in the stiffness between the two materials was observed. Batches comprised of 0% RPM–100% REM and 25% RPM–75% REM showed high stiffness performance. The Coulomb model assessed the PD behavior, and the results showed a similar response for all batches. Unlike the stiffness, blended mixtures did not show sensitivity to increased RPM content in the PD. This study may help end-users to understand the performance of REM given the documented threshold on the allowable quantity of RPM in REM.

**Keywords:** recycled excavation materials; recycled phyllite materials; resilient modulus; permanent deformation

check for updates

**Citation:** Adomako, S.; Engelsen, C.J.; Thorstensen, R.T.; Barbieri, D.M. Repeated Load Triaxial Testing of Recycled Excavation Materials Blended with Recycled Phyllite Materials. *Materials* **2022**, *15*, 621. https://doi.org/10.3390/ma15020621

Academic Editor: Dario De Domenico

Received: 9 December 2021
Accepted: 10 January 2022
Published: 14 January 2022

**Publisher's Note:** MDPI stays neutral with regard to jurisdictional claims in published maps and institutional affiliations.

**Copyright:** © 2022 by the authors. Licensee MDPI, Basel, Switzerland. This article is an open access article distributed under the terms and conditions of the Creative Commons Attribution (CC BY) license (https://creativecommons.org/licenses/by/4.0/).

## 1. Introduction

Construction and demolition waste (CDW) is by far the heaviest and voluminous waste stream, accounting for 35% of total waste produced globally [1]. However, thanks to environmental protection legislations and recycling technology, the operations of recovering, and reusing recycled aggregates (RA) from CDW has been successful. As a result, the application of RA in civil construction and performance has been studied for many years [2–5]. Given the origin and composition of CDW, RA mainly recovered and used in construction are recycled masonry aggregates (RMA), recycled concrete aggregates (RCA), mixed recycled aggregates (MRA), reclaimed asphalt pavement (RAP), and construction and demolition recycled aggregates (CDRA) [6]. RMA is sourced from crushed rubble, RCA is obtained from demolished concrete structures, whereas MRA consists of mixtures of RMA, ceramic tile, bricks and RCA. RAP is asphalt-based, and CDRA primarily consists of plastic, glass, wood, etc. [6].

Within the framework of CDW, little attention is given to excavation materials (soil and rock). In Europe, for example, the challenge of implementing a proper traceable system has made it difficult to determine the precise volume generated every year. In addition, today's viable technology for recycling construction waste materials is more focused on waste components such as glass, concrete, bricks, and wood [1,7]. However, the success of

applying recycled excavation materials is demonstrated in big projects such as the Gotthard base tunnel in Switzerland [8].

In Western Norway, Velde's modern aggregates recycling plant produces recycled aggregates (both soil and rocks) from excavation materials (REM), and occasionally phyllite materials are encountered [9]. Phyllites are low-grade metamorphic rocks characterized by phyllosilicates (mica and chlorite), and they usually have low engineering properties [10,11]. In addition, they are anisotropic, and weak planes develop following a preferred orientation, making it easier for a fracture to occur along the direction of the planar orientation [12]. Nevertheless, phyllites with good geometrical and mechanical properties may be applied in cement concrete [13].

Given the overall properties of RA, REM produced at Velde meets a range of technical requirements and is environmentally and economically efficient. In particular, good Los Angeles (LA) and micro-Deval (MD) performance are reported [9]. A comprehensive study of mixing different levels of recycled phyllite materials (RPM) with REM to assess the mechanical properties (LA and MD) and identify mechanically weak minerals was performed [14]. The results showed that intermixing RPM significantly affected the MD at high mixing levels (>40%). In addition, a good correlation was found between increased peaks of phyllosilicate minerals (mica and chlorites) when increasing RPM content. Hence the acceptable amount of RPM into REM was found. Generally, geological properties, particularly mineralogy, are reported to affect rock's LA and MD performance significantly [11]. In other studies, 50% of REM was incorporated into RCA obtained from CDW for concrete production [15]. The study showed that LA and MD performance of the mix were 30% and 20%, respectively. In addition, compressive strength after 28 days of three samples produced from the mix was reported in the region 57–65 MPa, and the acid-solubility was within 4–7%, which was reasonably lower than RCA produced from a single source of concrete rubble. REM use did not influence the physical characteristics, i.e., slump and density of concrete products [15]. Detailed technical assessment of REM in India showed good technical properties, i.e., specific gravity, LA, bulk density, soundness, and therefore these materials are suitable for a wide range of construction activities [16].

Despite this notable performance of REM, their potential application in unbound construction is not fully used in Norway due to limited research to characterize the behavior under repeated traffic. For instance, this type of mechanical response can be characterized by means of Repeated Load Triaxial Test (RLTT). Given this, REM may be applied as unbound granular material (UGM) in road pavement's base and subbase layers.

The RLTT investigates the mechanical performance of UGM in terms of resilient modulus ($M_R$) and resistance to permanent deformation (PD) [17–20]. In addition, the test simulates the behavior of UGM under repeated traffic loads in real applications [21]. UGM generally show anisotropic and nonlinear characteristics [22,23]. Therefore, the $M_R$ parameter adequately describes the behavior of these materials under cyclic compressive loads. In UGM, deformation behavior is classified by elastic (recoverable) and permanent (irrecoverable). Regarding the first behavior, high $M_R$ means high stiffness and is usually related to high load bearing capacity. Furthermore, an increase in confining stress usually leads to an increase in $M_R$ [24]. On the other hand, an excessive PD produces issues such as rutting, which is commonly related to high levels of deviatoric stress compared with the levels of triaxial stress.

The $M_R$ and PD behavior generally depends on several factors, including gradation, moisture content, fines content, grain size and shape, stress history, loading frequency, and stress level [24–27]. Given these factors, stress values and moisture content represent the most sensitive conditions with a significant effect on the elastic and plastic deformation properties.

The behavior of RA based on mixing levels and acceptable thresholds for sufficient stiffness and PD performance by RLTT is reported in several studies. For example, 25% of crushed brick (CB) blended with RCA and crushed rock (CR) showed optimal stiffness and PD characteristics, and therefore, the mixture makes a good alternative for subbase

material [28]. A similar study reported that 15% RAP and 85% RCA showed sufficient stiffness and deformation response at optimum moisture contents of 59–78%, compared with mixtures of increased RAP content at 30%, 50%, and 100% [29]. In conclusion, the authors emphasized the importance of respecting the mixing threshold of RAP to achieve an acceptable performance. The stiffness and PD behavior of RCA substituted with recycled clay masonry at 10–30% content was studied, and the result showed that the stiffness decreased while permanent strain increased with increased range of clay masonry, and the mixtures showed sensitivity to moisture content [30].

Regarding mixtures comprising of CDRA content, a study on the stiffness and PD behavior of mixtures of RCA and CR mixed with constant 1% crumb rubber and 1–5% of crushed glass showed that the mixtures were sensitive to increased content of crushed glass as both stiffness and PD improved [31]. In view of this, the authors recommended that approximately 1% crumb rubber and 5% crushed glass should be the optimum mixing level for both RCA and CR for base and subbase applications. In a similar study, different mix compositions of 10–50% recycled glass (5 mm) and CR were produced for stiffness and PD investigations [32]. The results showed that up to 30% recycled glass is regarded as optimum to be added to CR, considering that stiffness and PD behavior showed sufficient response just like natural aggregates. In addition, the authors mentioned that the degree of breakdown of the blends was within the acceptable limit as required of pavement subbase material. In another study, a recycled glass of 0–5 mm was mixed by volume with limestone 0–20 mm for stiffness and PD evaluation [33]. Different mixtures were prepared, but the optimum mix for sufficient stiffness and PD behavior was 25% recycled glass and 75% limestone. The authors observed that low traffic stress state corresponding to bulk stress of 82 and 276 kPa had a minor impact and all mixtures studied in these stress state performed similarly. However, a decreasing stiffness trend was observed at high-stress levels [33]. A study that evaluated the frictional strength properties of crushed glass, kaolin and fine quarry blends showed that frictional properties of the soil increased with increased crushed glass content, making the mix suitable for backfilling and embarkment applications [34]. Mixtures composed of glass gullet and caliche-weathered limestone showed that increasing the amount of glass gullet makes the combinations suitable for subbase applications [35].

Given the reported studies and previous research on RA, the almost non-existent research and knowledge of the stiffness and deformation behavior of REM and RPM mixes under repeated loads limit the use of REM composed of occasional amount of weak rocks. Unfortunately, this makes REM complete waste materials suffering the fate of landfill, which is not suitable from an environmental point of view. In addition, skepticism by end-users about the potentials of REM increases. Given that the stiffness and deformation behavior of blended mixtures composed of recycled materials vary, it is essential to assess the materials under consideration in the present study. Hence, the objective of the present study is to evaluate the performance of REM and RPM mixes in RLTT tests to establish an acceptable amount of phyllite or the content of weak rocks which may be present in REM. Finally, the findings may promote the use of REM as road construction materials.

## 2. Materials and Methods

The materials used in the investigation were produced by Velde AS located in Sandnes (Norway). Both REM and RPM were wet processed, i.e., scrubbing, washing, and screened into various fractions by the wet processing recycling facility. The grain size of the fractions used in the study is 4–16 mm as shown in Figure 1. RPM was blended by weight with REM, thus the notation 0 RPM–100 REM refers to 0% RPM and 100% REM, 25 RPM–75 REM refers to 25% RPM and 75% REM, 50 RPM–50 REM refers to 50% each, whereas 100 RPM–0 REM refers to 100% RPM and 0% REM.

The main geological composition of REM is feldspathic rock, granite, and gneiss, with an occasional presence of phyllites. REM shows predominant minerals of quartz, and feldspar group of minerals, i.e., plagioclase and microcline/orthoclase. In addition, a low amount of mica minerals of muscovite and biotite group and almost insignificant amount

of clinochlore were found. The minerals present in RPM are feldspar (i.e., typical traces of anorthite and microcline/orthoclase), quartz, chlorite (mainly clinochlore), and mica group (i.e., biotite, muscovite).

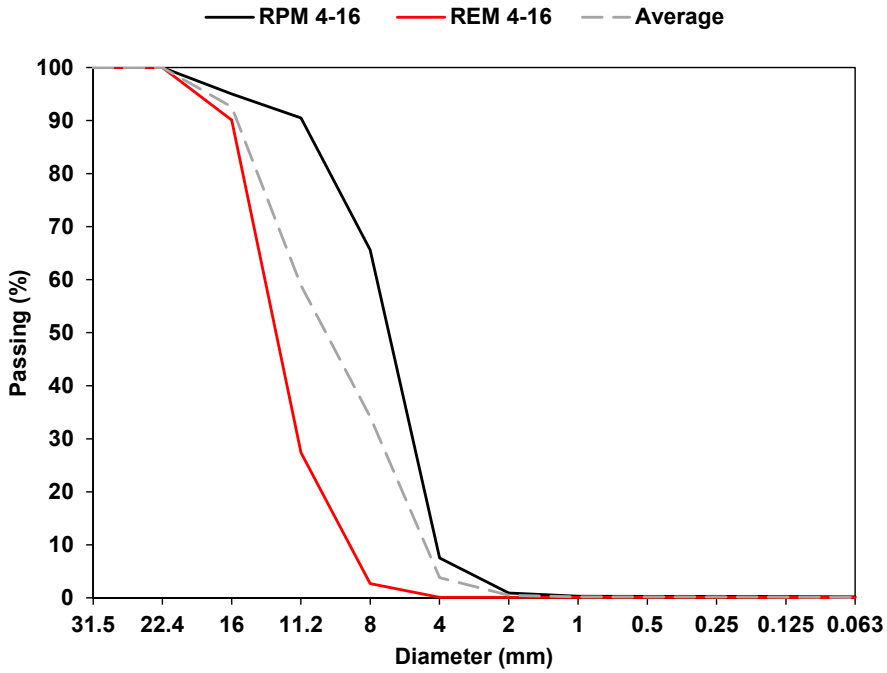


**Figure 1.** Grain size distribution curves for REM and RPM.

The physical and mechanical performance of REM and RPM is shown in Table 1 and Figure 2, respectively. The Flakiness Index (FI) of the two materials was essentially different, as expected, due to the layered shape of phyllite rocks. However, considering RA produced from CDW, FI is reported in the region 8–30% [36]. The water absorption of REM and RPM did not vary significantly, and both materials had the same particle density values. Water absorption and particle density values obtained for RA were reported to be 4–6% and 2.3–2.4 kg/cm$^3$, respectively [36].

**Table 1.** Physical properties of REM and RPM given as the arithmetic mean ± 1 standard deviation, n = 3.

| Sample Name | Flakiness Index (%) EN 933-3 | Water Absorption (%) EN 1097-6 | Particle Density (g/mL) EN 1097-6 |
|---|---|---|---|
| REM | 12.6 ± 2.5 | 0.3 ± 0.2 | 2.5 ± 0.1 |
| RPM | 31.1 ± 1.3 | 0.6 ± 0.1 | 2.5 ± 0.1 |

The LA and MD are critical mechanical properties to assess the strength of aggregates applied in road pavement. The LA determines the resistance to fragmentation, whereas MD evaluates wear resistance. The LA values for REM and RPM were 28% and 26%, respectively, whereas the MD was reported to be 6% and 26% [14]. The MD results varied significantly between REM and RPM. Compared to the performance of materials for base and subbase application defined by the Norwegian Public Roads Administration [37], the LA values met the base course and subbase limit requirement at ≤35%. Regarding the MD, only RPM exceeded the limit criteria of ≤15% for base and ≤20% for subbase. Hence, to comply with MD, the maximum content of RPM was found to be around 40%, see Figure 2.

Regarding the sample preparation for RLTT, a bulk mass of 8.500 g was measured in different quantities for pure REM and RPM based on the gradation specified in Figure 1. In addition, 25% and 50% RPM blended batches were prepared. Fractions of REM and

REM are shown in Figure 3a. Each bulk sample consisted of fractions obtained from the predefined gradation groups of 16–11.2 mm, 11.2–8 mm, 8–4 mm, to represent an effective distribution of particles. The distribution followed five individual groupings, (see Figure 3b for distribution example of REM), and each part was carefully placed into the mold and compacted. Milwaukee 2"SDS Max rotary hammer (hammer weight 12 kg, work per blow 27 Nm, tamping time 25 s) was used to compact each layer in the steel mold (see Figure 3c). The compacted specimen ready to be ejected from the mold is shown in Figure 3d. This operation requires special attention to avoid losing any particle, as shown in Figure 3e. Finally, the specimen is covered by two latex membrane and supported by two endplates, four plastic rings and two hose clamps to avoid penetration of water, see Figure 3f. Two Linear Variable Differential Transducers (LVDTs), are mounted to measure axial deformation, and three LVDTs measure the radial deformation, see Figure 3g. The complete test setup with the chamber filled with water is shown in Figure 3h, and Figure 3i shows the computer for data collection.

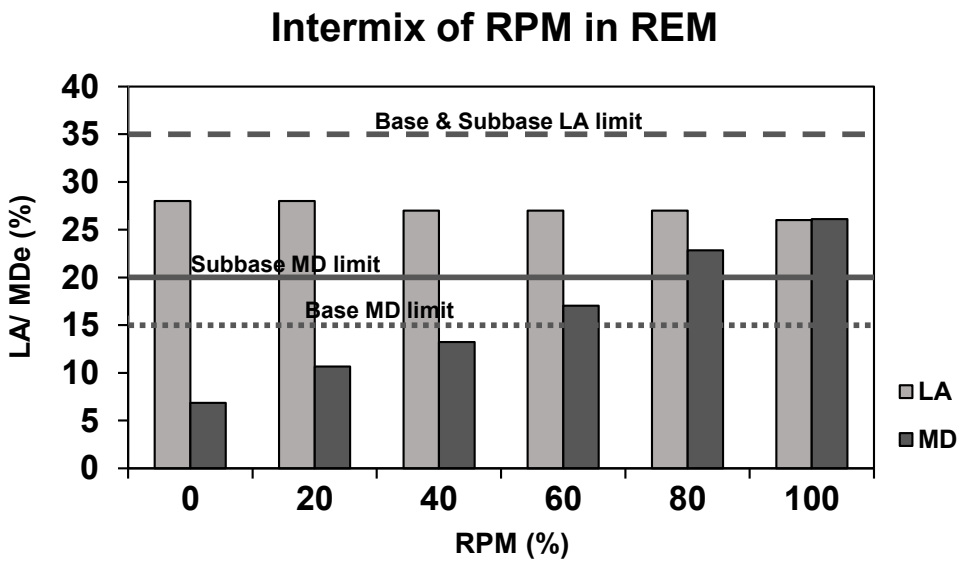


**Figure 2.** LA and MD performance of REM and mixed with RPM, adapted from [14].

The RLTT consists of a Multi-Stage Low-Stress Level (MS LSL) loading procedure on the specimen, according to the European Standard EN 13286-7 [38]. The process involves applying two stress paths, i.e., pressurized water acting in all directions and the hydraulic jack acting vertically. Thus, the pressurized water exerts a constant confining stress (triaxial stress, $\sigma_t$) at different stress levels. The hydraulic jack produces vertical dynamic stress (deviatoric stress, $\sigma_d$) following a sinusoidal pattern and increases stepwise at each sequence of $\sigma_t$. A minimum pressure value of 5 kPa produces contact between the hydraulic jack and the specimen. The loading sequence follows five incremental stages of $\sigma_t$ at 20, 45, 70, 100, and 150 kPa, with six varying load steps ($\sigma_d$). At each load sequence, about 10,000 load cycles of 10 Hz frequency result in a single load step (see Figure 4). In addition, Figure 4 indicates the loading sequence and load step in connection to the bulk stress $\theta$ ($\theta = \sigma_1 + \sigma_2 + \sigma_3 = \sigma_d + 3\sigma_t$, where $\sigma_1$, $\sigma_2$, and $\sigma_3$ are principal stresses-both deviatoric and triaxial stress). When the permanent axial deformation reaches 0.5%, the deviatoric stress automatically stops, and the operator is now able set the next load sequence.

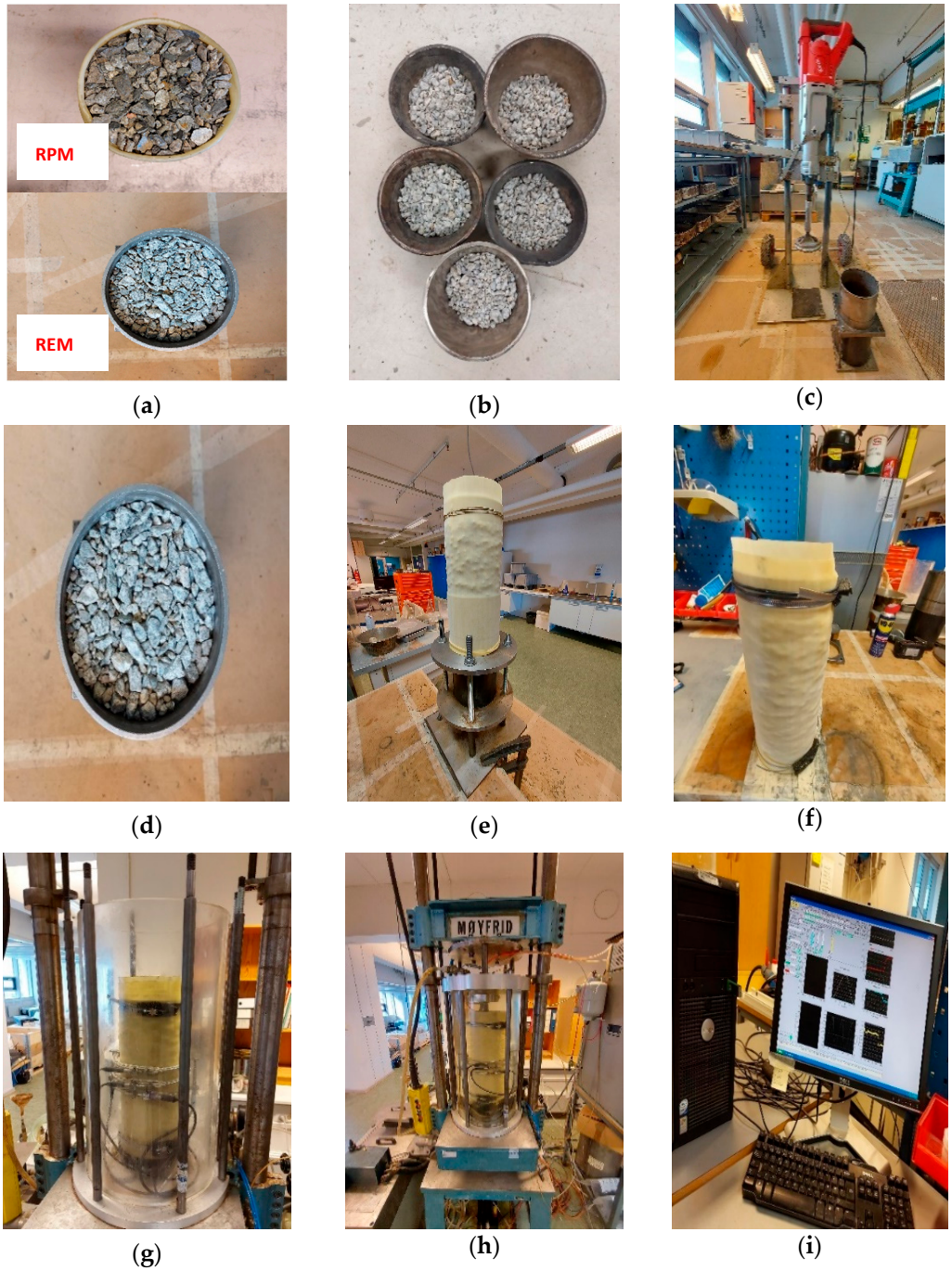


**Figure 3.** Repeated Load Triaxial Test set up. (**a**) Sample of REM and RPM; (**b**) Sample distribution into five different parts following specific gradation; (**c**) Vibrator hammer for sample compaction; (**d**) Fully compacted specimen in the steel mold; (**e**) Ejected specimen covered with first latex membrane; (**f**) Mounting of second latex membrane, plastic rings, and hose clamps; (**g**) Specimen placed in RLTT chamber with mounted two vertical and three horizontal linear variable differential transducers (LVDTs); (**h**) RLTT chamber filled with water and ready to begin test; (**i**) Computer setup for data collection.

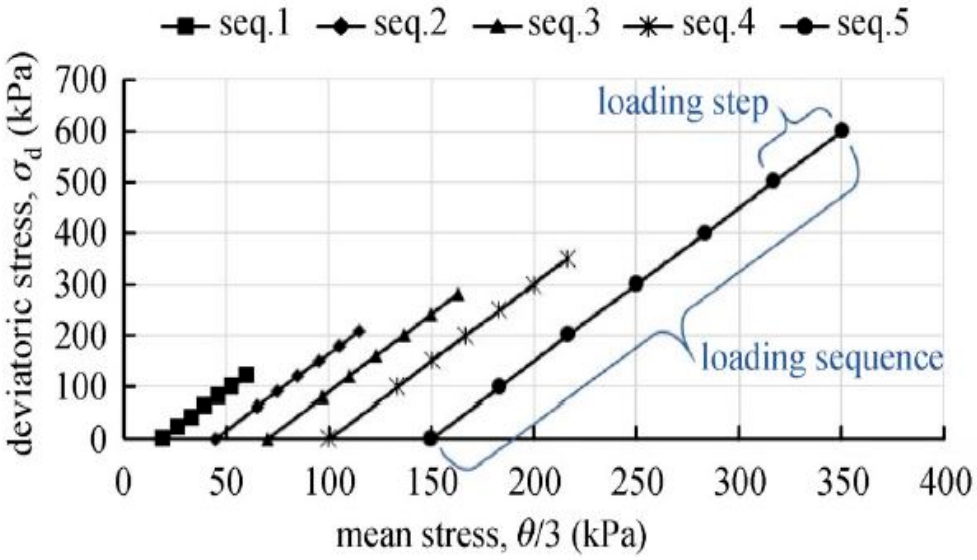


**Figure 4.** Loading sequence and load steps in a Multi-Stage Low-Stress level State (MS LSL), adapted from [39].

## 3. Results and Discussion

The following section discusses the resilient modulus and permanent deformation results obtained from the RLTT tests.

*Resilient Modulus ($M_R$) of REM and RPM*

The resilient modulus $M_R$ is the stiffness of materials and is given as the ratio between the change in deviatoric stress ($\Delta\sigma_d$) and the change in resilient or recoverable strain ($\Delta\varepsilon_r$),

$$M_R = \frac{\Delta\sigma_d}{\Delta\varepsilon_r} \tag{1}$$

Hence, $M_R$ is related to the stress state and it is an important parameter for pavement design. Several nonlinear models describe the relationship between $M_R$ and $\theta$. The most common formulation is the Hicks and Monismith's model [40], expressed in its dimensionless form:

$$M_R = k_1\,\sigma_a \left(\frac{\theta}{\sigma_a}\right)^{k_2} \tag{2}$$

where $k_1$ and $k_2$ are regression model parameters generated from the test results, $\sigma_a$ is a reference pressure taken to be the same as atmospheric pressure (100 kPa), and $\theta$ is the bulk stress. The model expresses the performance of the materials in a two-dimensional state. In the present study, the $M_R$ was calculated by this approach, and the result is presented in Figure 5. Uzan's model, which describes $M_R$ as a function of $\theta$ and $\sigma$ presents a three-dimensional plot [41] and, therefore, it is another valuable approach to compare the behavior of materials. The three parameters indicated in Uzan's model are ($M_R$, $\theta$, $\sigma_d$) and the model is expressed by:

$$M_R = k_1\,\sigma_a \left(\frac{\theta}{\sigma_a}\right)^{k_2} \left(\frac{\sigma_d}{\sigma_a}\right)^{k_3} \tag{3}$$

where $k_1$, $k_2$, $k_3$ are regression parameters.

As already mentioned above, moisture content represent one of the sensitive factors that affect the stiffness and PD behavior of UGM. Some studies have shown that moisture content significantly influenced the performance of RA at high-stress levels [28,30]. In addition, it is demonstrated regarding phyllite materials that they are sensitive to moisture

variations, and as a result, less cohesion and rapid development of plasticity may occur [42]. Given this, our test was performed on dry batches of REM and RPM.

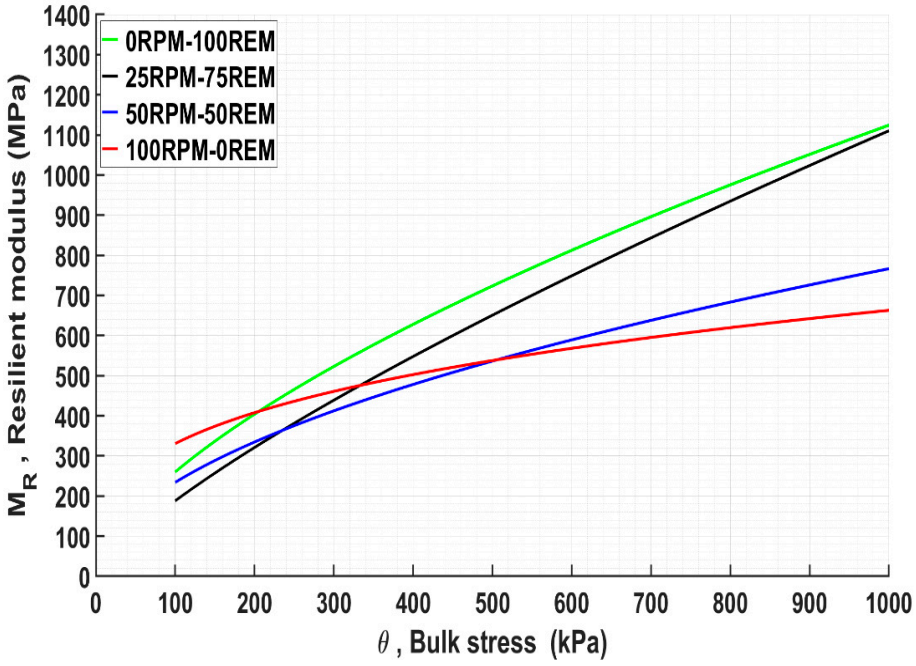


**Figure 5.** Resilient modulus of pure REM and RPM and blended mixtures by Hicks and Monismith model.

The stiffness performance of unblended and blended mixtures of REM and RPM at different $\theta$ is shown in Figure 5. Slightly high stiffness of 330 MPa was observed at the baseline 100 RPM compared with 260 MPa for 100 REM, at $\theta$ of 100 kPa. Foliated rocks of metamorphic origin composed of fine-grained felsic, and a significant amount of mica showed less stiffness of approximately 200 MPa at the same $\theta$ of 100 kPa [17]. Nevertheless, increased stiffness of 100 REM occurs at $\theta$ starting from 200 kPa, and the performance assumed better cohesion and frictional properties as the stiffness behaved almost linearly. This observation may be due to a considerable increase of $M_R$ properties as the confinement pressure and consolidation increased. A possible explanation for slightly high $M_R$ for 100 RPM at low bulk stress may be due to the slow packing density and particle re-orientation at the initial stage of the compaction process. In addition, the high surface area between the particles may have contributed to the initial performance since RPM is characterized by high FI. The stiffness response of both materials in a pure state indicates the vital role of material properties on performance.

For the blended mixtures, the stiffness decreased with an increased RPM content. 25 RPM–75 REM blends showed a performance pattern similar to 100 REM, whereas 50 RPM–50 REM performed similarly to 100 RPM. At a high-stress state, blended and unblended mixture 25 RPM–75 REM and 100 REM respectively provide higher stiffness performance. A similar conclusion was reached regarding the quantity of weak material in a mix for sufficient stiffness performance in the study [28]. In their study, the effect of CB in mixtures 25 CB–75 RCA and 25 CB–75 CR was consistent, except that the cemented part of RCA could potentially lead to significant permanent strain due to residual cement action. However, the authors mentioned that it is unlikely that such changes would significantly affect pavement performance over time. The LA values obtained in that study were 21%, 28%, and 36% for CR, RCA, and CB, respectively [28].

In other studies, effective stiffness response of RAP and RCA blends was achieved at 15 RAP–85 RCA combinations [29], and the LA of both materials in the pure state was reported as 42% and 28%, respectively. The LA for the mixture was 38% [29]. A comparative

study of deformation and stiffness behavior of two RCA and virgin quartzite rocks showed that the stiffness of RCA increased within the region of 490–1020 MPa, whereas quartzite performed within the region 480–685 MPa [43]. According to the authors, both materials' performance complied with the Australian requirement of 300 MPa, and the reported LA was 39% and 37% for both RCA and 25% for quartzite [43]. As found in the present study, the stiffness behavior of REM and RPM follows a similar pattern of mafic igneous rocks and metamorphic rocks classified as strong and weak rocks, respectively [17]. The authors mentioned that metamorphic rocks consisted of fine-grained felsic and micaceous texture, and the LA values reported were 17% and 30% for mafic igneous and metamorphic rocks, respectively. In the Netherlands, the stiffness values for natural aggregates, RMA, MRA and RCA are reported to be 100–400 MPa, 150–250 MPa, 400–600 MPa, and 600–800 MPa, respectively [44].

Given the baseline performance reported in the studies above, it is sufficient to mention that both REM and RPM showed optimal stiffness responses despite the significant performance variation between the two, which is certainly due to the inherent properties of the materials.

It is crucial to emphasize the effect of shape particle and FI regarding the performance of RPM. Although this was not experimentally demonstrated in this study, several researchers have investigated the effect of shape on the stiffness and deformation properties of unbound materials. As already shown in Table 1, a significant variation of FI performance was found between REM and RPM. Both materials meet the FI requirement reported as $\leq$35% by the Norwegian Public Roads Administration [37]. A study of gneiss rocks with different textural and shape properties (flaky, flaky rounded, cubic, and cubic rounded) was performed [45], and the results showed that for the same $\theta$ of 200 kPa, cubic and cubic rounded particles had the highest stiffness performance in the region of 300–400 MPa, whereas that of flaky particles was <300 MPa. It was observed in the same study that as the $\theta$ increased to 1000 kPa, a marginal drop of stiffness in the cubic particles was observed; nevertheless, the study concluded that cubic particles showed highest stiffness response. Additionally, for recycled aggregates, some authors have established strong relationships between FI and stiffness and deformation properties [46,47]. Hence, it is necessary to study the effect of other physical properties and, in this case, FI to understand the behavior altogether.

Uzan's model presents a three-dimensional view plot of the relationship between $M_R$ $\theta$ and $\sigma_d$ as discussed above. The model was applied to the RLTT data, and the regression parameters used in both Hicks and Monismith's and Uzan's models are shown in Table 2.

**Table 2.** Regression parameters of Hicks and Monismith's and Uzan's models.

| Sample | Hicks and Monismith | | Uzan | | |
|---|---|---|---|---|---|
| | $k_1$ | $k_2$ | $k_1$ | $k_2$ | $k_3$ |
| 0 RPM–100 REM | 2363 | 0.59 | 779 | 1.66 | −0.94 |
| 25 RPM–75 REM | 1881 | 0.77 | 575 | 1.88 | −1.01 |
| 50 RPM–50 REM | 2597 | 0.44 | 1026 | 1.30 | −0.76 |
| 100 RPM–0 REM | 4122 | 0.29 | 1306 | 1.46 | −1.11 |

Regarding Uzan's model, the results showed similar performance of $M_R$ for the materials in pure and mixed conditions, see Figure 6.

Permanent Deformation Behavior of REM and RPM

In this study, the Coulomb approach was adopted to investigate the PD of the materials. The Coulomb approach, which derives from the shakedown approach characterizes the mobilized friction angle $\rho(^\circ)$ and incremental friction angle $\varphi(^\circ)$, which describes the degree of mobilized and maximum shear strength, respectively [48] as shown in Figure 7. These two angles illustrate the behavior of materials according to three ranges, i.e., elastic,

elasto-plastic, and failure, see Figure 7. Table 3 shows the permanent strain rate for each performance range.

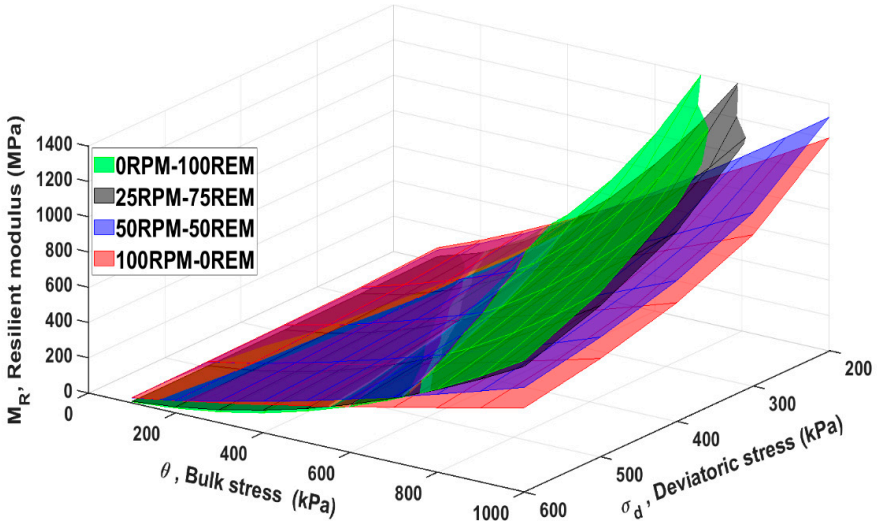


**Figure 6.** Resilient modulus of pure REM and RPM and blended mixtures by Uzan's model.

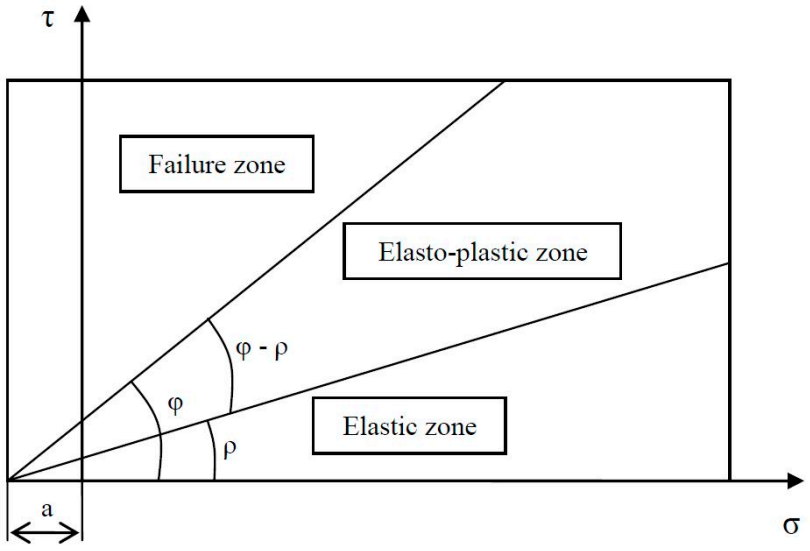


**Figure 7.** Material behavior classified according to mobilized shear strength $\rho(^\circ)$ and maximum shear to failure $\varphi(^\circ)$ in three ranges. The Coulomb approach applied to cyclic load triaxial testing is demonstrated in a τ-σ plot, adapted from [45].

**Table 3.** Classification of the deformation behaviour according to Coulomb model.

| Permanent Strain Rate ($\dot{\varepsilon}$) | Performance Range |
|---|---|
| $\dot{\varepsilon} < 2.5 \times 10^{-8}$ | elastic range |
| $2.5 \times 10^{-8} < \dot{\varepsilon} < 1.0 \times 10^{-7}$ | elasto-plastic range |
| $\dot{\varepsilon} > 1.0 \times 10^{-7}$ | failure range |

The accumulation of PD is classified into the three performance ranges according to the aforementioned angles in the Coulomb model and is represented by best-fit lines. Each load step is defined by the average strain rate $\dot{\varepsilon}$ developed within 5.000 to 10.000 load

cycles [48], which is described as a measure of the speed to PD [45]. Regarding the elastic limit and failure limit, they are respectively defined by the following equations.

$$\sigma_d = \frac{2\sin\rho\ (\sigma_3 + a)}{1 - \sin\rho} \tag{4}$$

$$\sigma_d = \frac{2\sin\varphi\ (\sigma_3 + a)}{1 - \sin\varphi} \tag{5}$$

where $a$ is the apparent attraction considered equal to 20 kPa [45].

The mobilized friction angle $\rho(^\circ)$ and incremental friction angle $\varphi(^\circ)$ of REM and RPM in unblended and blended mixtures resulting from the loading sequence are shown in Figure 8, and Table 4 illustrates the limit values obtained for $\rho(^\circ)$ and $\varphi(^\circ)$, respectively. To present a typical raw data trend, Figure 9 shows the pattern of accumulated axial permanent deformation (PDaxial) for each of the five loading sequences (LS) in each tested mix percentage. There is no variation in the degree of mobilized angle for the samples as the values are the same. Regarding the incremental friction angle $\varphi(^\circ)$, 50% RPM–50% REM batch had the lowest value. Overall, the samples tested in this study offered a similar response when the resistance to PD was determined. Unlike stiffness, blended mixtures assessed for PD behavior did not show sensitivity to increased RPM content. Comparing the performance to crushed rocks in the studies [17,39,49], the values of mobilized friction angle $\rho(^\circ)$ obtained in this study is small; nevertheless, the incremental friction angle $\varphi(^\circ)$ is similar to the results obtained in the studies mentioned above. Such changes could be the differences in material properties, as emphasized by [49] that differences in the grading envelope reflected the discrepancies in the PD behavior. A basic friction angle for unweathered rock surfaces falls between 25° and 35° [50]. Regarding RA, it was found that the friction angle was small in the blends of 25 CB–75 RCA and 25 CB–75 CR [28].

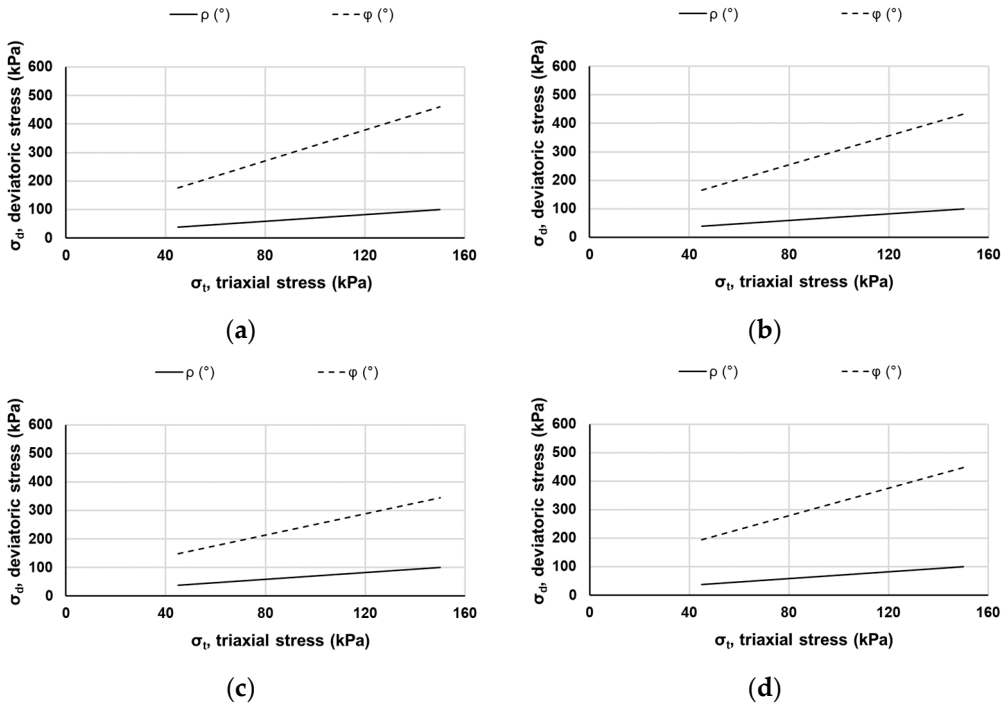


**Figure 8.** Degree of mobilized shear strength $\rho(^\circ)$ and maximum shear strength $\varphi(^\circ)$ of (**a**) 0% RPM–100% REM; (**b**) 25% RPM–75% REM; (**c**) 50% RPM–50% REM; and (**d**) 100% RPM–0% REM.

**Table 4.** Mobilized angle of friction $\rho(^\circ)$ and incremental angle to failure $\varphi(^\circ)$ for REM and RPM in pure and blended state.

| Sample | Limit Angles | |
|---|---|---|
| | $\rho(^\circ)$ | $\varphi(^\circ)$ |
| 0 RPM–100 REM | 30.4 | 69.7 |
| 25 RPM–75 REM | 30.4 | 68.5 |
| 50 RPM–50 REM | 30.4 | 66.4 |
| 100 RPM–0 REM | 30.4 | 71.4 |

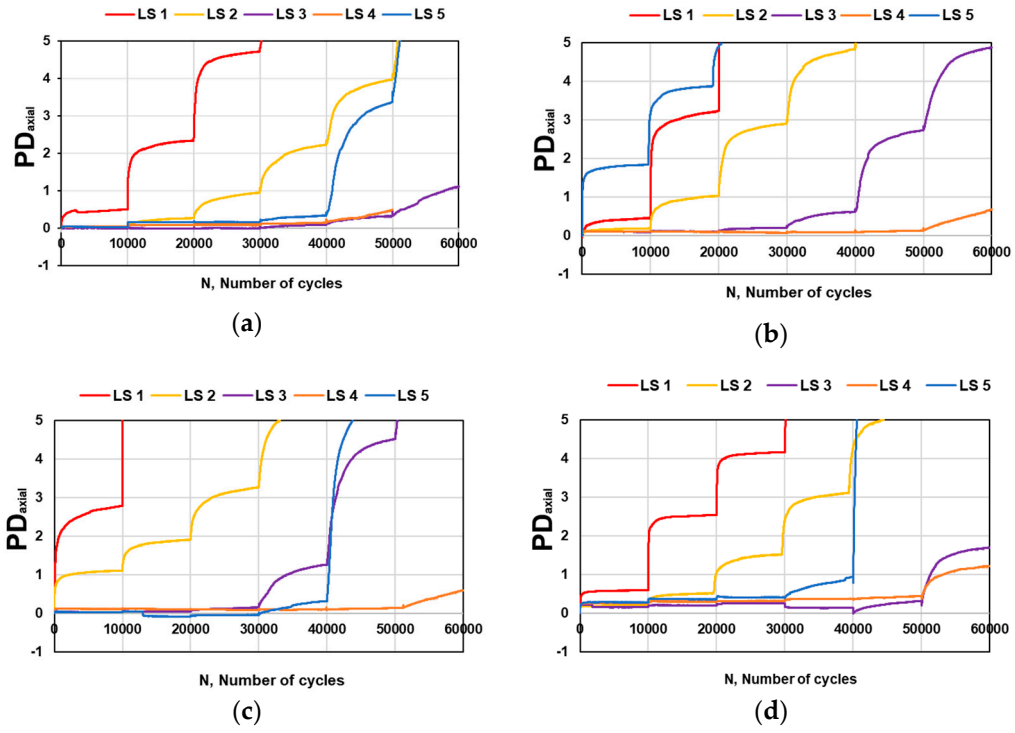


**Figure 9.** Permanent deformation (PD) of REM and RPM as function of the load cycles (N) for (**a**) 0% RPM–100% REM; (**b**) 25% RPM–75% REM; (**c**) 50% RPM–50% REM, and (**d**) 100% RPM–0% REM.

The PD of the materials gave a true reflection of the performance concerning degradation behavior in the LA tests. There is a strong relationship between PD, fine particles, and high fouling index [51]. In other words, rocks susceptible to fragmentation or crushing may develop a significant number of fine particles over time, resulting in excessive PD. Similarly, a conclusion was reached that angularity and surface texture positively influenced the elastic and plastic shakedown thresholds for cubic aggregates [45]. Based on these findings, it is possible to infer that the PD performance of both REM and RPM are satisfactory. Therefore, the use of REM with some amount of RPM should not be considered detrimental to overall performance.

## 4. Conclusions

This work investigated the resilient modulus ($M_R$) and permanent deformation (PD) behavior of Recycled Excavation Materials (REM) blended with Recycled Phyllite Materials (RPM) by Repeated Load Triaxial Test (RLTT). RPM was systematically incorporated into REM at 0%, 25%, 50%, and 100% to document the maximum substitution ratio without compromising the performance. Hicks and Monismith's model and Uzan's model assessed the stiffness, while the Coulomb model was used to evaluatethe PD.

The investigation findings showed that the stiffness behavior of REM and RPM in a pure state varied considerably, with 0% RPM–100% REM exhibiting high stiffness strength. Regarding blended mixtures, 25% RPM–75% REM achieved almost the same strength characteristics as REM in a pure state, whereas 50% RPM–50% REM performed similarly to RPM. The behavior of the materials in this regard showed sensitivity to the increased content of RPM.

The PD response of both materials did not show significant differences as the degree of mobilized friction angle $\rho(^{\circ})$ for the samples was the same. Regarding the incremental friction angle $\varphi(^{\circ})$, 50% RPM–50% REM had the lowest value; however, no sensitivity to increased RPM content in the PD was shown. The study's findings may be helpful to end-users regarding the maximum quantity of RPM in REM considering the application of REM in unbound construction.

Given the influence of physical properties, as demonstrated in other studies on the stiffness and deformation characteristics of unbound materials, the authors recommend that future research should focus on the effect of material properties such as the shape and flakiness index of unblended and blended REM and RPM mixtures.

**Author Contributions:** Conceptualization, S.A.; methodology, S.A. and D.M.B.; software, S.A. and D.M.B.; validation, C.J.E., R.T.T., S.A. and D.M.B.; formal analysis, S.A., C.J.E., R.T.T. and D.M.B.; investigation, S.A.; resources, C.J.E., R.T.T. and D.M.B.; writing—original draft preparation, S.A.; writing—review and editing, C.J.E. and D.M.B.; supervision, C.J.E. and R.T.T. All authors have read and agreed to the published version of the manuscript.

**Funding:** The work presented in this paper is part of the ongoing project MEERC (More Efficient and Environmentally friendly Road Construction), partly funded by the Research Council of Norway (NFR) [project number 273700] and Sorlandets Kompetansefond.

**Institutional Review Board Statement:** Not applicable.

**Informed Consent Statement:** Not applicable.

**Data Availability Statement:** The data presented in this paper is available upon request from the corresponding author.

**Acknowledgments:** The authors express profound gratitude to Velde Pukk in Sandnes (Norway) for providing the materials used in this study. In addition, the kind support of Bent Lervik at NTNU is acknowledged.

**Conflicts of Interest:** The authors declare no conflict of interest.

## Abbreviations

| | |
|---|---|
| CB | Crushed Brick |
| CDW | Construction and Demolition Waste |
| CDRA | Construction and Demolition Waste Recycled Aggregates |
| CR | Crushed Rock |
| FI | Flakiness Index |
| LA | Los Angeles Test |
| LSL | Low-Stress Level |
| LVDT | Linear Variable Differential Transducers |
| MD | Micro-Deval Test |
| MS | Multi-Stage |
| MRA | Mixed Recycled Aggregates |
| MR | Resilient Modulus |
| PD | Permanent Deformation |
| PDaxial | Axial Permanent Deformation |
| RA | Recycled Aggregates |
| RAP | Recycled Asphalt Pavement |
| RCA | Recycled Concrete Aggregates |
| REM | Recycled Excavation Materials |

| | |
|---|---|
| RLTT | Repeated Load Triaxial Test |
| RMA | Recycled Masonry Aggregates |
| RPM | Recycled Phyllite Material |
| UGM | Unbound Granular Material |

## References


1. Ng, S.; Engelsen, C.J. Construction and demolition wastes. In *Waste and Supplementary Cementitious Materials in Concrete*; Elsevier: Amsterdam, The Netherlands, 2018; pp. 229–255. [CrossRef]
2. Bianchini, G.; Marrocchino, E.; Tassinari, R.; Vaccaro, C. Recycling of construction and demolition waste materials: A chemical–mineralogical appraisal. *Waste Manag.* **2005**, *25*, 149–159. [CrossRef]
3. Chung, S.-S.; Lo, C.W. Evaluating sustainability in waste management: The case of construction and demolition, chemical and clinical wastes in Hong Kong. *Resour. Conserv. Recycl.* **2003**, *37*, 119–145. [CrossRef]
4. Huang, W.-L.; Lin, D.-H.; Chang, N.-B.; Lin, K.-S. Recycling of construction and demolition waste via a mechanical sorting process. *Resour. Conserv. Recycl.* **2002**, *37*, 23–37. [CrossRef]
5. Poon, C.S.; Chan, D. Feasible use of recycled concrete aggregates and crushed clay brick as unbound road sub-base. *Constr. Build. Mater.* **2006**, *20*, 578–585. [CrossRef]
6. Cardoso, R.; Silva, R.V.; de Brito, J.; Dhir, R. Use of recycled aggregates from construction and demolition waste in geotechnical applications: A literature review. *Waste Manag.* **2016**, *49*, 131–145. [CrossRef] [PubMed]
7. Tam, V.W.; Tam, C.M. A review on the viable technology for construction waste recycling. *Resour. Conserv. Recycl.* **2006**, *47*, 209–221. [CrossRef]
8. Lieb, R. Experience in spoil management on conclusion of excavations for the Gotthard base tunnel. In *Tagung der italienischen Tunnelbaugesellschaft Convegno SIG (Società Italiana Gallerie), Samoter, VeronaFiere*; Societa Italiana Gallerie: Milano, Italy, 2011.
9. Norby, M. Nytt Resirkulert Tilslag Produsert fra Grave-og Byggavfall. Master's Thesis, University of Agder, Kristiansand, Norway, 2020.
10. Voit, K.; Kuschel, E. Rock material recycling in tunnel engineering. *Appl. Sci.* **2020**, *10*, 2722. [CrossRef]
11. Adomako, S.; Engelsen, C.J.; Thorstensen, R.T.; Barbieri, D.M. Review of the relationship between aggregates geology and Los Angeles and micro-Deval tests. *Bull. Eng. Geol. Environ.* **2021**, *80*, 1963–1980. [CrossRef]
12. Singh, M.; Samadhiya, N.; Kumar, A.; Kumar, V.; Singh, B. A nonlinear criterion for triaxial strength of inherently anisotropic rocks. *Rock Mech. Rock Eng.* **2015**, *48*, 1387–1405. [CrossRef]
13. Adom-Asamoah, M.; Afrifa, R.O. A study of concrete properties using phyllite as coarse aggregates. *Mater. Des.* **2010**, *31*, 4561–4566. [CrossRef]
14. Adomako, S.; Engelsen, C.J.; Thorstensen, R.T.; Barbieri, D.M. Recycled aggregates derived from excavation materials—Mechanical performance and identification of weak minerals. *Resour. Conserv. Recycl.* **2021**. *submitted*.
15. Mujica, E.V.H.; Engelsen, C.J.; Nodland, M.S. Recycled aggregates produced from two different feedstock materials—Applied in ready-mixed concrete. In Proceedings of the International Conference on Sustainable Materials, Systems and Structures, Rovinj, Croatia, 18–22 March 2019.
16. Engelsen, C.J.; Malhotra, S.K.; Bhatiani, G.; Nath, K. Detailed assessment of the technical properties of recycled aggregates from mixed C&D waste. *Indian Concr. J.* **2020**, *94*, 32–39.
17. Barbieri, D.M.; Hoff, I.; Mørk, M.B. Innovative stabilization techniques for weak crushed rocks used in road unbound layers: A laboratory investigation. *Transp. Geotech.* **2019**, *18*, 132–141. [CrossRef]
18. Barbieri, D.M.; Hoff, I.; Mørk, M.B. Organosilane and lignosulfonate as innovative stabilization techniques for crushed rocks used in road unbound layers. *Transp. Geotech.* **2020**, *22*, 100308. [CrossRef]
19. Barbieri, D.M.; Tangerås, M.; Kassa, E.; Hoff, I.; Liu, Z.; Wang, F. Railway ballast stabilising agents: Comparison of mechanical properties. *Constr. Build. Mater.* **2020**, *252*, 119041. [CrossRef]
20. Erlingsson, S.; Rahman, M.S. Evaluation of permanent deformation characteristics of unbound granular materials by means of multistage repeated-load triaxial tests. *Transp. Res. Rec.* **2013**, *2369*, 11–19. [CrossRef]
21. Barksdale, R.D. Compressive stress pulse times in flexible pavements for use in dynamic testing. *Highw. Res. Rec.* **1971**, *345*, 32–44.
22. Kim, M.; Tutumluer, E.; Kwon, J. Nonlinear pavement foundation modeling for three-dimensional finite-element analysis of flexible pavements. *Int. J. Geomech.* **2009**, *9*, 195–208. [CrossRef]
23. Tutumluer, E.; Seyhan, U. Laboratory determination of anisotropic aggregate resilient moduli using an innovative test device. *Transp. Res. Rec.* **1999**, *1687*, 13–21. [CrossRef]
24. Lekarp, F.; Isacsson, U.; Dawson, A. State of the art. I: Resilient response of unbound aggregates. *J. Transp. Eng.* **2000**, *126*, 66–75. [CrossRef]
25. Tian, P.; Zaman, M.M.; Laguros, J.G. Gradation and moisture effects on resilient moduli of aggregate bases. *Transp. Res. Rec.* **1998**, *1619*, 75–84. [CrossRef]
26. Ekblad, J. Influence of Water on Coarse Granular Road Material Properties. Ph.D. Thesis, KTH University, Stockholm, Sweden, 2007.

27. Attia, M.; Abdelrahman, M. Effect of state of stress on the resilient modulus of base layer containing reclaimed asphalt pavement. *Road Mater. Pavement Des.* **2011**, *12*, 79–97. [CrossRef]
28. Arulrajah, A.; Piratheepan, J.; Bo, M.; Sivakugan, N. Geotechnical characteristics of recycled crushed brick blends for pavement sub-base applications. *Can. Geotech. J.* **2012**, *49*, 796–811. [CrossRef]
29. Arulrajah, A.; Piratheepan, J.; Disfani, M.M. Reclaimed asphalt pavement and recycled concrete aggregate blends in pavement subbases: Laboratory and field evaluation. *J. Mater. Civ. Eng.* **2014**, *26*, 349–357. [CrossRef]
30. Cameron, D.; Azam, A.; Rahman, M. Recycled clay masonry and recycled concrete aggregate blends in pavement. In *GeoCongress 2012: State of the Art and Practice in Geotechnical Engineering*; ASCE: Reston, VA, USA, 2012. [CrossRef]
31. Saberian, M.; Li, J.; Setunge, S. Evaluation of permanent deformation of a new pavement base and subbase containing unbound granular materials, crumb rubber, and crushed glass. *J. Clean. Prod.* **2019**, *230*, 38–45. [CrossRef]
32. Ali, M.; Arulrajah, A.; Disfani, M.; Piratheepan, J. Suitability of using recycled glass-crushed rock blends for pavement subbase applications. In *Geo-Frontiers: Advances in Geotechnical Engineering*; ASCE: Reston, VA, USA, 2011; pp. 1325–1334.
33. Amlashi, S.M.H.; Vaillancourt, M.; Carter, A.; Bilodeau, J.-P. Resilient modulus of pavement unbound granular materials containing recycled glass aggregate. *Mater. Struct.* **2018**, *51*, 1–12. [CrossRef]
34. Wartman, J.; Grubb, D.G.; Strenk, P. Engineering properties of crushed glass-soil blends. In *Geotechnical Engineering for Transportation Projects*; ASCE: Reston, VA, USA, 2004; pp. 732–739. [CrossRef]
35. Senadheera, S.; Rana, A.; Nash, P. Characterization of the behavior of granular road material containing glass cullet. In Proceedings of the International Conferences on the Bearing Capacity of Roads, Railways and Airfields, Trondheim, Norway, 25–27 June 2005.
36. Silva, R.; De Brito, J.; Dhir, R. Use of recycled aggregates arising from construction and demolition waste in new construction applications. *J. Clean. Prod.* **2019**, *236*, 117629. [CrossRef]
37. Norwegian Public Roads Administration. *Håndbok N200 Vgbygging*; NPRA: Vejdirektoratet, Norway, 2014.
38. The European Committee for Standardization (CEN). *Cyclic Load Triaxial Test for Unbound Mixture*; European Committee for Standardization: Brussels, Belgium, 2004.
39. Barbieri, D.M.; Hoff, I.; Ho, C.-H. Crushed rocks stabilized with organosilane and lignosulfonate in pavement unbound layers: Repeated load triaxial tests. *Front. Struct. Civ. Eng.* **2021**, *15*, 412–424. [CrossRef]
40. Hick, R.; Monismith, C. Factors influencing the resilient response of granular materials. *Highw. Res. Rec.* **1971**, *345*, 15–31.
41. Uzan, J. Characterization of granular material. *Transp. Res. Rec.* **1985**, *1022*, 52–59.
42. Hu, K.; Feng, Q.; Wang, X. Experimental research on mechanical property of phyllite tunnel surrounding rock under different moisture state. *Geotech. Geol. Eng.* **2017**, *35*, 303–311. [CrossRef]
43. Gabr, A.; Cameron, D. Properties of recycled concrete aggregate for unbound pavement construction. *J. Mater. Civ. Eng.* **2012**, *24*, 754–764. [CrossRef]
44. RBBS (Recycling-Branchevereniging Beren en Sorteren). Use of Recycled Aggregate—The Best Road Base Material on Earth. Technical Report. 2017. Available online: https://www.researchgate.net/publication/313106736_Use_of_recycled_aggregate_-_The_best_road_base_material (accessed on 9 January 2022).
45. Uthus, L. Deformation Properties of Unbound Granular Aggregates. Ph.D. Thesis, Norwegian University of Science and Technology (NTNU), Trondheim, Norway, 2007.
46. Nataatmadja, A.; Tan, Y. Resilient response of recycled concrete road aggregates. *J. Transp. Eng.* **2001**, *127*, 450–453. [CrossRef]
47. Bozyurt, O.; Tinjum, J.M.; Son, Y.-H.; Edil, T.B.; Benson, C.H. Resilient modulus of recycled asphalt pavement and recycled concrete aggregate. In *GeoCongress 2012: State of the Art and Practice in Geotechnical Engineering*; ASCE: Reston, VA, USA, 2012; pp. 3901–3910. [CrossRef]
48. Hoff, I.; Bakløkk, L.J.; Aurstad, J. Influence of laboratory compaction method on unbound granular materials. In Proceedings of the 6th International Symposium on Pavements Unbound (UNBAR 6), Nottingham, UK, 6–8 July 2004; pp. 6–8.
49. Barbieri, D.; Hoff, I.; Mork, H. Laboratory investigation on unbound materials used in a highway with premature damage. In *Bearing Capacity of Roads, Railways and Airfields*; CRC Press: Boca Raton, FL, USA, 2017; pp. 101–108.
50. Barton, N.; Choubey, V. The shear strength of rock joints in theory and practice. *Rock Mech.* **1977**, *10*, 1–54. [CrossRef]
51. Qian, Y.; Tutumluer, E.; Hashash, Y.M.; Ghaboussi, J. Effects of ballast degradation on permanent deformation behavior from large-scale triaxial tests. In Proceedings of the ASME/IEEE Joint Rail Conference, Colorado Springs, CO, USA, 2–4 April 2014; Volume 45356, p. V001T01A022.

**Paper D**

**S. Adomako**, C. J. Engelsen, L.T. Døssland, T. Danner, and R. T. Thorstensen "Technical and environmental properties of recycled aggregates produced from concrete sludge and excavation materials," *Case Studies in Construction Materials*, (In press). https://doi.org/10.1016/j.cscm.2023.e02498

Case Studies in Construction Materials 19 (2023) e02498

Contents lists available at ScienceDirect

Case Studies in Construction Materials

journal homepage: www.elsevier.com/locate/cscm

# Technical and environmental properties of recycled aggregates produced from concrete sludge and excavation materials

Solomon Adomako [a,*], Christian John Engelsen [b], Line Teigen Døssland [b], Tobias Danner [c], Rein Terje Thorstensen [a]

[a] Department of Engineering and Science, University of Agder, 4879 Grimstad, Norway
[b] SINTEF Community, Department of Building and Infrastructure, P.O.Box 124 Blindern, NO-0314 Oslo, Norway
[c] SINTEF Community, Department of Architecture, Building Materials and Construction, Høgskoleringen 7B, 7034 Trondheim, Norway

ARTICLE INFO

*Keywords:*
Los angeles
Micro-deval
Recycled aggregates
Wet treatment
Re-Con zero
Admixture

ABSTRACT

This study presents a Re-Con Zero dry washing technology used to produce recycled aggregates from concrete sludge (RCZ) and combined as a feedstock in wet recycling excavation materials (EM) for unbound applications. A two-component admixture i.e, high water absorbing polymer and aluminum sulphate was used in producing RCZ. RCZ0, RCZ50 and RCZ100 were produced with EM within the range 0–100%. Analysis by the Los Angeles (LA) and micro-Deval (MD) test demonstrated RCZ to be of high-quality, hence a clear trend of improved performance as the content increased was observed in the LA and MD values. X-ray diffraction analysis performed on original and pulverized residues (<1.6 mm) showed that feldspar, quartz, phyllosilicates (mica and chlorite) and minor amounts of pyroxene (diopside) were present together with paste minerals such as portlandite and residual clinker, and calcite. Acid solubility results demonstrated the relation to increased paste content as particle size reduced. This observation was more prevalent in < 1.6 mm RCZ fraction which further indicated the significant amount of remained paste after wet treatment. Low levels of the content of chemical species of potential concern were in general found and were mostly complying to Norwegian regulations. Total Cr exceeded the criteria of 100 mg/kg, but the leachable Cr(VI) was not detected which showed that remaining Cr after recycling process was present mostly on the trivalent form. This indicated low leaching of Cr upon carbonation and a decrease in pH.

## 1. Introduction

Construction and demolition waste (C&DW) is one of the largest solid waste stream on a global scale [1,2]. The composition of C&DW varies from country to country due to economic structure, environmental and construction policies [1], and about 70–80% of total waste is composed of concrete and bricks [3]. Today, recycling C&DW waste into recycled aggregates is a common practice as it reduces the exploit of aggregate reservoir and environmental pollution [4,5]. Currently, there is a wide range of technological methods which can be applied to process recycled aggregates from C&DW. Many demonstrations have been conducted for the past 15–20 years [6,7], and many significant developments in applying final products have been achieved. For example, considering their application in fresh concrete, some authors have reported stabilized mechanical and durability performance [8,9].

* Corresponding author.
*E-mail address:* solomon.adomako@uia.no (S. Adomako).

https://doi.org/10.1016/j.cscm.2023.e02498
Received 7 June 2023; Received in revised form 8 August 2023; Accepted 19 September 2023
Available online 21 September 2023
2214-5095/© 2023 The Authors. Published by Elsevier Ltd. This is an open access article under the CC BY license (http://creativecommons.org/licenses/by/4.0/).

In order to further increase circular economy, the Norwegian concrete industry is developing solutions to recycle aggregates derived from returned concrete sludge (RCSA). By definition, concrete sludge or returned concrete is residual concrete which remains in the mixing truck and by nature appears in fresh condition with a significant amount of cement mortar [10,11]. Globally, it is estimated that over 125 million tons of these wastes are produced annually depending on quality control during production and use in construction [12]. Currently in Norway, returned concrete are discharged and treated in sedimentation basins, temporarily stored, and finally disposed in a landfill. While one recoverable product is generally known to be RCSA [13], a summary of management strategies to process the waste has been outlined as (a) Recycling in new downgraded products by a process of delivering fresh concrete for pre-cast concrete products or use in backfilling. (b) Reuse in new batches of concrete mixture with or without chemical admixtures or additives. (c) Recycling after hardening of fresh concrete waste by crushing into recycled concrete aggregates (RCA). (d) Reclaiming by a wash-out process using mechanical aggregate reclaiming system to reclaim aggregates and grey water [13]. The outlined management strategies for treatment vary in different countries and are also linked to economic and environmental and logistics issues [13–15].

New emphasis on turning returned concrete into aggregates has been the use of non-toxic additives. For example, one study converted returned concrete into RCSA by using a polymer with high water binding capacity (dosage of 0.4–0.8 m3 of concrete) and thereafter aluminum sulphate to further enhance the water binding process by ettringite formation. The RCSA was produced in the mixer of a concrete truck with the objective of dry washing the drum. The performance in concrete by 30% replacement to natural aggregates was good, i.e., no significant difference between RCSA concrete and reference concrete regarding water permeable capacity, compressive strength development, water absorption, frost resistance and chloride penetration [11]. The authors, however, mentioned that the interface transition zone of concrete produced with RCSA improved and this contributed to the resistance to water penetration. Similar procedure of applying dry washing technology with high water absorbing polymers has gained interest in Norway and a study demonstrated the Los Angeles strength of RCSA to be 25% by applying this type of polymer [16].

Some studies have also demonstrated the possibility to cease cement hydration of RCSA and to prolong its fresh state using stabilizing additives and activators to allow for reuse in new concrete [17–19]. In other studies, RCSA have been produced by conventional curing and separation of aggregates from waste source. These studies replaced RCSA with natural aggregates in a new concrete at various levels and only a slight decrease in durability properties and almost same strength development was found [20,21]. However, reduced strength development has been reported for concrete with 25–100% RCSA [22,23]. So far, the performance of concrete seems to be dependent on the replacement level of natural aggregates with RCSA and the initial quality. This means that careful control of the substitution level and curing of the sludge are essential to achieve desired properties. Furthermore, the same precautions applying to the use of recycled materials (from regular concrete waste) need to be taken for RCSA. While recycled aggregates from concrete waste is also known for unbound construction, the use of RCSA for the same purpose is not widely considered. A few studies have reported their behavior for similar applications. For example, a study that investigated the use of fine RCSA which was incorporated into mortar for soil stabilization reported increased bearing capacity of the mix [20]. In Norway, a large pilot demonstrated the use of RCSA in road base layer as one of the first of its kind [24].

Failing to demonstrate the extended use of these materials in unbound construction may limit the opportunity to achieve current sustainable targets for the concrete industry. Hence, in the present study a new method for producing recycled aggregates by recycling a mix of concrete sludge and excavation materials was demonstrated. The recycled concrete sludge used in the study has been developed by a two-component admixture Re-Con Zero Evo (high water absorbing polymer and aluminum sulphate). The objective was to use Re-Con Zero dry washing technology to produce recycled aggregates from concrete sludge (RCZ) [25] in combination with wet recycling of excavation materials. To the authors best knowledge, this combined approach has not been reported before, including a technical assessment of the recycled materials separately and in mixed conditions. The present study is part of the RECONC project (www.reconc.no) with the objective of developing RCZ with a lower $CO_2$ footprint and reduced heavy metal leaching.

## 2. Materials and methods

### 2.1. Preparation of RCZ

RCZ was produced using a dry wash method for cleaning returned concrete from concrete mixer trucks [25]. In this method, aggregates were fed into concrete mixer trucks containing the sludge and rotated a number of times until the sludge appeared to adhere onto the aggregates. They were later poured from the barrel of the truck. The process was repeated in another scenario with other concrete trucks. This method has the advantage of reducing the volume of water used while cleaning the concrete mixer truck and subsequently reducing the pH of the water. In addition, the process reduces the amount of sludge in the sedimentation basins on the concrete batching plants. By adopting this procedure, granular RCZ was produced. Specifically, 4000–6000 L 4/8 aggregates were fed into a hopper and 2000 L of the aggregates was transferred into a concrete truck containing 500 L of return concrete. The drum of the concrete mixer truck was rotated for 3–5 min before the contents were emptied into a storage bin. The entire process took around 15 min. The dry washing aggregates were stored for 8–12 h before larger agglomerates were crushed with a front loader. Following this the aggregates were moved into a separate storage bin and used for feeding the hopper to enter the next dry washing cycle. The dry washing aggregates were used in subsequent cycles until the surface of the aggregate appeared like a sludge surface and saturated. The feedstock derived from this approach was processed at Ølen Betong and sampled at two different places. The first sampling denoted as (RCZ-$F_0$) took place at Ølen Betong. The feedstock was transported and stockpiled outside the concrete recycling facility at Velde where the second sample of the feedstock (RCZ-F) was collected. The rest of the materials were converted into recycled aggregates (see Section 2.2).

### 2.2. Production of recycled aggregates

The (CDE, Northern Ireland) recycling plant installed at Sandnes (Norway) was used to recycle and produce the RCZ and excavation materials. It has an operation capacity of processing 350 tons per hour of excavation materials or C&DW. The materials are produced in different fractions 0/2 mm, 2/4 mm, 4/16 mm, 16/32 mm, 20/100 mm, including a residual fraction of <63 μm. The primary scalping unit with a grizzly feeder of 100 mm opening grid, receives the feedstock, screens, and separates the large materials or boulders. Hence, masses $<$ 100 mm are transported to the log-washer where they are intensely washed and scrubbed. During this process, the in-built over band magnet traps ferrous metals and any lightweight floating material is dewatered and separated through another chamber. The materials are further dewatered and separated into different fractions before passing through secondary magnetic separation. Final processed fractions appear in sizes described above. One benefit of this technology is that more than 90% of processed water is recycled and pumped back into the system for reuse. The processing of 15 tons of waste excavation materials and 15 tons of RCZ was conducted in a full-scale trial at the Velde facility where the final recycled aggregates were sampled directly from the conveyer belts as shown in Fig. 1. The plant was operated without feeding for 10 min before and in between feeding the target materials to avoid cross contamination.

The mixing volumes in the feeding and the samples (final recycled aggregates) collected from the end of conveyor belt are shown in Table 1. Samples denoted RCZ0, RCZ50 and RCZ100 have been produced with 0–100% of excavation materials. The feeding was conducted by a front loader by equal load distribution. Three samples were also collected from the feedstock piles RCZ-$F_0$, and RCZ-F. For processed materials, six samples were collected from the 4/16 mm conveyer belt. The materials investigated in the study are shown in Fig. 2.

### 2.3. Physical and mechanical tests

The laboratory experiments comprised of physical, mechanical, and chemical tests. Tests for physical properties were particle-size distribution (NS-EN 933–1), particle density, and water absorption (NS-EN 1097–6). Both particle density and water absorption (WA) were performed on fractions passing through 31 mm sieves but retained on 4 mm. The mechanical tests comprised of LA (NS-EN 1097–2) and MD tests (NS-EN 1097–1). Regarding the LA, a test mass of 5000 $\pm$ 5 g of particle size 10/14 mm was derived from the laboratory sample, and a total of eleven steel balls were gently added to the mass in the test drum. A test cycle completes at 500 revolutions, i.e., 15 min, and after the test, the aggregates were washed and sieved on a 1.6 mm sieve and dried. The mass loss (%) was then determined. For MD, a test mass of 500 g of size 10/14 was derived. Spherical balls amounting to 5000 g were gently added to the test mass plus 2.5 $\pm$ 0.5 L of water in the cylindrical steel drum. One complete test cycle took about 2 h, and after the test, the aggregates were washed and sieved on a 1.6 mm sieve and dried. The average mass loss (%) of two test specimens were measured and calculated as the MD coefficient. These experiments were conducted at the laboratory of University of Agder (UiA) and the laboratory of the recycling site in Sandnes by Velde.

### 2.4. Chemical and mineralogical analysis

Determination of Al, As, Ca, Cd, Cr, Cu, Fe, K, Na, Ni, Mg, Mn, P, Pb, Si, Ti and Zn in the solid samples was conducted by inductively

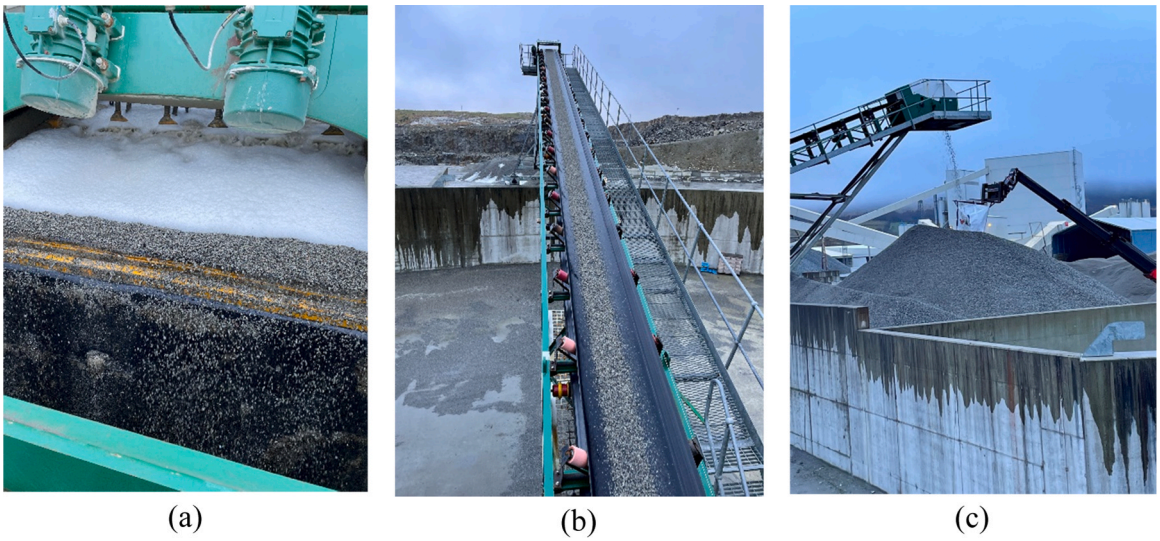


**Fig. 1.** Production and sampling of recycled materials during full-scale pilot: (a) washing and sieving process (b) conveyor belt with recycled materials (c) direct sampling.

**Table 1**
Samples collected with the mix ratio given in volume (%).

| Sample | Wet processing | RCZ | EM |
|---|---|---|---|
| RCZ-$F_0$ | No | - | - |
| RCZ-F | No | - | - |
| RCZ0 | Yes | 0 | 100 |
| RCZ50 | Yes | 50 | 50 |
| RCZ100 | Yes | 100 | 0 |

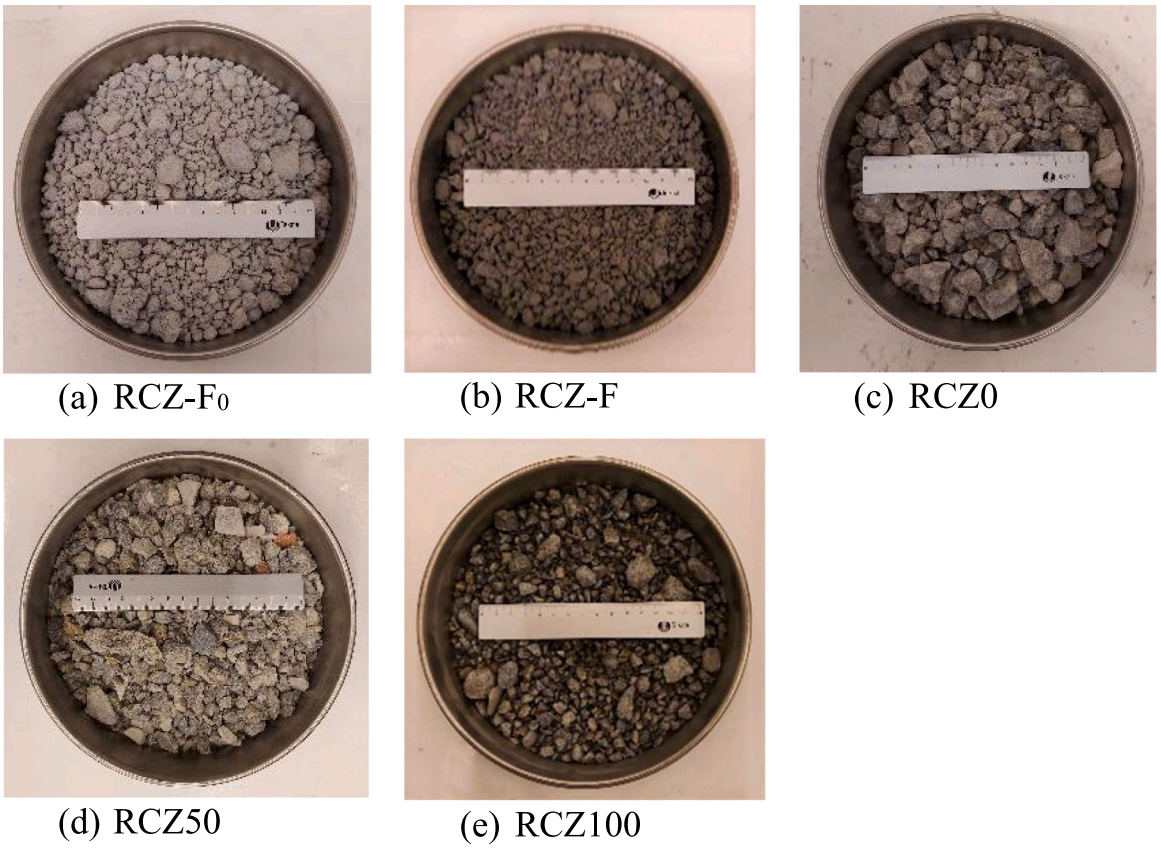


**Fig. 2.** Materials used in the study: (a) RCZ-$F_0$; Feedstock from raw feed pile, (b) RCZ-F; Feedstock stockpiled in open environment, (c) RCZ0; wet-processed (recycled) excavation materials, (d) RCZ50; 50% blends of wet processed (RCZ). (e) RCZ100; wet-processed (recycled) concrete sludge.

coupled plasma mass spectrometry (ICP-MS) according to ISO 17294–2 and EPA method 200.8. Analysis of Hg was done by Atomic Fluorescence Spectrometry (AFS) and Cr(VI) was analysed by ion chromatography with spectrophotometric detection according to ISO 15192:2010.

Acid solubility test was performed following the procedures described in NT Build 437. The acid solubility test comprised of samples milled and reduced to a test portion size. The test was performed on samples before and after the LA test. Fractions bearing the sample name RCZ-$F_0$, RCZ-F, RCZ0, RCZ50, and RCZ100 were analyzed before LA. They were dried over night at 105 °C before they were pulverized in a disk mill (Siebtechnik, Labor-Scheibenswingmühle T.250). Fractions composed of $RCZ0_{LA}$, $RCZ50_{LA}$ and $RCZ100_{LA}$ were received from $< 1.6$ mm after LA and therefore did not need further size reduction before drying. $4.0 \pm 0.1$ g of the sample were weighed (Mettler AE 260 Delta Range) directly in a beaker, the weight of the beaker had been determined with an accuracy of 1 * 10–3 g in advance. After this the samples were dried for 2 h at 105 °C before the weight was determined with an accuracy of 1 * 10–3 g. A large magnet was put into the glass before the addition of 3 mL absolute ethanol by use of pipette. Then 150 mL Type I water was added. The mix was then stirred by use of a magnet stirrer while 10 mL of $HNO_3$ was carefully added to the mixture using a pipette. The stirring continued for 10 min after the addition of $HNO_3$. After the samples had settled for at least two hours or overnight, the samples were filtrated using a water suction apparatus and Ø 55 mm Whatman filter paper. Sand and fine particles that were not dissolved were transferred back to the beaker which were dried over night at 105 °C. Samples and beakers were then weighed again.

X-ray powder diffraction analysis was performed using a Bruker D8 Focus X-ray diffractometer in Bragg–Brentano geometry ($\theta/2\theta$) for the materials before and after removal of paste content by the wet technology. The samples were prepared by the back-loading

technique to minimize potential mineral orientation effects. Samples were scanned from 5 to 60 °2θ with Cu-Kα radiation, a step size of 0.2 °2θ and 0.8 s time per step. The diffractograms were qualitatively analyzed with EVA V4.3. Quantitative analysis was done by Rietveld refinement and profile fitting using TOPAS V.6, the ICDD PDF4 + and COD mineral structure databases. The Chebychev background model and sample displacement were refined. For the mineral structures, lattice parameters and scale were refined. Crystallite sizes were refined within reasonable limits. For mica, preferred orientation in (002) direction was additionally refined. In order to describe and quantify the mineral phases present in the materials, pulverized fragments obtained from < 1.6 mm sieve after LA was analyzed and compared with original samples. Hence, the minerals phases which shows the mineralogy of samples investigated is shown in Table 6. The results are normalized to 100% crystalline content. Uncertainty of the Rietveld results can be expected due to certain small amounts of non-carbonated X-ray amorphous C-S-H phases in the residual cement paste. However, the expected overall error of the quantitative analysis was expected to be in a similar range as the amount of potential X-ray amorphous hydration phases itself.

## 3. Results and discussion

### 3.1. Physical properties

The particle-size distribution (PSD) of the materials investigated in this study is shown in Fig. 3. There was no significant difference between the PSD determined at UiA and Velde. However, the PSD of feedstock RCZ-$F_0$ and RCZ-F as determined at UiA varied. The cause of changes in the gradation of RCZ-F may be due to the effect of rainfall action and the storage time outside the recycling facility before sampled to UiA. In the case of Velde, RCZ-$F_0$ was not determined. The PSD of RCZ0, RCZ50 and RCZ100 was consistent with the 4/16 mm production line of the facility. Although RCZ100 was obtained from the same concrete sludge source, significant differences in textural characteristics resulting from efficient removal of poorly cured cement paste by intense washing and scrubbing unit of the recycling facility was observed (see Fig. 3).

The density and WA values as reported in Table 2 were obtained from the tests performed at UiA and Velde. In general, these parameters are influenced by the porous structure of mineral aggregates, hence they demonstrate the amount of water that can be absorbed. They are vital material properties required for road pavement and concrete production. The density results obtained from both test centers showed a similar trend. Reported values between the feedstock and recycled aggregates RCZ50 and RCZ100 did not significantly vary although poorly cured cement paste were removed from recycled aggregates during treatment. Nevertheless, it was observed that the density increased as RCZ content increased. Regarding RCZ0, Adomako et al., (2022) reported similar values in a study that investigated the mechanical performance of recycled aggregates derived from EM. Other studies have also reported the density for recycled aggregates obtained from ready mixed concrete waste within the range 1.65–2.72% [11,16,20,26]. It can also be mentioned that Norwegian rocks typically have a density within the range of 2.65–3.10 g/mL [16]. The values obtained for density clearly show that RCZ have similar density characteristics compared to other recycled and natural aggregates.

Unlike the density, significant differences were observed for WA, especially for the feedstocks. This observation may be due to differences in storage time at the recycling facility- Velde and UiA. Hence, the feedstock tested at UiA demonstrated high WA values. In this case, it may be suggested given the ambient storage conditions that the hardened and or dried nature of cement paste increased the pore structure [27]. Evidence of dry cement paste can be seen in Fig. 2. Regarding the feedstock at Velde, the low WA value may be related to the densification and refinement of microstructure of cement composites given its exposure to open environment and resulting carbonation [28]. It is well accepted in literature that carbonation treatment improves the WA of recycled aggregates from concrete waste [29]. The WA values for recycled aggregates at UiA were slightly higher than Velde. Generally, the WA of recycled aggregates from concrete waste are known to be high and this has a negative impact on overall performance. Low WA values recorded for processed materials indicate the effectiveness of the recycling technology on removal of loose components e.g., uncured cement paste.

For RCZ0, the WA obtained is higher than 0.3% reported for similar material in the study [30]. Studies that have investigated the performance of RCSA reported WA values within the margin 4–13% [20,22]. Given the variation of WA in RCSA, it is important to consider factors such as substitution level and water- cement ratio if used in concrete. [16,23]. Overall, the results demonstrated that RCZ have better quality performance.

**Table 2**
Particle density and water absorption values of investigated materials.

| Sample | Particle density (g/mL) | | Water absorption (%) | |
|---|---|---|---|---|
| | UiA | Velde | UiA | Velde |
| RCZ-$F_0$ | 2.68 | 2.64 | 7.62 | 3.10 |
| RCZ-F | 2.63 | n.d.[a] | 6.68 | n.d.[a] |
| RCZ0 | 2.58 | 2.59 | 2.78 | 1.95 |
| RCZ50 | 2.62 | 2.62 | 2.58 | 1.86 |
| RCZ100 | 2.68 | 2.66 | 2.05 | 1.63 |

[a] Not determined

**Table 3**
LA and MD performance of the materials.

| Sample | UiA | | Velde | |
|---|---|---|---|---|
| | LA | MD | LA | MD |
| RCZ-$F_0$ | 25 | 20 | 22 | 15 |
| RCZ-F | 23 | 18 | n.d.[a] | n.d.[a] |
| RCZ0 | 24 | 12 | 26 | 10 |
| RCZ50 | 22 | 10 | 24 | 11 |
| RCZ100 | 18 | 11 | 20 | 11 |

[a] Not determined

**Table 4**
Acid soluble contents (wt%) in the samples with various particle size given as arithmetic mean ± 1 standard deviation, (n = 3) and (n = 4, $_{LA}$).

| Sample | Acid soluble part, % | Standard deviation,% | RSD, % |
|---|---|---|---|
| RCZ-$F_0$ | 13.29 | 0.19 | 1.41 |
| RCZ-F | 13.80 | 0.05 | 0.35 |
| RCZ0 | 4.58 | 0.18 | 3.96 |
| RCZ50 | 8.27 | 0.41 | 4.96 |
| RCZ100 | 7.14 | 0.07 | 0.93 |
| $RCZ0_{LA}$ | 9.46 | 0.28 | 3.00 |
| $RCZ50_{LA}$ | 12.04 | 0.28 | 2.34 |
| $RCZ100_{LA}$ | 18.53 | 0.68 | 3.66 |

**Table 5**
Major oxide composition in the samples expressed in wt%.

| Element | RCZ-$AF_0$ | RCZ-AF | RCZ 0 | RCZ 50 | RCZ 100 | RCZ $0_{LA}$ | RCZ $50_{LA}$ | RCZ $100_{LA}$ |
|---|---|---|---|---|---|---|---|---|
| $Al_2O_3$ | 14.4 | 13.3 | 14.6 | 14.4 | 14.3 | 13.0 | 12.8 | 12.6 |
| CaO | 6.0 | 5.9 | 2.3 | 4.0 | 3.0 | 4.6 | 5.9 | 8.9 |
| $Fe_2O_3$ | 4.6 | 4.8 | 2.9 | 4.3 | 4.9 | 2.3 | 2.8 | 3.2 |
| $K_2O$ | 3.4 | 3.4 | 3.9 | 3.3 | 3.3 | 3.8 | 3.6 | 3.6 |
| MgO | 1.0 | 1.0 | 0.6 | 0.9 | 1.0 | 0.6 | 0.7 | 0.9 |
| $MnO_2$ | 0.1 | 0.1 | 0.0 | 0.1 | 0.1 | 0.0 | 0.1 | 0.0 |
| $Na_2O$ | 2.9 | 2.8 | 3.8 | 3.2 | 3.2 | 2.7 | 2.6 | 2.5 |
| $P_2O_5$ | 0.3 | 0.3 | 0.1 | 0.2 | 0.3 | 0.1 | 0.1 | 0.2 |
| $SiO_2$ | 70.8 | 64.8 | 74.5 | 70.8 | 68.2 | 74.6 | 71.2 | 65.8 |
| $SO_3$ | 0.3 | 0.3 | 0.1 | 0.2 | 0.2 | 0.2 | 0.3 | 0.5 |
| $TiO_2$ | 0.6 | 0.7 | 0.3 | 0.6 | 0.7 | 0.2 | 0.3 | 0.4 |
| LOI- 1000° C | 3.3 | 3.5 | 1.3 | 1.8 | 1.2 | 2.6 | 3.4 | 5.1 |

**Table 6**
Mineral phase contents (%) in the samples investigated in the study.

| Mineral | RCZ-$AF_0$ | RCZ-AF | RCZ 0 | RCZ 50 | RCZ 100 | RCZ $0_{LA}$ | RCZ $50_{LA}$ | RCZ $100_{LA}$ |
|---|---|---|---|---|---|---|---|---|
| Quartz | 28.2 | 35.6 | 31.6 | 31.6 | 30.2 | 31.3 | 32.4 | 31.7 |
| Feldspar | 52.9 | 43.3 | 53.8 | 52.8 | 41.6 | 50.8 | 46.7 | 52.5 |
| Calcite | 4.8 | 5.1 | 1.6 | 1.4 | 10.9 | 2.4 | 3.9 | 1.9 |
| Portlandite | 0.5 | 0.3 | 0.0 | 0.1 | 1.7 | 0.4 | 1.2 | 0.4 |
| Chlorite | 0.4 | 0.5 | 2.2 | 1.6 | 0.9 | 3.3 | 3.3 | 0.4 |
| Mica | 8.4 | 6.5 | 5.9 | 5.9 | 6.3 | 6.3 | 5.2 | 8.6 |
| Diopside | 1.6 | 5.1 | 3.8 | 3.4 | 2.7 | 4.3 | 2.5 | 1.4 |
| Clinker | 3.2 | 3.6 | 1.1 | 3.2 | 5.7 | 1.2 | 4.8 | 3.1 |
| Total | ~100 | ~100 | ~100 | ~100 | ~100 | ~100 | ~100 | ~100 |

### *3.2. The Los Angeles and micro-Deval performance*

The Los Angeles (LA) and micro-Deval (MD) test investigate the resistance to fragmentation and wear, respectively and are two most common tests used to analyze the performance of aggregates for concrete and in unbound applications. The results obtained for LA and MD are shown in Table 3. First, marginal differences in the performance can be seen in the results obtained from the two test sources. Considering the feedstock materials, the values obtained at UiA is slightly higher than Velde. It was observed in this case that the paste adhering to the surfaces of samples tested at UiA had severely disintegrated and this reflected in the sieving process as large

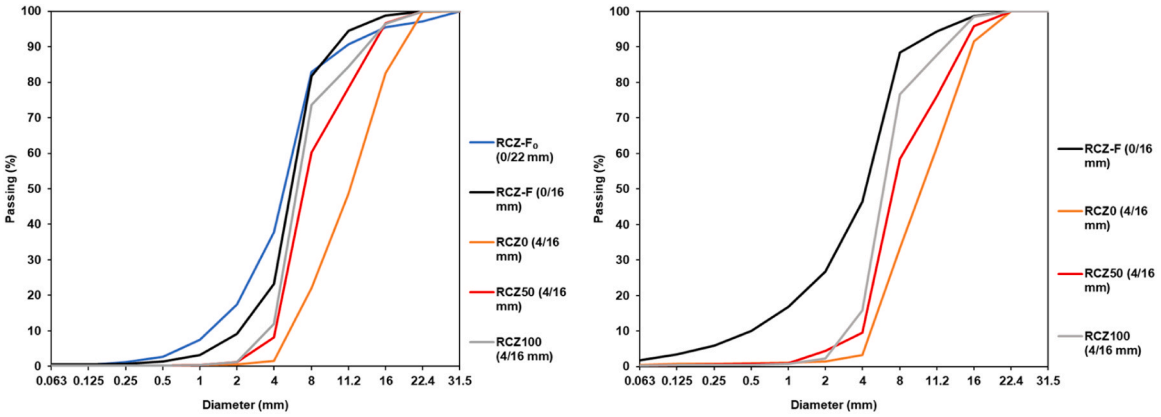


**Fig. 3.** PSD as determined at UiA (left), and Velde (right).

amount of < 1.6 mm fractions contained such content. This resulted in increased mass loss when the LA coefficient was measured. This observation changed regarding processed materials as the values obtained at Velde were slightly higher. Overall, a clear trend in improved performance can be seen with increased RCZ. This was expected given that RCZ was composed of a significant amount of natural aggregates derived from concrete sludge. Secondly, this trend indicates that the developed admixture under proper curing conditions stabilizes the performance of recycled aggregates.

Regarding the LA for RCZ0, other studies have reported stabilized results for excavation materials within the range of 24–28% [30,31]. The LA for RCZ50 also show the optimal intermix of recycled aggregates RCZ and excavation materials. The positive effect of RCZ intermix can be explained by removal of weak paste (poorly cured). However, the results from acid solubility still revealed that RCZ100 contained a significant cement paste after wet treatment (see Section 3.3). Typical LA value for recycled aggregates from returned concrete waste has been reported to be 25% [16]. Generally, comparing the performance of materials investigated in this study to others e.g. recycled concrete aggregates, generic conclusion regarding the LA performance is that such materials have lower performance than natural aggregates. This is due to the crushing effect on residual mortar at the interfacial transition zone i.e., region of paste around aggregate particles [32,33]. For example, in a study that reported the LA of recycled concrete aggregates within the range of 35–42%, it was mentioned that the tendency to achieve less crushing resistance was due to increased amount of paste content [33]. Similarly, another study reported the LA of three different recycled concrete aggregates within the range of 38–41% [34].

The Norwegian road construction guideline report the LA limit criteria for natural aggregates for base at ≤ 35% [35]. Similarly, maximum LA values for different applications ranging from 30% to 50% are reported in the study[36]. Another study reported averaged LA values for eleven limestone, eleven marble and ten andesite rocks as 26%, 27% and 16%, respectively [37]. Based on these, it may be concluded that the performance of materials investigated is good and therefore they qualify to be used in unbound applications.

Regarding the MD results significant differences were seen in feedstock materials. Recycled materials demonstrated a consistent trend in both cases. This observation again confirmed the effect of the wet technique on removing weak paste on the interface of RCZ. The MD performance obtained in this study is significantly better compared to reported MD of 31% for recycled aggregates obtained from ready mixed concrete waste [16]. Slight differences in MD occurred for RCZ0. Nevertheless, they are consistent with reported MD values within the range 6–20% for excavation materials [31]. In Norway, a recent study proposed LA and MD criteria for intermix of recycled concrete aggregates and excavation materials of ≤ 35% and ≤ 20%, respectively [38]. These limit criteria were met by all materials investigated, especially RCZ50. In comparing the MD performance to recycled concrete aggregates, one study reported the MD within the region 28–30% [39]. The MD for natural aggregates i.e., basalt, granitoid and gabbroid rocks has been reported within the margin 8–9%. [40,41]. Another study have also reported the MD values for natural aggregates used in different applications within the range ≤ 13–30% [42]. It is clear given these findings that RCZ advances the opportunity to increase the use of recycled materials from returned concrete waste under proper production and treatment.

### 3.3. Acid soluble content and particle size

Acid solubility test were performed on samples obtained from UiA only and the results are reported in Table 4. The solubility rate of the feedstock were found to be the same. Similar observation was realized in RCZ50 and RCZ100 whereas RCZ0 was the main insoluble material given a 5% soluble part. Generally, the results followed a consistent pattern in relation to the LA performance. By this, RCZ-F$_0$, and RCZ-F which recorded LA of 25% and 23%, respectively were shown to be highly soluble. This was not surprising given the source and the fact that both feedstocks did not receive wet treatment, subsequently indicating more amount of cement paste. Recycled RCZ50 and RCZ100 demonstrated low amount of paste content which also reflected in the LA values of 22% and 18%, respectively. Further, this confirmed the removal of loose paste content by applied treatment and maximizes the benefits of producing recycled aggregates RCZ and excavation materials. The relation that high paste content reduces the LA performance has been demonstrated in some studies [33,43].

Samples denoted $_{LA}$ were obtained from < 1.6 mm sieve after LA. $RCZ0_{LA}$, $RCZ50_{LA}$ and $RCZ100_{LA}$ showed increased solubility rate which means the paste content was more profound in small particle size fractions. This trend can be seen by the increased solubility for < 1.6 mm samples by increased RCZ content. Generally, the relation that acid soluble content increases as the particle size reduces is consistent with the findings reported earlier [44]. In view of this, it is feasible to expect that the fine fraction will contain a higher amount of cement paste than the coarse fraction of recycled materials at the production facility. In the case of increased solubility for $RCZ0_{LA}$ the reason may be due to the presence of residual paste from $RCZ50_{LA}$ and $RCZ100_{LA}$ since all materials were tested in the same machine.

### 3.4. Oxide composition and change in mineralogy

The results for oxide and heavy metal composition are reported in Table 5 and Table 6, respectively. Regarding the major oxides,

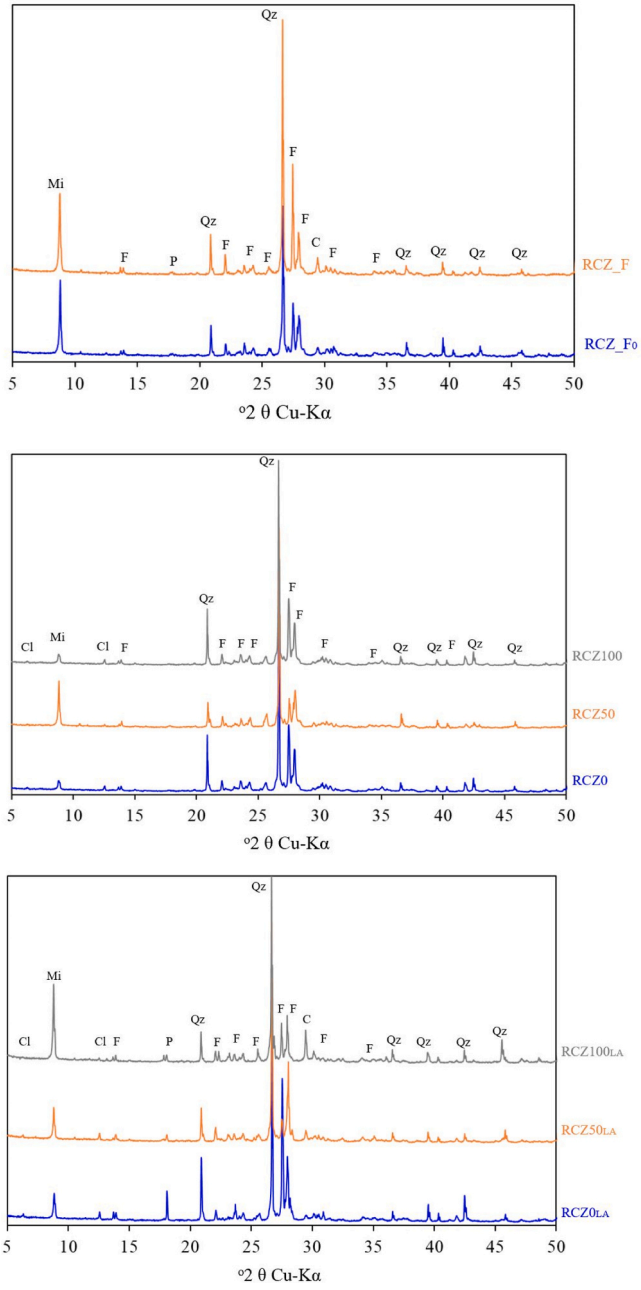


**Fig. 4.** X-ray diffractograms pattern of samples investigated and marked with the prominent peaks of the main mineral phases Mi = Mica, F = feldspar, Qz = Quartz, C= Calcite, P = Portlandite, Cl = Chlorite.

slight differences were observed between the materials. The content of CaO found in the feedstock was higher than recycled materials. Again, this observation means that some of the paste were removed during the wet process. A clear trend of increased CaO content was found in the fine fraction of RCZ samples after LA which supports that paste content is susceptible to crushing. In addition, these findings were in accordance with the trend observed in the acid soluble results as demonstrated in Table 4. This again supports the theory that some of the paste is removed during the wet process. Some studies show that the major element oxides are influential factors given their effect on durability, hardness, toughness, and soundness properties [40,45]. The most apparent element is $SiO_2$ as expected due to the mineralogy (discussed below). It can be observed that $SiO_2$ content decreases with increasing RCZ because more properly cured cement paste is introduced.

The quantified mineral phases in both original and pulverized residues (<1.6 mm) are shown in Table 6. The dominant minerals identified were typical for Norwegian aggregates, i.e. feldspar, quartz, phyllosilicates (mica and chlorite) and minor amounts of pyroxene (diopside). The main feldspar minerals identified were albite, while anorthite, microcline and orthoclase was also found. In addition, paste minerals like portlandite and residual clinker phases were identified besides calcite. The clinker minerals were mainly larnite ($Ca_2SiO_4$) and brownmillerite ($Ca_2(Al,Fe)_2O_5$). The results are normalized to 100% crystalline phase content. The discrepancy between the acid soluble amount and the paste phases detected is probably due to the X-ray amorphous phases of calcium silicate hydrate which were not considered here. Some differences in mineral content were observed between the samples before and after LA. Considering calcite, RCZ100 recorded the highest amount but there was a significant reduction in $RCZ100_{LA}$. Other recycled materials RCZ0 and RCZ50 recorded lower concentrations but slightly increased amounts were observed in $RCZ0_{LA}$ and $RCZ50_{LA}$. All samples reported a low amount of Portlandites. The clinker phases were not marked in the figures. This was because of peak overlap with other main minerals and low overall intensities in comparison to feldspar and quartz. Note that the presence of mechanically weak minerals e.g., Chlorite is slightly higher in RCZ0 and RCZ50, and $RCZ0_{LA}$ and $RCZ50_{LA}$. This is because the excavation materials used in the study is originally characterized by different geological make up i.e., phyllites [30]. Nevertheless, the content of mica is consistent and present in all samples. Generally, these primary minerals identified as quartz, phyllosilicates, and feldspar, are known to influence the mechanical performance of rocks, [30,36,46,47]. Unlike quartz and feldspar which contributes to performance improvement, phyllosilicates are mechanically weak minerals. However, in this study, the content of mica and chlorite as found in excavation materials did not compromise overall mechanical performance. This phenomenon is not only attributed to the content but also the disposition through distribution and structural formation of the grain boundaries [47]. Hence, the LA reported for excavation materials as 24% and 26% from both test centers are equivalent to the LA of some rocks (e.g., Arkose, Granite, Pegmatite) found in Norway [42]. Fig. 4.

### 3.5. Chemical species of potential concern (COPC)

The environmental applicability of RCZ was screened by assessing the COPC level in the feedstock and new aggregates. In addition, the LA fine samples (< 1.6 mm) were included to disclose any increased concentrations in the weak mineral part of the RCZ. Furthermore, Norwegian content limits for concrete waste, that recently have been developed by Norwegian Environmental Agency (NEA) were used to evaluate the COPC level [48]. They were derived from risk assessments based on COPC leaching evaluation and Norwegian soil quality limits [49]. Concrete and masonry waste that comply with these limits can be used without calculating the environmental risk in case-by-case for recycling scenarios above groundwater level and not submerged in water (e.g. sub-base in road construction). The limits are often used as first-stage evaluation of waste-derived binders and recycled aggregates used for concrete, since the unbound recycling scenarios (granular condition) are more critical for unacceptable release of COPC than the use in concrete (monolithic condition). Hence, compliance with the Norwegian NEA limits ensures limited spreading of COPC to the environment in the practical recycling application scenarios[48]. The results are shown in Table 7 and the concentrations were found to be low with some exceptions, i.e., elevated concentrations for Cu, Cr and Zn were found in the washed RCZ which exceeded the NEA limits. If the RCZ0 (washed excavation materials) are compared to the concrete sludge feedstocks $RCZ\text{-}AF_0$ and RCZ-AF, it can be observed that the elevated levels originated from the excavation feedstock. In addition, these levels decrease significantly as concrete sludge content was introduced in the recycling process.

Furthermore, under oxidised conditions hexavalent Cr ($CrO_4^{2-}$) may form, which in earlier studies has been identified experimentally [50] and by geochemical speciation modelling [51] as bound in ettringite solid solution in recycled concrete aggregates. In the present study, the Cr(VI) level was low in RCZ samples (see Table 7) which will ensure low leaching of Cr upon carbonation and a decrease in pH. Moreover, all Cr(VI) values were below the Norwegian soil quality criteria of 2 mg/kg [49]. It can also be seen that the wet recycling process decreased the Cr(VI) level when the feedstock and RCZ100 are compared. It can be noted that the recycling facility has full treatment of polluted water and the removal of Cr(VI) in the present process may be found to be a viable solution.

If the fine fractions (<1.6 mm) are examined, a significant concentration increase was only found for Zn and Cu when the concrete sludge feedstock increased. The cement paste content also increased in the fine fractions upon increased sludge content (shown in Table 4), which explained the elevated concentrations in RCZ100. However, the COPC levels in the fine fractions were low which is promising regarding potential impact on soil and groundwater, since the cement paste is the most chemically active part regarding the release from recycled aggregates.

## 4. Conclusions

This paper investigates the technical and environmental properties of Re-Con Zero dry washing technology used to produce recycled aggregates from concrete sludge (RCZ) and combined as a feedstock in wet recycling excavation materials. The production followed sample classification RCZ0, RCZ50 and RCZ100 within the range 0–100%. The Los Angeles (LA) and micro-Deval (MD)

**Table 7**
Content of COPC in the materials compared to Norwegian criteria for concrete waste. Concentrations are given in mg/kg.

| Element | RCZ-$AF_0$ | RCZ-AF | RCZ 0 | RCZ 50 | RCZ 100 | RCZ $0_{LA}$ | RCZ $50_{LA}$ | RCZ $100_{LA}$ | NEA limit[a] |
|---|---|---|---|---|---|---|---|---|---|
| As | < 3 | < 3 | < 3 | < 3 | < 3 | < 3 | < 3 | < 3 | 15 |
| Cd | < 0.1 | < 0.1 | < 0.1 | < 0.1 | < 0.1 | < 0.1 | < 0.1 | < 0.1 | 1.5 |
| Cr | 131 | 105 | 168 | 139 | 107 | 30.2 | 24.8 | 32.7 | 100 |
| $Cr^{6+}$ | 0.8 | 0.7 | < 0.3 | < 0.3 | < 0.3 | 1.4 | 1.4 | 1.9 | 8 |
| Cu | 49 | 47.5 | 206 | 33.4 | 29 | 38.5 | 36.8 | 49.4 | 100 |
| Hg | < 0.01 | < 0.01 | < 0.01 | < 0.01 | < 0.01 | < 0.01 | < 0.01 | < 0.01 | 1 |
| Ni | 11.7 | 12.9 | 10.4 | 8.3 | 7.4 | 8.3 | 10.9 | 9.4 | 75 |
| Pb | 28.5 | 27.7 | 35.9 | 25.8 | 23.3 | 32.9 | 33.8 | 29.6 | 60 |
| Zn | 96.5 | 99 | 250 | 72.6 | 87.1 | 49 | 56.7 | 70.7 | 200 |

[a] Waste regulation limits for concrete waste developed and issued by Norwegian Environmental Agency (NEA, 2022)

performance demonstrated RCZ to be a good material and therefore increasing the amount of RCZ enhanced the performance of final product. This observation was clearly visible in reported LA and MD values. X-ray diffraction analysis performed on original and pulverized residues (< 1.6 mm) identified dominant mineral phases to be feldspar, quartz, phyllosilicates (mica and chlorite) and minor amounts of pyroxene (diopside). Furthermore, some differences in paste mineral (calcite) were observed, e.g., while a significant amount was found in RCZ100, the amount in $RCZ100_{LA}$ significantly reduced. Conversely, low concentrations were reported for RCZ0 and RCZ50 with a marginal increase in $RCZ0_{LA}$ and $RCZ50_{LA}$. Regarding the acid solubility, the study showed that paste content in particle sizes (<1.6 mm) obtained after LA test was significantly higher than in the coarse fractions. This phenomenon confirmed the presence of paste in RCZ after wet treatment although the treatment process removed poorly cured paste. The contents of chemical species of potential concern (COPC) were found to be low and mostly complying to Norwegian environmental criteria. It was also found that Cr(VI) was not detected in wet treated RCZ and strongly indicate low leaching of Cr upon carbonation and a decrease in pH. Hence, the results were promising and can be used for further development of separate RCZ and in combination with excavation materials. The approach may increase the extended use of both materials and offer significant technical and environmental benefits.

## Declaration of Competing Interest

The authors declare no conflicts of interest.

## Data Availability

Data will be made available on request.

## Acknowledgement

The work was part of the RCN (Research Council of Norway) projects MEERC (More Efficient and Environmentally friendly Road Construction, RCN 273700) and RECONC (Recycled aggregates from Concrete sludge with $CO_2$ binding properties, RCN 309959).

## References

[1] K. Chen, J. Wang, B. Yu, H. Wu, J. Zhang, Critical evaluation of construction and demolition waste and associated environmental impacts: a scientometric analysis, J. Clean. Prod. 287 (2021), 125071, https://doi.org/10.1016/j.jclepro.2020.125071.
[2] H. Wu, J. Zuo, G. Zillante, J. Wang, H. Yuan, Status quo and future directions of construction and demolition waste research: a critical review, J. Clean. Prod. 240 (2019), 118163, https://doi.org/10.1016/j.jclepro.2019.118163.
[3] M. Bernardo, M.C. Gomes, J. de Brito, Demolition waste generation for development of a regional management chain model, Waste Manag. 49 (2016) 156–169, https://doi.org/10.1016/j.wasman.2015.12.027.
[4] J. Hu, Z. Wang, Y. Kim, Feasibility study of using fine recycled concrete aggregate in producing self-consolidation concrete, J. Sustain. Cem. -Based Mater. 2 (2013) 20–34, https://doi.org/10.1080/21650373.2012.757832.
[5] C. Shi, Y. Li, J. Zhang, W. Li, L. Chong, Z. Xie, Performance enhancement of recycled concrete aggregate–a review, J. Clean. Prod. 112 (2016) 466–472, https://doi.org/10.1016/j.jclepro.2015.08.057.
[6] H. Mujica, E. Velde, C.J. Engelsen, M.S. Nodland, Recycled aggregates produced from two different feedstock materials – applied in ready-mixed concrete. International Conference on Sustainable Materials, Systems and Structures (SMSS 2019). Rovinj, Croatia.
[7] C.J. Engelsen, K.P. Nath, S. Kandasami, Recycled concrete aggregates in new concrete – full scale demonstration in Navi Mumbai, Indian Concr. J. 96 (1) (2022) 49–57.
[8] L. Peng, Y. Zhao, H. Zhang, Flexural behavior and durability properties of recycled aggregate concrete (RAC) beams subjected to long-term loading and chloride attacks, Constr. Build. Mater. 277 (2021), 122277, https://doi.org/10.1016/j.conbuildmat.2021.122277.
[9] Y. Zhao, L. Peng, W. Zeng, C. sun Poon, Z. Lu, Improvement in properties of concrete with modified Rca by microbial induced carbonate precipitation, Cem. Concr. Compos. 124 (2021), 104251, https://doi.org/10.1016/j.cemconcomp.2021.104251.
[10] S.L. Correia, F.L. Souza, G. Dienstmann; A.M. Segadaes, Assessment of the Recycling Potential of Fresh Concrete Waste Using a Factorial Design of Experiments Waste management, 29(11) (2009) 2886–2891. https://doi.org/10.1016/j.wasman.2009.06.014.
[11] G. Ferrari, M. Miyamoto, A. Ferrari, New Sustainable Technology for Recycling Returned Concrete Construction and Building Materials, 67 (2014) 353–359. https://doi.org/10.1016/j.conbuildmat.2014.01.008.
[12] A. Kazaz, S. Ulubeyli, B. Er, V. Arslan, M. Atici, A. Arslan, Fresh ready-mixed concrete waste in construction projects: a planning approach organization, Technol. Manag. Constr.: Int. J. 7 (2015) 1280–1288, https://doi.org/10.5592/otmcj.2015.2.2.

[13] D. Xuan, C.S. Poon, W. Zheng, Management and sustainable utilization of processing wastes from ready-mixed concrete plants in construction: a review resources, Conserv. Recycl. 136 (2018) 238–247, https://doi.org/10.1016/j.resconrec.2018.04.007.
[14] N.N. Gebremichael, S.M.M. Karein, M. Karakouzian, K. Jadidi, Investigation of Setting Time and Compressive Strength of Ready-Mixed Concrete Blended with Returned Fresh Concrete Construction and Building Materials, 197 (2019) 428–435. https://doi.org/10.1016/j.conbuildmat.2018.11.201.
[15] L.B.P. Vieira, A.D. de Figueiredo, T. Moriggi, V.M. John, Waste Generation from the Production of Ready-Mixed Concrete Waste Management, 94 (2019) 146–152. https://doi.org/10.1016/j.wasman.2019.05.043.
[16] S. Adomako, A. Heimdal, R.T. Thorstensen, From Waste to Resource–Utilising Residue from Ready-Made Concrete as New Aggregate, 64(1) (2021a) 1–10. https: doi.org/10.2478/ncr-2021–0010.
[17] Y. Okawa, H. Yamamiya, S. Nishibayashi, Study on the Reuse of Returned Concrete Magazine of Concrete Research, 52(2000)109–115. https://doi.org/10.1680/macr.2000.52.2.109.
[18] F. Kinney, Reuse of Returned Concrete by Hydration Control: Characterization of a New Concept Special Publication, 119(1989)19–40.
[19] J.F. Papí, Recycling of Fresh Concrete Exceeding and Wash Water in Concrete Mixing Plants Materiales de Construcción. 264 (2914) e004-e004.
[20] E. Anastasiou, M. Papachristoforou, D. Anesiadis, K. Zafeiridis, E.-C. Tsardaka, Investigation of the Use of Recycled Concrete Aggregates Originating from a Single Ready-Mix Concrete Plant Applied sciences. 8 (2018)2149. https://doi.org/10.3390/app8112149.
[21] L.B.P. Vieira, A.D. de Figueiredo, Evaluation of Concrete Recycling System Efficiency for Ready-Mix Concrete Plants Waste Management, 56(2916)337–351. https://doi.org/10.1016/j.wasman.2016.07.015.
[22] M. Sérifou, Z.M. Sbarta, S. Yotte, M.O. Boffoué, E. Emeruwa, F. Bos, A study of concrete made with fine and coarse aggregates recycled from fresh concrete waste, J. Constr. Eng. (2013) 1–5, https://doi.org/10.1155/2013/317182.
[23] S.-C. Kou, B.-J. Zhan, C.-S. Poon, Feasibility Study of Using Recycled Fresh Concrete Waste as Coarse Aggregates in Concrete Construction and Building Materials, 28(2012) 549–556. https://doi.org/10.1016/j.conbuildmat.2011.08.027.
[24] T. Søndenaa, Large initiative in South Norway: New research on rehabilitation of old county roads. In Våre Veger 06 (2020) 19–21.
[25] Y.-M. Miniggio, Concrete Waste Recovery and Emissions Reductions in the Norwegian Concrete Industry. Master Thesis (2022), University of Agder, Norway.
[26] A. Diotti, L. Cominoli, G. Plizzari, S. Sorlini, Experimental evaluation of recycled aggregates, washing water and cement sludge recovered from returned concrete, Appl. Sci. 12 (1) (2021) 36, https://doi.org/10.3390/app12010036.
[27] F. Thérèné, E. Keita, J. Nael-Redolfi, P. Boustingorry, L. Bonafous, N. Roussel, Water absorption of recycled aggregates: measurements, influence of temperature and practical consequences, Cem. Concr. Res. 137 (2020), 106196, https://doi.org/10.1016/j.cemconres.2020.106196.
[28] B.J. Zhan, D.X. Xuan, C.S. Poon, K.L. Scrivener, Characterization of interfacial transition zone in concrete prepared with carbonated modeled recycled concrete aggregates, Cem. Concr. Res. 136 (2020), 106175, https://doi.org/10.1016/j.cemconres.2020.106175.
[29] B. Lu, C. Shi, Z. Cao, M. Guo, J. Zheng, Effect of carbonated coarse recycled concrete aggregate on the properties and microstructure of recycled concrete, J. Clean. Prod. 233 (2019) 421–428, https://doi.org/10.1016/j.jclepro.2019.05.350.
[30] S. Adomako, C.J. Engelsen, T. Danner, R.T. Thorstensen, D.M. Barbieri, Recycled Aggregates Derived from Excavation Materials—Mechanical Performance and Identification of Weak Minerals Bulletin of Engineering Geology and the Environment, 81(2022),1–12.
[31] M. Norby, Nytt resirkulert tilslag produsert fra grave-og byggavfall. Master Thesis (2021), University of Agder, Norway.
[32] K. McNeil, T.H. Kang, Recycled concrete aggregates: a review, Int. J. Concr. Struct. Mater. 7 (2013) 61–69, https://doi.org/10.1007/s40069-013-0032-5.
[33] M.S. De Juan, P.A. Gutiérrez, Study on the influence of attached mortar content on the properties of recycled concrete aggregate, Constr. Build. Mater. 23 (2009) 872–877, https://doi.org/10.1016/j.conbuildmat.2008.04.012.
[34] S. Silva, L. Evangelista, J. De Brito, Durability and shrinkage performance of concrete made with coarse multi-recycled concrete aggregates, Constr. Build. Mater. 272 (2021), 121645, https://doi.org/10.1016/j.conbuildmat.2020.121645.
[35] Norwegian Public Roads Administration (NPRA), Håndbok N200 Vgbygging, Vejdirektoratet, 2022.
[36] S. Adomako, C.J. Engelsen, R.T. Thorstensen, D.M. Barbieri, Review of the relationship between aggregates geology and Los Angeles and micro-deval tests, Bull. Eng. Geol. Environ. 80 (2021) 1963–1980, https://doi.org/10.1007/s10064-020-02097-y.
[37] O. Yilmaz, Predicting Los Angeles abrasion of rocks from some physical and mechanical properties, Sci. Res. Essays 6 (2011) 1612–1619, https://doi.org/10.5897/SRE10.1164.
[38] C.J. Engelsen, K.R. Lysbakken, Utnyttelse av resirkulert tilslag N200 Vegbygging (REN 200): Kunnskap og erfaringer med resirkulerte betong og gravemasser (2021) (In Norwegian).
[39] A. Gabr, D. Cameron, Properties of recycled concrete aggregate for unbound pavement construction, J. Mater. Civ. Eng. 24 (2012) 754–764, https://doi.org/10.1061/(ASCE)MT.1943-5533.0000447.
[40] Ö.F. Apaydın, M. Yılmaz, Correlation of petrographic and chemical characteristics with strength and durability of basalts as railway aggregates determined by ballast fouling, Bull. Eng. Geol. Environ. 80 (2021) 4197–4205, https://doi.org/10.1007/s10064-019-01654-4.
[41] E. Johansson, K. Miškovský, M. Bergknut, Š. Šachlová, Petrographic Characteristics of Intrusive Rocks as an Evaluation Tool of Their Technical Properties Geological Society, London, Special Publications, 416(2016) 217–227. https://doi.org/10.1144/SP416.19.
[42] S. Adomako, C.J. Engelsen, T. Danner, R.T. Thorstensen, D.M. Barbieri, Recycled aggregates derived from excavation materials—mechanical performance and identification of weak minerals, Bull. Eng. Geol. Environ. 81 (2022), 340, https://doi.org/10.1007/s10064-022-02817-6.
[43] P. Saravanakumar, K. Abhiram, B. Manoj, Properties of treated recycled aggregates and its influence on concrete strength characteristics, Constr. Build. Mater. 111 (2016) 611–617, https://doi.org/10.1016/j.conbuildmat.2016.02.064.
[44] C.J. Engelsen, H.A. van der Sloot, G. Wibetoe, G. Petkovic, E. Stoltenberg-Hanssone, W. Lund, Release of Major Elements from Recycled Concrete Aggregates and Geochemical Modelling Cement and Concrete Research 2009, 39,446–459. https://doi.org/10.1016/j.cemconres.2009.02.001.
[45] İ. Gökalp, V.E. Uz, The effect of aggregate type and gradation on fragmentation resistance performance: testing and evaluation based on different standard test methods, Transp. Geotech. 22 (2020), 100300, https://doi.org/10.1016/j.trgeo.2019.100300.
[46] D.M. Barbieri, I. Hoff, M.B.E. Mørk, Innovative stabilization techniques for weak crushed rocks used in road unbound layers: a laboratory investigation, Transp. Geotech. 18 (2019) 132–141, https://doi.org/10.1016/j.trgeo.2018.12.002.
[47] E. Kuznetsova, A.P. Pérez Fortes, S. Anastasio, and S.Willy Danielsen, Behavior of Crushed Rock Aggregates Used in Road Construction Exposed to Cold Climate Conditions, EGU General Assembly Conference Abstracts, (2016).
[48] Norwegian Environmental Agency (NEA). ⟨https://www.environmentagency.no/⟩, 2022 (accessed 31.12.2022).
[49] Norwegian Polluation Regulation (NPR), Chapter 2: Cleaning of polluted ground originating from construction and excavation activities, Attachment 2: Norm values, FOR-2004–06-01–93, (2004).
[50] M. Mulugeta, G. Wibetoe, C.J. Engelsen, W. Lund, Optimization of an anion-exchange high performance liquid chromatography-inductively coupled plasma-mass spectrometric method for the speciation analysis of oxyanion-forming metals and metalloids in leachates from cement-based materials, J. Chromatogr. 1217 (2010) 6186–6194, https://doi.org/10.1016/j.chroma.2010.07.082.
[51] C.J. Engelsen, H.A. van der Sloot, G. Wibetoe, H. Justnes, W. Lund, E. Stoltenberg-Hansson, Leaching characterisation and geochemical modelling of minor and trace elements released from recycled concrete aggregates, Cem. Concr. Res. 40 (12) (2010) 1639–1649, https://doi.org/10.1016/j.cemconres.2010.08.001.